HASAN KALYONCU UNIVERSITY
GRADUATE SCHOOL OF
NATURAL & APPLIED SCIENCES

VOLTAGE REGULATION FOR GRID CONNECTED PHOTOVOLTAIC SYSTEMS USING REACTIVE POWER

M.Sc. THESIS
IN
ELECTRONICS AND COMPUTER ENGINEERING

BY
Buray Eray TANKUT
MAY 2019

"Voltage Regulation For Grid Connected Photovoltaic Systems Using Reactive Power"

M.Sc. Thesis

in

Electronics and Computer Engineering

Hasan Kalyoncu University

Supervisor

Asst. Prof. Dr. Bilal Mouneir Saeed Eid

By

Buray Eray TANKUT

MAY 2019

GRADUATE SCHOOL OF NATURAL & APPLİED SCIENCES INSTITUTE M.Sc. ACCEPTANCE AND APPROVAL FORM

Electronics and Computer Engineering Department, Electrical and Electronics Engineering M.Sc. (Master of Science) programme student **Buray Eray TANKUT** prepared and submitted the thesis titled **Voltage Regulation For Grid Connected Photovoltaic Systems Using Reactive Power** defended successfully on the date of **23/05/2019** and accepted by the jury as a M.Sc. thesis.

Position	**Title, Name and Surname** **Department/University**	**Signature**
Supervisor	Asst. Prof. Dr. Bilal Mouneir Saeed EID Electrical and Electronics Engineering Deparment Hasan Kalyoncu University	
Jury Member	Asst. Prof. Dr. Kadir Sercan BAYRAM Electrical and Electronics Engineering Deparment Hasan Kalyoncu University	
Jury Member	Asst. Prof. Dr. Burhan BEZEKÇİ Electrical and Electronics Engineering Deparment Kilis 7 Aralık University	

This thesis is accepted by the jury members selected by the institute management board and approved by the institute management board.

Prof. Dr. Mehmet KARPUZCU
Director

I hereby declare that all information in this document has been obtained and presented in accordance with academic rules and ethical conduct. I also declare that, as required by these rules and conduct, I have fully cited and referenced all material and results that are not original to this work.

Buray Eray TANKUT

ABSTRACT

VOLTAGE REGULATION FOR GRID CONNECTED PHOTOVOLTAIC SYSTEMS USING REACTIVE POWER

TANKUT, BURAY ERAY

M.Sc. in Electronics and Computer Engineering.

Supervisor: Dr. Bilal Mouneir Saeed Eid

May 2019, 143 pages

Nowadays the microgrids with renewable energy sources (RESs) usage and development rapidly increase due to govermentel incentives,dropping the price of DERs and improvement of the technology. The high penetration of DERs espicialy if it is intermittent sources such as Photovoltaic (PV) sources, will effect the stability of the distribution network and causes disturbances for the voltage. To solve this issue the connected PV sources have to contribute to the stability of the distribution network.

The conventional control of distrubition networks generally controlled by human which has many limitations and slow response time, so the it is important to use a real time controllers.Currently, the nine-zone diagram control (NDC) is widely used in the reactive power control (VQC) to keep voltage and reactive power within limits. This NDC plane is divided into nine regions, which determine on-load tap-changer (OLTC) and Static Var Compensators (SVCs) control strategy according the location of real-time measured voltage and reactive power. In this research the already available infrastructures (such as OLTC and SVCs) will be used in coordenation with PV sources to contribute to the voltage regulation via reactive power. The developed solution will elemenate some device failures, save budgets and improve the reialibility for both consumer and distribution network operator

A case study have been carried out on a 8 bus distribution system to illustrate the effectiveness of the proposed method. This study showed how the voltage and reactive power problem can be resolved in a timely and economical way.

A small scale microgrid has been simulated in this thesis and the results helped companseting distrubition grids. Matlab/Simulink have been used to verify the developed controller.

Key Words: Photovoltaic Cell, Reactive Power, Voltage Regulation, DERs

ÖZET

REAKTİF GÜÇ KULLANARAK ŞEBEKEYE BAĞLI FOTOVOLTAİK SİSTEMLER İÇİN GERİLİM REGÜLASYONU

TANKUT, BURAY ERAY

Yüksek Lisanas Tezi, Elektronik Bilgisayar Müh. Bölümü

Tez Yöneticisi: Dr. Bilal Mouneir Saeed Eid

Mayıs 2019, 143 Sayfa

Günümüzde yenilenebilir enerji kaynaklarına sahip mikrogridlerin (RES) kullanımı ve gelişimi, devlet teşvikleri, dağıtılmış enerji kaynaklarının (DER'lerin) fiyatının düşmesi ve teknolojinin gelişmesi nedeniyle hızla artmaktadır. DER'lerin yüksek oranda dağıtım şebekesine nüfuzu, dağıtım ağının kararlılığını etkileyerek voltaj dalgalanmalrına neden olmaktadır. Bu sorunu çözmek için DERlerin dağıtım ağının istikrarına yapacağı etkiler izlenmelidir.

Dağıtım ağları genel olarak insan kontrolünde çalışır bu durum yavaş tepki süresi başta olmak üzere bir sürü sıkıntı ortaya çıkarır, bu nedenle gerçek zamanlı kontrol cihazlarının kullanılması önemlidir. Şu anda, dokuz bölgeli diyagram kontrolü (NDC) reaktif güç kontrolünde yaygın olarak kullanılmaktadır. (VQC) voltajı ve reaktif gücü sınırlar içinde tutınak için dokuz bölgeye ayrılmış bir düzlem öngörülmüştür. Bu NDC düzlemi, yük kademe değiştiricisi (OLTC) ve statik reaktif güç kompensatörleri kullanarak (SVC'ler) kontrol stratejisini gerçek zamanlı ölçülen gerilimin ve reaktif gücün konumuna göre belirleyen dokuz bölgeye ayrılmıştır. Bu araştırmada hali hazırda mevcut olan altyapılar (OLTC ve SVC'ler gibi) reaktif güç ve voltaj regülasyonunda PV kaynakları ile koordinasyonlu bir şekilde kullanılacaktır. Geliştirilen çözüm, bazı cihaz arızalarını ortadan kaldıracak, bütçelerden tasarruf sağlayacak ve hem tüketici hem de dağıtım ağı operatörü için yeniden uygunluğu artıracaktır.

Önerilen yöntemin etkinliğini göstermek için 8 bus içeren bir dağıtım sistemi üzerinde bir vaka çalışması yapılmıştır. Bu çalışma, gerilim ve reaktif güç sorununun zamanında ve ekonomik şekilde nasıl çözülebileceğini göstermiştir. Geliştirilmiş kontrol cihazını doğrulamak için Matlab / Simulink kullanılacaktır.

Anahtar Kelimeler: Fotovoltaik Hücre, Reaktif Güç, Voltaj Regülasyonu

ACKNOWLEDGEMENTS

I would like to express my deepest gratitude to my supervisor **Dr. Bilal Mouneir Saeed Eid**, not only for his guidance, suggestions and criticisms but also for his endless encouragements and confidence in me. His positive attitudes made the problems endurable.

TABLE OF CONTENTS

LIST OF TABLES

LIST OF FIGURES

LIST OF ABBREVIATIONS

DERs	: Distributed Energy Resources
PV	: Photovoltaic
SVC	: Static Var Compensator
OLTC	: On Load Tap Changer
DG	: Distribution Grid
MG	: Microgrid
AC	: Alternating Current
DC	: Direct Current
MPPT	: Maximum Power Point Tracking
CBs	: Capacitor Banks
MW	: Mega Watt
VA	: Volt Amper
VAr	: Volt Amper Reactive
MPP	:Maximum Power Point

CHAPTER 1

INTRODUCTION

1.1. Background

Energy is one of the fundamentals of existence and the demand for energy in the world gradually increases. The electrical energy is produced by using such resources as chemical (fossil fuels), nuclear sources, gravitational fields (tidal waves), wind power and solar power. The block diagram for producing the electrical energy is shown in Figure 1.1 (L. Freris, and D. Infield, 2008).

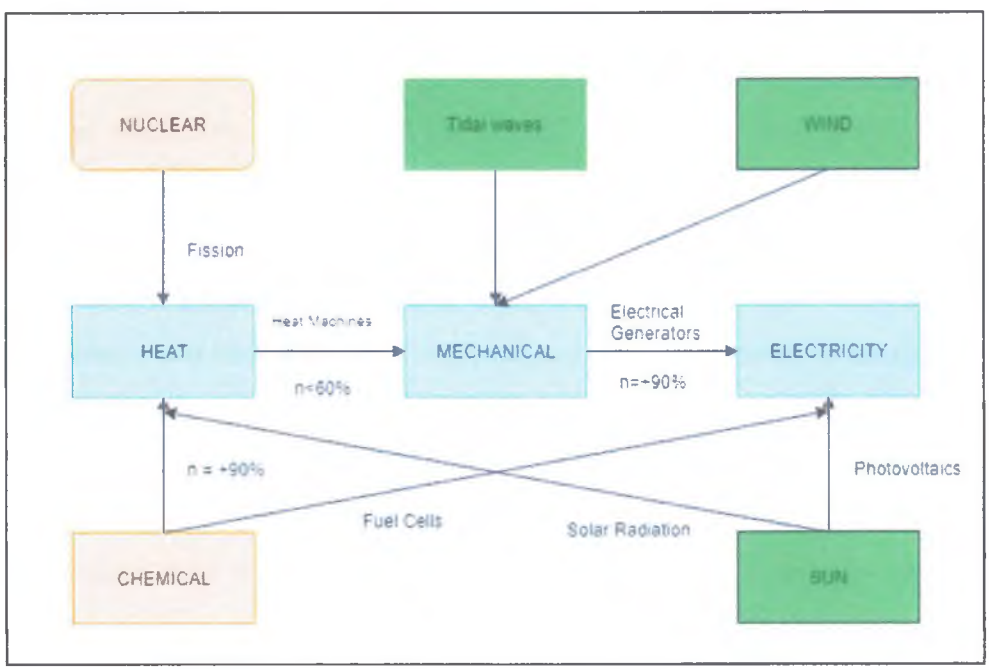

Figure 1.1. The energy conversion of different energy sources to electrical energy

Most of the electrical power is produced from chemical and fossil sources such as petroleum and natural gas. It is known that the development of these sources in nature takes a long time. And the rapid consumption of fossil fuels constitutes negative effects on the environment and human health. The developing technology and the industrial production increase the energy consumption. And the likelihood of

a possible energy crisis also increases. The International Energy Agency (IEA) estimates that the demand for energy in the world will increase with an amount of 55% by the year 2030, and the fossil fuels would take part in this increase with an amount of 84% (A. Goldthau, 2008). In this context, the depletion of the fossil-based fuels increases, the concerns over the global warming and leads people towards finding alternative energy sources.

Solar, wind, geothermal and wave energies can be given as examples of alternative energy sources. The solar energy which is one of the alternative energy sources is a result of the fusion reactions that takes place in the Sun. The radiation that comes out of these reactions is named as solar energy. About half of the solar power reaches to earth passing through the atmosphere, resulting in the increase of the temperature of the Earth and the continuation of life. As a result of the variation in the temperature, the wind and the movements in the ocean occurs. The amount of the solar power s about 1370W/m^2 just outside of atmosphere and between 0 and 1100 W/m^2 at the surface of the Earth. In this context, it can be said that even a small portion of the energy that reaches to the Earth is more than the total energy consumption. The literature shows that the studies for producing electrical energy with solar energy increases after 1970's. The eco-friendly solar energy systems which is also named as photovoltaic (PV) systems, has been less expensive over the last technologic developments and it had made itself accepted as a new and renewable energy source.

The known energies in the world convert into different energy sources through different conversion processes. The sources such as the Sun, tide and the center of the world constitutes a source for energies such as PV, wind, tide, geothermal and other renewable energy sources. The technologies that are used in these processes are shown Figure 1.2 (M.K. Daugherty, and V.R. Carter, 2010).

Turkey is more advantageous than many other countries in terms of energy potential when its geographical location is considered. In a study that has been conducted with the data of "the reception of light and amount of light" that is obtained from the National Meteorology Affairs (DMİ), it is shown that the light reception time in Turkey is 7.2 hours per day which is equal to 2640 hours per year and the amount of light is 3.6kWh/m^2 which is equal to 1311kWh/m^2 (H., Erdoğan, et al., 2009) E.İ.G.

(Müdürlüğü, and U.E.T. 1997). The solar energy map of Turkey has been announced according to the data from DMİ and it has been released in the General Directorate of Electric Power Resources Survey and Development Administration (EİEİ). After 2008 the measurements for the reception of light and the amount of light showed that the yearly reception of light duration is about 2740 hours and the received amount of light daily is measured to be 4.14 kWh/m^2. Also, the most amount of electricity is produced from sunlight is produced in June. The literature shows that in our country there is an area of 4.600 km^2 that is suitable for electrical energy production (A. Bedeloğlu, A. Demir, and Y. Bozkurt, 2010).

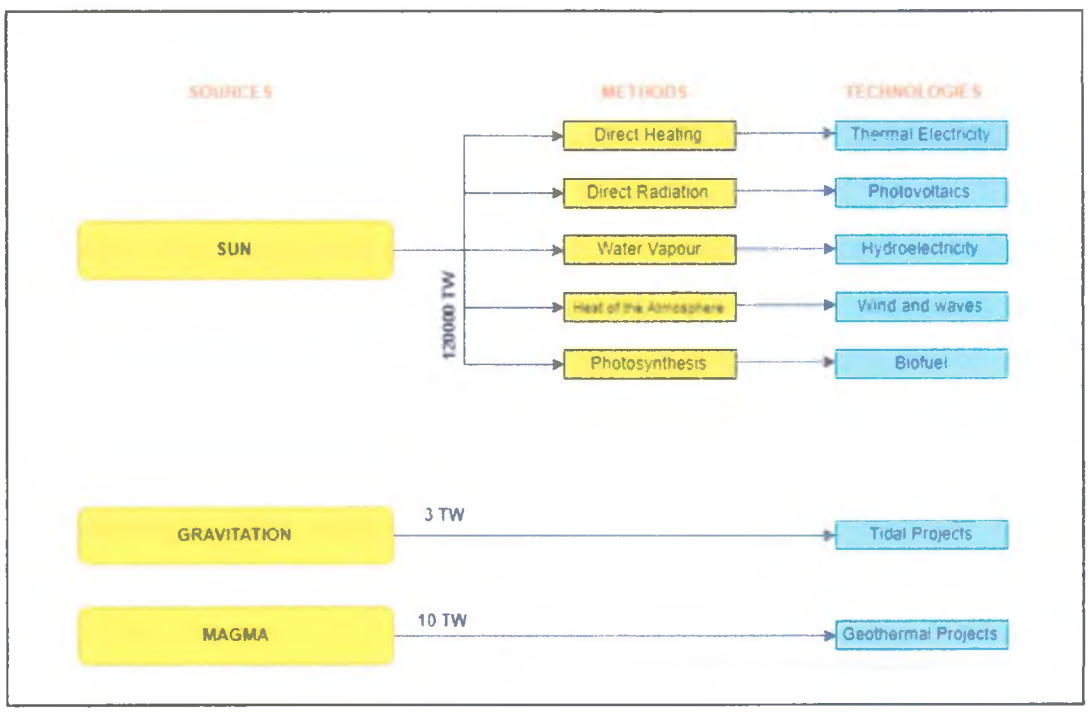

Figure 1.2. Renewable energy formation

The increase in the demand in energy may cause shortages. This situation can be explained with physical and economic reasons such as the power loss over the energy transmission to the further locations, lack of investments even though the demand is high, and the unbalanced power distribution.

The DER units can be used for reducing the distance between the source and the load and the reactive power consumption to increase the power and voltage quality. They can also eliminate the demand for energy in the transmission and distribution lines

and decrease the line losses. But the controlling of the Voltage Source Inverter (VSI) shows different results when only one DER is used and multiple DERs are used. Only one DER can be controlled with one Current Control Strategy (CCS). A grid that has multiple DERs need a more rapid adjustment for having multiple production characteristics and capacity (M. Meiqin, L. Chang, and D. Ming. 2008),(F. Katiraei, and M.R. Iravani, 2006). For this reason, the fulfilment of the real time control needs in the load swings is hard to maintain.

DERs can be explained as the energy production that takes place near a consumer. In a clearer way, it means producing the energy closer to the consumer instead of producing it in a further place. DERs are efficient power sources with less losses and cost. This is a technology that produces energy from different sources depending on the purpose and the location (J. Von Appen,et al., 2013). This can be a facility for producing electricity for a settlement or for a large military base. DERs are connected to the energy lines and they support the energy lines for a more clean and renewable energy (M., Shamshiri, C.K. Gan, and C.W. Tan. 2012). DERs are used to produce electricity for houses and offices as a renewable energy source. In this context, they reduce the release of the hazardous gases such as carbon monoxide. Just like this, a clean energy is produced, and the power losses are minimized. For such advantages, many changes throughout the world has been conducted to adopt more renewable energy sources to the power system (E. Filoğlu, 2011).

Renewable energy sources are known for such problems as voltage regulation during the connection to the grid or during changing the load, and power quality. The following chapter presents the hardships for the voltage regulation.

1.2. Problem Statement

The quality of the energy that is produced, transmitted and distributed in a proximity of the consumer is important. In the production facilities, the most important aspects to consider are the amplitude, frequency and the consistency of the waveform. So, the variations in amplitude, imbalance, and defects in the waveform and inconsistency in the frequency shows a system of a poor quality. Different consumers define "poor quality" in different ways. But in a general way, it is defined as the mis

operation of the devices due to variation in the current, voltage or frequency. The literature shows that many studies have been carried out to enhance the quality in electrical energy (A. Kusko, and M.T. Thompson, 2007).

There are various kinds of PV panels and the studies in this field to increase the quality are still being carried out. The desired current and voltage values can be obtained by connecting different number of PV panels in series or in parallel (B.I. Rani, G.S. Ilango, and C. Nagamani, 2013). But the energy that is obtained from a PV panel is highly dependent on the ambient light and temperature. And this energy is a DC current while the grid demands for an AC power. This results in the need of using DC/DC converters and DC/AC invertors (X. Huijie, et al. 2010), (S. Saridakis, E. Koutroulis, and F. Blaabjerg, 2013). Along with the traditional invertors and convertors, new generation convertors such as SEPIC (S. Saridakis, E. Koutroulis, and F. Blaabjerg, 2013), CUK (S. Chiang, H.-J. Shieh, and M.-C. Chen, 2009), (D. Riawan, and C. Nayar. 2007) and Fly back and Forward (A. Safari, and S. Mekhilef, 2011) are also used. In invertor design, the invertors such as half bridge (B. Vermulst, C. Wijnands, and J. Duarte. 2012), full bridge (A. Testa, et al. 2012), PWM (D.P. Shankar, U. Govindarajan, and K. Karunakaran, 2013) and DC/AC invertors are used. So, the main purpose of this study is to increase the power efficiency.

The problems associated with the power quality can be classified as the long-term or short-term voltage fluctuations, the time dependent changes in the voltage value, the distortions in the sinusoidal waveform and harmonics, flickers and frequency changes. These problems not only cause the increase of the cost of the grid but also cause time and money loss for the customer, thus constituting an economical problem (D. Middleton, I.o. Electrical, and E. Engineers, 1996). There are two committees which were formed by (Institute of Electrical and Electronic Engineers) I.O.f. Standardization, and I.E. Commission, (2001) and IEC (International Electrotechnical Commission) to classify and set the standards for the problems associated with the power (R. Gazete, 2010).

The PV systems are connected to the distribution systems with different voltage values when the installed power (Z.E. Aygen, 2002). In this context the power quality and/or the voltage regulation becomes more important.

The reasons for these are given below

- The sensitive electronic hardware is affected by the imbalance in the grid
- Damaging the integrity of the harmonics by using capacitors and driver circuits to enhance the efficiency of the grid
- The expectancy of the customers in terms of quality of the power when they get more knowledgeable about the concept
- The problems that affect the whole system which arise from interconnected and interdependent devices in the distribution systems.

The voltage drop in the grid is caused by elimination of one or some of the devices in either one of the productions, transmission or distribution systems, thus having difficulties while maintaining the voltage regulation control. This forms a power quality problem. In fact, the energy quality problem is caused by not being able to meet the reactive power needs of the system with an increasing power demand. In this regard, the main cause of the voltage defects should be detected and the needed solution for the problem to be solved need to be specified. Regulating the grid is carried out with the active power (P) and the load angle (δ) while the regulation of the voltage is carried out with the voltage (V) and reactive power (Q) and the relationship among them. The traditional studies concerning the voltage regulation are performed with data of static load or the steady state voltage regulation. The studies that are performed in this context show that the static data is not enough, and the dynamic data should also be supplied.

1.3. Research Objectives

The main goal of this study is to contribute to the involment of DERs, PV systems, to the main grid. The voltage criteria should be applied to DERs that must withstand different conditions.

The main goals of the study are given below

- To increase the DERs' stability under the presence of great penetrations of PV sources.
- To solve the voltage and reactive power problems in time and economically by using the already installed equipment (such as: SVC and OLTC)

1.4. Scope of Work

In this thesis we control voltage level of sytem by using onload tap changer (oltc), static var compensator (svc) and voltage regulation of photovoltaic array with implementation of nine zone diagram algorithm. The simulation has run one day along without any regulation and data has collect from all specific buses and the simulation has run again by controlling with OLTC, SVC, and PV based on datas which have previous result for example we looked at voltage, active and reactive power on known bus and when voltage rises or droped dramatically we change tap of oltc and regulate the voltage also we checked reactive power and try to compensate according to the previous result. Matlab/Simulink has been used as simulation program, the simulation has 8 buses which is; voltage source, OLTC, SVC, PV Farm, ASM and Residential loads,

1.5. Methodology

The method has begun with studying the previous works in this field. The voltage regulations are one of the most vital parts of DERs and they can be controlled. This makes it to a subject to the study. After all these works the system were modeled in MATLAB/Simulink with all its components such as voltage source, OLTC, SVC, PV Farm, ASM and Residential loads and grid. A case study was performed to show the effectivity of the proposed solution in the system. By using a nine zone diagram algorithm. MATLAB/Simulink was used to validate the NDC controller. Many cases such as load change, dynamic reference voltage, voltage regulation. Based on these measurements such as active power, reactive power, RMS voltage value are analyzed. And the data is compared with the outcome of two different cases.

1.6. Thesis Outline

The structure of the thesis consists of the chapters that are given below

Chapter 1; A Quick introduction is given in this chapter

Chapter 2; The literature review is given in and the studies that were performed in the field of voltage regulation in distribution lines was mentioned. And the studies that have a control strategy were summarized.

Chapter 3; In this chapter methodology of thesis given and simulation and circuit are explained briefly.

Chapter 4; Results and discussion are given in this chapter, two case compared each other.

Chapter 5; The evaluation and recommendations were given in this chapter.

CHAPTER II

LITERATURE REVIEW

2.1. Introduction

The first studies in this field has been performed on the structure of the microgrid, the working state when connected to the grid, the existing problems, the ways of utilization of clean energy in the most possible way and the increase the effect of the microgrid in the power system. Katiraei, Iravani (M., Bayat, et al., 2016), has developed an active and reactive power strategy to respond towards the transient currents in the microgrid by using power electronics components. Weiss, Zhong (X. Wang, F. Blaabjerg, and W. Wu, 2014) has designed an H^{∞} repetitive DC-AC converter which reduces the nonlinear harmonic distortions that are originated from the load or the grid itself.

When the microgrid operation is approached as an optimization problem while it is connected to the grid, the goal is to minimize the operation cost in when the grid connection points, the electrical boundary conditions and the production capacity of the microgrid are concerned. The mode in which the sparsely placed production systems are concerned for meeting the energy consumption in the microgrid when they are independent of the main grid is called as the island mode. In the island mode the operation cost is the secondary concern while maintaining nonstop energy supply is the primary goal (G. Diaz,et al., 2010).

Meeting the power demand and supplying the power with high quality are among the goals of a microgrid. But the variations in the active and reactive power of the DERs and the voltage distortions that arise from the nonlinear loads damages the stability of the grid. (Wang, Blaabjerg M. Abdollahi, and S. Bathaee. 2008) has modeled an AC microgrid in MATLAB/Simulink along with the loads and the production plants. With this simulation the possible harmonic distortions that may arise due to the

operation of the system were determined and it was shown that the proposed solutions would work well with the micro grid integration. Diaz, Gonzalez-Moran (H., Kanchev, et al., 2011) has determined the frequency and voltage variations in a power system (or in other words drop coefficients) with the aid of the bifurcation theory. In the proceeding study, the effect of the determined coefficient was investigated in terms of micro grid stability for a microgrid that works in the island mode. A Sliding Mode Control was developed for preventing the variations in a system when there is addition to the DERs to the grid or when some of the DERs are disabled (S., Conti, et al., 2012). This controller is placed inside the DERs and they offer a practical usability.

It is seen that the most recent studies in this field mainly focus on investigating the response of the microgrid to various types of loads and this constitutes a vital point in energy management. Kanchev, Lu (F.S. Gazijahani, et al. 2017), has investigated a system that can produce energy from a PV unit which has a battery unit and aims for residential use. This system was considered as a multipurpose optimization problem. For this an energy management mechanism which aims for minimizing the CO_2 emission and the operation cost. For the utilization of the DER and the energy storage system, an optimization-based approach has been purposed in reference (J., Hernández, et al., 2011) by reducing the effect of the the conventional fuel-based systems in a microgrid. Gazijahani, Hosseinzadeh (G. Chicco, J. Schlabbach, and F. Spertino, 2009), has proposed a scheduling model by taking such properties of the microgrid as stochastic nature and the unpredictability of the power demand into account. But none of the energy management studies have mentioned the effects of the demand response and the electrical device usage on the operation of the microgrid.

In order to preserve the quality of the energy that is used by the consumer it is a must to maintain the consistency of the amplitude and the frequency of the voltage and also the sinusoidal structure of the wave should be preserved. It is known that the variations in the amplitude of the voltage, unstable voltage values and distortions, the variations in the frequency and interrupts are the indication of the poor quality of the power. The output voltage of a PV system varies depending on the weather conditions. This causes instabilities in the grid. For this reason, the possible harmonic

effects that may arise in the grid brings some doubts alongside with the PV systems and investigating these distortions get more and more important every day. PV systems produce DC current while the grid uses AC currents. For this reason, the PV units are connected to the grid via invertors. The components that are used in this connection are components that produce harmonics (S. Ozdemir, N. Altin, and I. Sefa, 2014). In recent years the density of the studies that focus on the quality of the power in PV systems has increased (W.N. Macêdo, and R. Zilles, 2009). These studies are mentioned below.

2.2. Voltage on Distribution Network

The number of studies on improving the energy quality of the PV systems that are connected to the grid is increasing in recent years (M.A. Eltawil, and Z. Zhao, 2010). It is seen in the literature that the measurements were performed at the connection point of a 11kW PV system to the grid in September, October, November (2009) to determine the voltage quality (K. Fekete, Z. Klaic, and L. Majdandzic, 2012). In another study that is also conducted in 2009, the effects of the convertors that are used in the PV systems which are connected to the grid. (A. Pan, Tian, Y., Zhao, H., Yang, X., & Jin, J. 2012).. A 10 kW PV system has been installed in Zagreb in 2011 (K.H. Chua, et al., 2011) and a 6.7 kW PV system has been installed in Shanghai, and the measurements have been carried out to determine the energy quality at the points where the systems were connected to the grid. A PV system that is installed in China has been subjected to an experimental study for the voltage distortions (Y.S. Lim, and J.H. Tang, 2014). In Ref. (M. Ortega, J. Hernández, and O. García, 2013), a PV powerplant that is connected to the grid has been carried out for the harmonics and the flicker effects it may cause in the grid. In Ref. (S.K. Gawre, N. Patidar, and R. Nema, 2012), an experimental study has been performed to determine the flicker effect that arises at the connection point of a 15kW PV system that is installed in 2013 in Malaysia. Another study has been performed in Australia in the same year on the effects of the harmonic effects of the current in the grid and the output power of the invertor (E. Fuchs, and M.A. Masoum, 2011). The problems regarding the power quality has been classified as short-term, medium-term and long-term problems. They can also be classified as the instability in the voltage, distortions in the waveform, long-term/short-term variations in the voltage, flickers in the voltage and

frequency distortions etc. The studies that are in the literature and the classification of these studies are given in Table 2.1 (S. Chattopadhyay, M. Mitra, 2011).

A common problem regarding the voltage quality is named as the voltage imbalance can be defined as the measuring the amplitude and the phase angle different than the value that it is supposed to be. In 3 phase circuits, the voltage imbalance arises when the voltage amplitudes are not the same or when the angles that are between the phases are not 120 degrees. Various solutions regarding these problems are proposed in the literature (K. Basaran, N.S. Cetin, and S. Borekci, 2016).

The system's instability results in the voltage imbalance. Voltage imbalance causes the excess of reactive power in the system, it causes the devices operate with faults and it reduces the usability of the grid .

The causes of the voltage imbalance have been given in Ref. (K. Basaran, N.S. Cetin, and S. Borekci, 2016) as;

- The imbalance of the three phase circuits: In three phase systems, most of the loads are one-phase loads. The voltage needs to be distributed evenly but this prevents the evenly distribution of the voltage.
- The imbalance occurs when the overhead energy lines are not transposed.
- In one-phase systems, the imbalance boundary should be 5%.

Table 2.1. The classification of the problems regarding the power quality

ORDER	CATEGORY	DURATION	VOLTAGE
Short Term Variations	Voltage Sag		
	Instantaneous	0,5 – 30 Period	0,1 - 0,9 pu
	Momentary	30 Period – 3 Sec.	0,1 - 0,9 pu
	Temporary	3 Sec. – 1 Min	0,1 - 0,9 pu
	Voltage Swell		
	Instantaneous	0,5 – 30 Period	1,1 – 1,8 pu
	Momentary	30 Period – 3 Sec.	1,1 – 1,8 pu
	Temporary	3 Sec. – 1 Min	1,1 – 1,8 pu
	Interruption		

	Momentary	0,5 period – 3 Sec.	< 0,1 pu
	Temporary	3 Sec. – 1 Min	< 0,1 pu
Long Term Variations	Interruption	>1 Min	0,0 pu
	Under Voltage	>1 Min	0,8 – 0,9 pu
	Over Voltage	>1 Min	1,1 – 1,2 pu
Transient State	Impulsive		
	Nanoseconds	<50ns	0,4 pu
	Microseconds	50ns – 1 ms	0,8 pu
	Milliseconds	>1 ms	0,4 pu
	Oscillatory		
	Low Frequency	0,3 – 50 ms	
	Medium Frequency	20 Microseconds	
	High Frequency	5 Microseconds	
Distortions in the waveform	DC Offset	Steady State	0 – %0,1
	Harmonics	Steady State	0 – %20
	Interharmonics	Steady State	0 – %2
	Noise	Steady State	%0,1
Voltage Imbalance		Steady State	0,5 – %0,2

Here, the voltage imbalance can be explained with the symmetric components. In this case the imbalance factor (*IF*) is (*IF*):

$$IF = \frac{v^-}{v^+} \tag{2.1}$$

In Equation 2.1'de v^+ is for the positive component and v^- is for the negative component. The voltage imbalance can be found with the aid of this formula.

The decrease of the rms voltage to the range of 10-90 % of the normal value is called a voltage sag and the increase of the voltage value over 110% of the normal value is called a voltage swell. These situations are shown in Figure 2.1 (K. Basaran, N.S. Cetin, and S. Borekci, 2016).

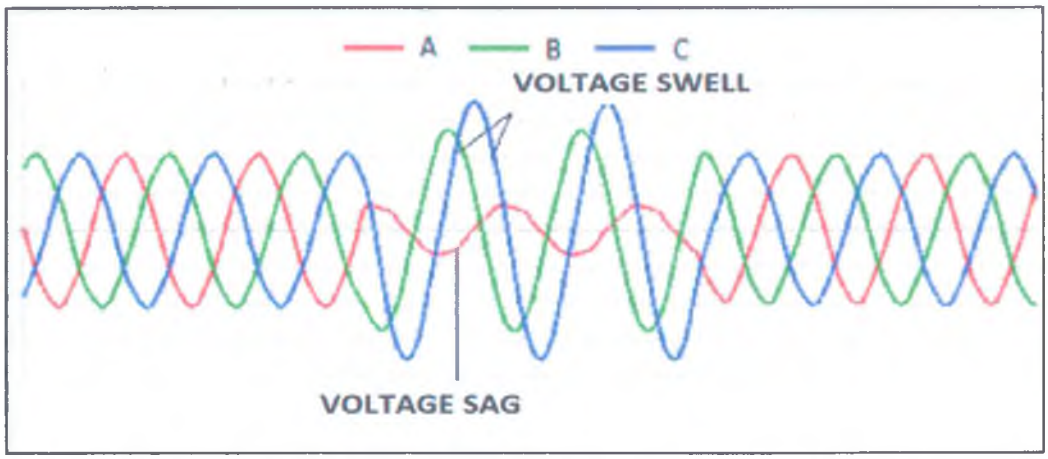

Figure 2.1. A one period of voltage sag and voltage swell in 3 phase systems

The harmonics can be found via the Fourier analysis if the waveform is not in sinusoidal form. Here, the frequency that belongs to every sinusoidal form is equal to the frequency of the distorted wave's frequency with the corresponding integer. In this way every harmonic that belongs to a system can be investigated independently. Fourier analysis is used to solve such problems because of this property (K. Basaran, N.S. Cetin, and S. Borekci, 2016).

Alongside with the PV systems, the use of solar invertors increases as well. The voltage and the current that are produced from a PV system are direct voltage and current. In order to connect this to a grid, invertors are used to convert DC to AC. And this may cause some problems. One of the integration problems are the harmonics and the DC/AC invertors cause this problem (S. Chowdhury, and P. Crossley, 2009).

The literature recommends the use of the stepped voltage regulators (SVR). SVR performs the voltage regulation by changing the step of the coil level. SVR interferes with the system in 32 different states. 16 of these states are downwards and 16 of them are upwards. SVR changes the output voltage by 0.625% at each step. SVRs are available in both ANSI and IEEE standards. There are two types of SVRs that are compatible with both standards, which are type A and type B. Type B is the more common one between these types (A., Baggini, 2008). In type B, the coils that belong to the primary side are connected to the SVR coils through the steps.

2.3. Reactive Power Management

The power flow analysis is needed when designing an electrical grid system in order not to face problems regarding the voltage regulation, to control the capacity of the load in the distribution line and to meet the power demand. Because of the reason that the production capacity of the DERs change during daytime, more complex and different systems are needed to ensure the security and stability of the system (H.B. Çetinkaya, and F. Dumlu, 2013). The control mechanisms that are used so far have met the requirements in terms of maintaining the security and the stability but the ever changing needs and the technology makes the use of the new ways and tools necessary. The recent studies in this field shown that improvement in both the control mechanisms and the tools used in the active grids are necessary (R. Idris, and N. Zaid. 2016). In this context, the studies that are given below can be shown as examples for reactive power compensation and voltage control.

When the system works under a load, the use of the method that is called "on-load tap-changer" is considered as one of the simplest methods to use and this is the most common method in the voltage regulation (H.-C. Chin, 1995). If the voltage value of the system exceeds a pre-determined value, the tap changers interferes with the system and the change the ratio of the transformer. In this context, they are used with the Automatic Voltage Control (AVC).

The shunt capacitors are used in the reactive power management as well. When integrating the shunt capacitors to the system, they should be placed either near the transformer or near the load. Many studies are in the literature about the most efficient ways of using capacitors. These are named heuristic, numerical, analytics, artificial intelligence etc. (W. Kersting, 2009).

One of the components that are used as voltage regulators is called as static voltage compensator (SVC). Also known as static reactive power compensators, these devices are mainly used as reducing the effects of the voltage ripples in the system, compensating the reactive power etc. SVC ensures the safety of the system by controlling the power via the power electronics components at the place where it is

connected to the system. They can induce capacitive and inductive currents to the system to ensure that the bus voltages remain in the limitations (D. Parlak, 2014).

Another SVC structure contains tristor controlled capacitors. The tristors are connected in opposite ways and in parallel. This defines the capacitor group that planned to be connected in either delta or wye connection right after the SVC transformer. These capacitor groups supply reactive power to the grid by performing switching at the desired rate. Delta connected TSC prevents the third harmonic to enter the power system by inverting the component. The delta connected capacitor groups are used in the industrial applications in a wider manner (P. Chopade, et al. 2011).

Reactive power control is referred as VAr (Volts, Ampere, and Reactive) in the literature. VAr is performed to reduce the system losses. It is also used to regulate the reactive power coefficients, to make the coefficient as close to 1 as possible, when the coefficient at the places such as generator-to-transmission and transmission-to-distribution line are concerned. VAr is generally installed where the distribution transformers or where the loads are located. They are connected to the system as constant or switching capacitor groups. The VAr control is ensured with an independent controller. This controller uses some controlling parameters such as;

- Voltage,
- Temperature,
- VAr control,
- Current Control,
- Voltage/Temperature,
- Time,

and the combinations of these parameters are used as controlling parameters. (S., Borlase, 2016).

Until 20 years ago, it was not possible to control the switching capacitors remotely. But the controllers that are available today have the technology that allows mono/bi directional communication. All the parameters were entered to the controller manually when such communication was not available. Today's technology offers a

more efficient controlling over the systems by making it possible to enter different parameters at any desired time. (J.J. Burke, 1994). The cost of the systems that are used today varies from the older technologies. The cost of the sensors, measuring devices etc. may seem like a disadvantage. But when it is considered in terms of the control strategies that belong to 20 years ago, it is realized that the controlling performance was reduced by the unexpected factors when the work plans were adjusted to the expected yearly calendar. The capacitor groups that conducts a time dependent control over the system ensures that the load works better in the unpredictable and varying circumstances (L. Jun-Wei, et al., 2015).

2.4. Nine Zone Diagram Control

The nine-zone diagram control (NDC) is widely used in the reactive power controlling to hold the voltage and the reactive power in the desired limits. Also known as On-load tap changer (OLTC) and the capacitor banks (CBs) control strategy, NDC splits the plane into 9 zones according to the voltage and reactive power that is measured in real time. NDC lessens the work of the distribution line operators and reduces the human induced faults. The traditional nine zone control has many advantages. Operating the same reactive power compensation component frequently, can be mentioned as a disadvantage (Z. Peng-hui, S. Shi-Ping, and H. Yan, 2014).

A new VQC control is proposed to prevent such disadvantage that is mentioned above and to establish a control model and algorithm in Ref. (S.-l. Lei, et al., 2013). In the study, the system moves the OLTCs and CBs minimally to hold the voltage and reactive power values in the desired limit.

In Ref (Y.-z., Zhang, W.-z. XU, and H.-y. FU, 2009), by studying the different aspects of TSC and MSC, the nine-zone control has been developed and it was merged with artificial neural networks controls. The proposed system reduces the regulation of the capacitor banks and the transformer switches to ensure the stability of the system. Ref (W.-Q. Han, et al., 2012) has stated that a second level reactive power control is accepted as a universal voltage and reactive power control. And it

proposed an adjusting strategy for the global voltage of the main station and to the input sensitivity of the reactive.

Ref (H., Erdoğan, et al., 2009) proposes a new reactive power control algorithm based on the real time measurements. It also proposes an optimization algorithm for solving the problems in the existing reactive power integration control algorithm. In this section the studies about the NDC were investigated. The studies above have developed the NDC approach. But there are still some problems. The traditional transformer voltage and the reactive power control strategy ignores the effects of the load characteristics. And it is realized that there are so much to study on in this field.

2.5. Voltage and Frequency Control

It is known that there are loads and DERs that are connected to the grid. It is both possible to connect either load or the DERs to be connected to the grid before the other. Both situations require a different supervision method. When a group of DERs that are connected to the load are started, there arises a voltage instability. Because of this the reason of the voltage distortion and which regions are exposed to problems need to be clearly stated and the solutions that are to be applied need to be clearly stated. The traditional grid regulation studies are performed with the relationship between the active power and the load angle whereas the voltage regulation is performed with the relationship between the voltage and the reactive power. The studies that are performed for the voltage regulation are performed based on the static load data or the steady state voltage regulation. In this context the studies Show that static load data is not enough to explain the dynamic behavior of the voltage regulation and along with it the dynamic load data need to be analyzed in great detail (R.H. Lasseter, 2011).

The voltage and the frequency supervision are the most vital need for the low voltage grid to work in a stable state. The controllable DERs need to be in control of the voltage and frequency if there are drops in both. Because of the decrease in the line impedance there arises a problem about the reactive current and this makes the voltage instable (X., Wang, et al., 2012), (Z., Zhang, et al., 2010). For this the

problems that are in the DERs' connection and work states in distribution grid need to be solved.

2.6. P and Q Power Sharing

The power sharing is important for both in grid and the islanded modes. The sharing is important for supplying each DERs previously determined steady state; F.Z. Peng, Y.W. Li, (2009), the high-power quality performs in the DER limit, (J. Rocabert, et al., 2012), (T.C. Green, and M. Prodanović, 2007), (H. Hanaoka, M. Nagai, and M. Yanagisawa. 2003), low harmonic distortion (S.K. Mazumder, M. Tahir 2008), (E. Barklund, et al., 2008) to operate in a determined voltage range, (C.K. Sao, and P.W. Lehn, 2008), (M.R. Miveh, S. Mirsaeidi 2012) and to supply the minimum power loss for the system. For the micro RES to operate regularly the criteria above should be considered.

2.7. Protection

The protection is one of the most vital problems in a micro grid application. When a micro grid is established, the main issue is to protect the DERs, the load and the line. There are two AC current limiting algorithms available to protect the microgrid from the overcurrent and the grid voltage instabilities (A. Salam, A. Mohamed, 2008). A guided protection plan is recommended for the microgrids. In this plan the overcurrent relays are used for both connected to. The grid and used in the islanded modes to protect the lines. This question may come to minds: how can a protection can be applied for both systems. For this the system need to be connected to the distribution line with a static key to protect the microgrid for the faults that may arise (R.H. Lasseter, 2011).

2.8. Large-Scale PVs in Grid

The importance of PV units in the energy systems is increasing over the last years. Even though the micro renewable energy source units such as PV systems and wind energy systems are used widely due to the easy installation and low cost, the renewable energy sources in larger scales draw attention due to the highly clean energy integration and lower cost per the installed power. Most large-scale projects

integrate different types of DERs and loads. For this, it is needed to study on the larger scale micro RES parameters and components in order to investigate the effects on the low voltage distribution lines (H., Saadat, 1999).

2.9. PV Systems

The PV Batteries are defined as the devices which converts the sunlight that illuminates the surface of the unit to electrical energy via the semiconductor materials they contain. A PV system is obtained by connecting PV solar cells together. The surfaces are in different geometrical forms, and the surface area and thickness are about 25 cm^2 and 0.2-0.4 mm. The PV cells work with the power production capacity of 1-2 W and with the efficiency of 5-25%. This depends on the material that is used in the battery and the structure of the battery (D. Song, et al. 2012).

In the literature it is seen that the semiconductor material that is used to investigate the electrical response of the solar cell has been modeled as a p-n junction element with a nonlinear characteristic. A mathematical model has been developed for analyzing the solar cell. This model contains the mathematical expressions for the input and the output parameters used in the system. Three distinct technologies are used in converting the solar energy into electrical energy, and these are called as PV, concentrated PV and concentrated solar power (CSP) (F. Blaabjerg, and D.M. Ionel, 2017).

2.9.1. PV System Basics

PV systems convert the solar power into electrical energy. It should be noted that even though they convert a small amount of energy into electrical energy they have no negative effects to the environment and they are low cost. They are a very important source of energy. With the advance technology, different materials are used in the PV systems. The inner structure of a PV cell is shown in Figure 2.2

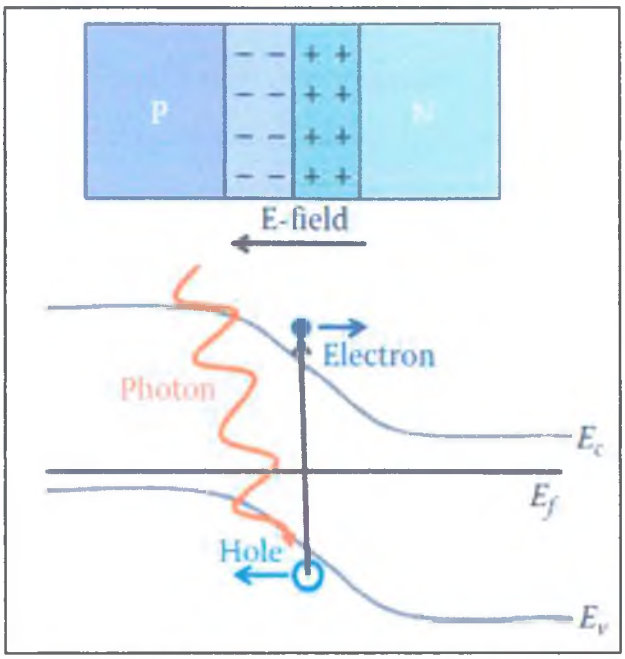

Figure 2.2. The inner structure of a PV cell

Here the main structure of a PV is broken into the main components and structures and they are modeled discretely. In Figure 2.3, the various components in a PV cell that form up the PV are shown.

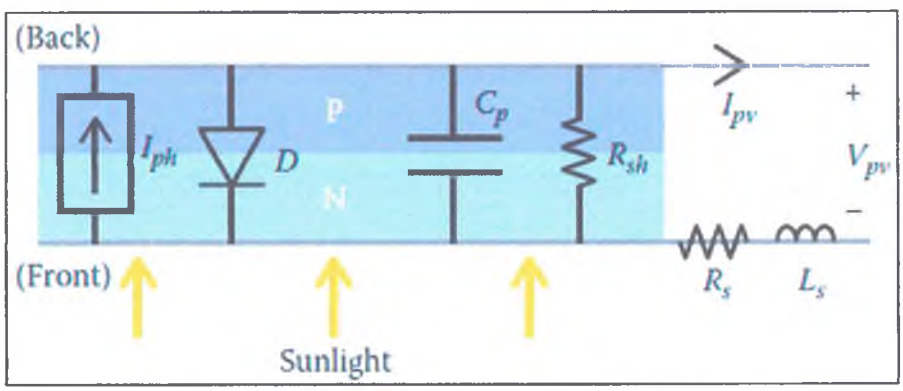

Figure 2.3. The main structure of a PV cell

Even though there are many characteristics that affect how the PV system works, the solar radiation, G (W / m^2), and the temperature, T (°C) are the most important of them. The PV system can be modeled mathematically based on these two parameters. The photocurrent I_{ph}, depends on both radiation and the temperature.

$$I_{ph}(G,T) = \left[I_{scn} + K_i\left(T - T_n\right)\right]\frac{G}{G_n} \tag{2.2}$$

Here

I_{scn}, is the nominal short circuit current

K_i, is the temperature coefficient

G_n, is the nominal solar radiation, usually taken as 1000 W/m^2.

T_n, is the nominal temperature of the PV cell, usually taken as 25 °C.

These values for a PV cell can be obtained from the listed datasheets for the PVs that are commercially available. And the diode current I_d and the diode voltage V_d, can be expressed as an exponential function.

$$I_d(T,V_d) = I_s(T)\left[\exp\left(\frac{V_d}{aV_t(T)}\right)-1\right] \tag{2.3}$$

Here

I_s, is the diode saturation current

a, is the diode coefficient

V_d, is the diode voltage

V_t, is the semiconductor thermal voltage

The diode saturation current depends on the temperature

$$I_s(T) = \frac{I_{scn} + K_i(T - T_n)}{\exp\left(\frac{V_{ocn} + K_v(T - T_n)}{aV_t(T)}\right)-1} \tag{2.4}$$

There

I_{scn} is the nominal short circuit current

K_i is the temperature coefficient

T_n, nominal cell temperature

V_{ocn} nominal open circuit voltage

K_v voltage temperature coefficient

a ideal diode coefficient

V_t thermal voltage

It should be noted that in the ideal model, the diode voltage V_d, and the PV voltage V_{pv} are the same. And the thermal voltage V_t, depends on the temperature T, and it is defined as;

$$V_t(t) = \frac{kT}{q} N_s \tag{2.5}$$

Here

k is the Boltzmann constant (approximately 1.3807×10^{-23} J·K^{-1})

q is the charge of an electron ($1.60217662 \times 10^{-19}$ C)

N_s, is the number of PV cells in the system

Using Kirchhoff's laws as well, we can describe the relationship between I_{pv} and V_{pv} as;

$$I_{pv} = I_{ph}(G,T) - I_d(T,V_{pv}) \tag{2.6}$$

According to these formulas, the ideal current-voltage characteristics is given in Figure 2.4 and the power-voltage characteristics is given in Figure 2.5. In Figures, G = 1000 W/m² and T = 25 °C; VOC: open-circuit voltage; ISC: short-circuit current; MPP: Maximum power point.

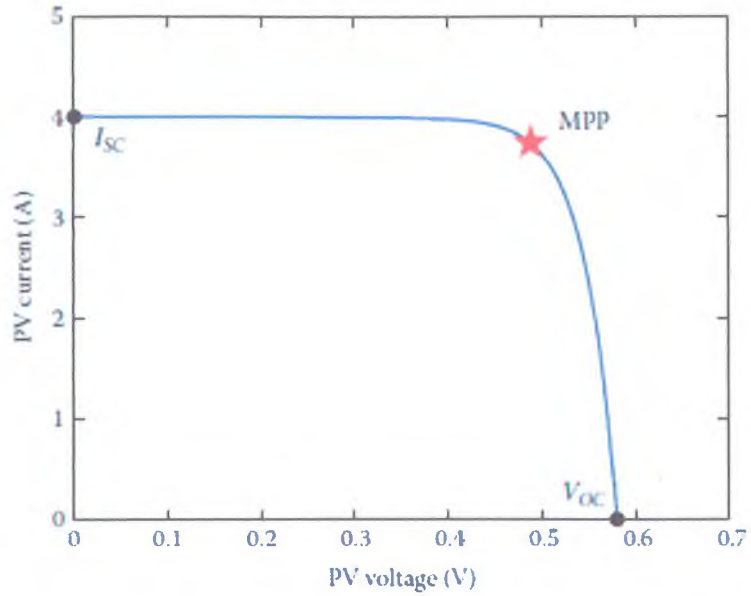

Figure 2.4. I-V curve for a PV cell

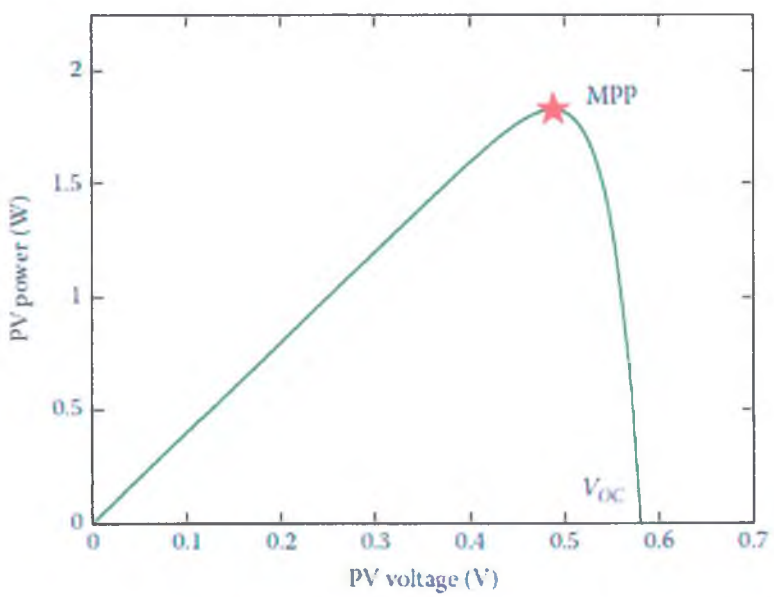

Figure 2.5. W-V curve for a PV cell

2.9.2. PV Panel Structure

In many applications where the PV cells are used, many PV cells are combined to produce more power. In such applications, the cells can be connected in series, in parallel or in both, depending on the situation. If the cells are connected in series, the voltages are added up. If they are connected in parallel, the currents are added up.

One single cell can produce a voltage of 0.5 volts depending on the surface area. The PV cells are connected in series to produce higher voltages. In the commercial uses, it is seen that 72-96 cells are connected in series. The resulting voltage is between 30 and 60 Volts. A similar PV panel configuration is shown in Figure 2.6. Each diode that is used in 24 cells is used to bypass the problems in the lower line.

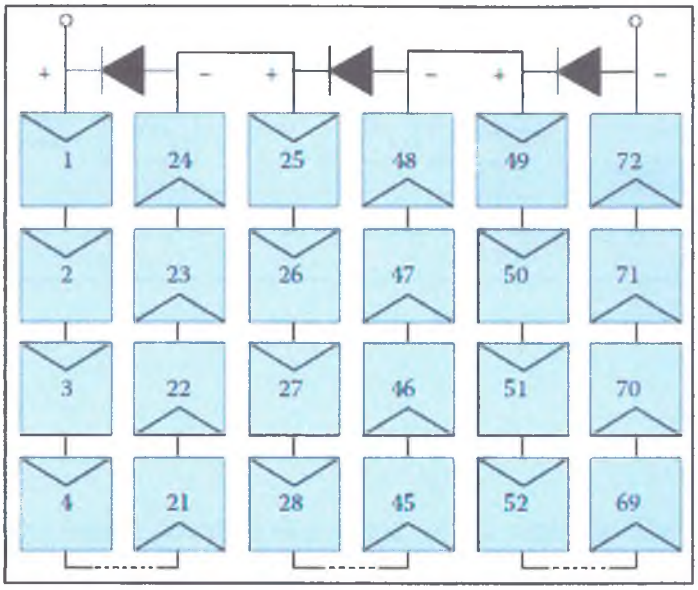

Figure 2.6. PV panel configuration

2.9.3. Three Phase PV Panel Structure

The voltage that is obtained from a PV cell group is a direct voltage (DC). This voltage is converted into AC while it is integrated into a grid. During this conversion process, the components that are known as invertors and/or convertors are used. These components are designed so that they can convert a DC voltage into a 3-phase AC voltage. The general scheme of the 3-phase convertors is shown in Figure 2.7.

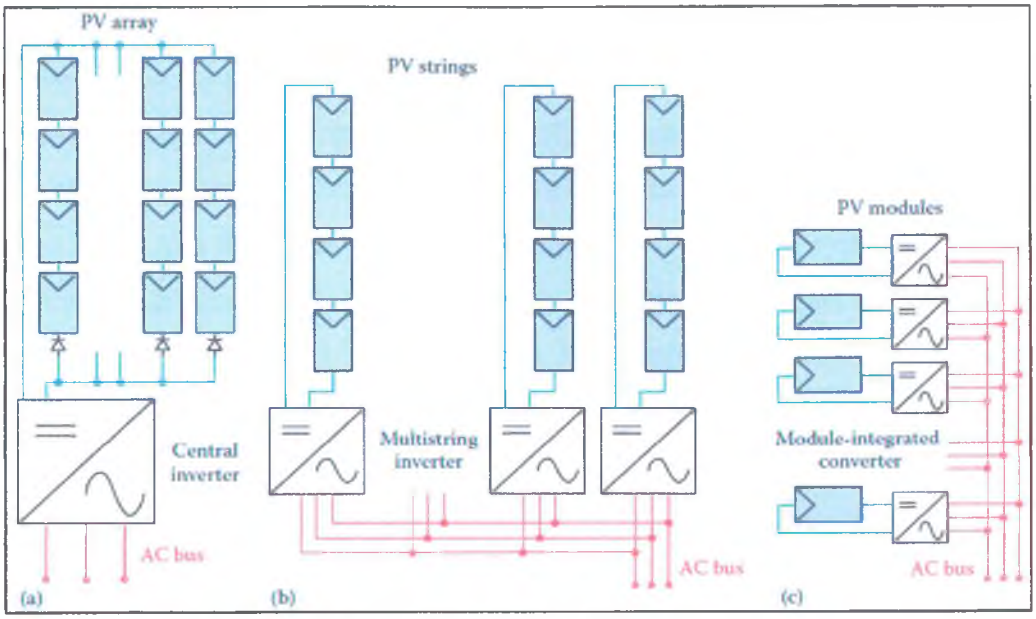

Figure 2.7. The scheme of the 3-phase convertors

2.9.4. Structure of Grid-Connected Photovoltaic Systems

In PV systems, the output power is dependent on the sunlight. The variations in the output power of the PV is time dependent. In this case, the PV systems that are connected to the grid cause some harmonic distortions, so investigating these systems constitutes a big importance. The single line diagram of a PV system that is connected to the grid is given in Figure 2.8 (Y. Du, et al., 2013).

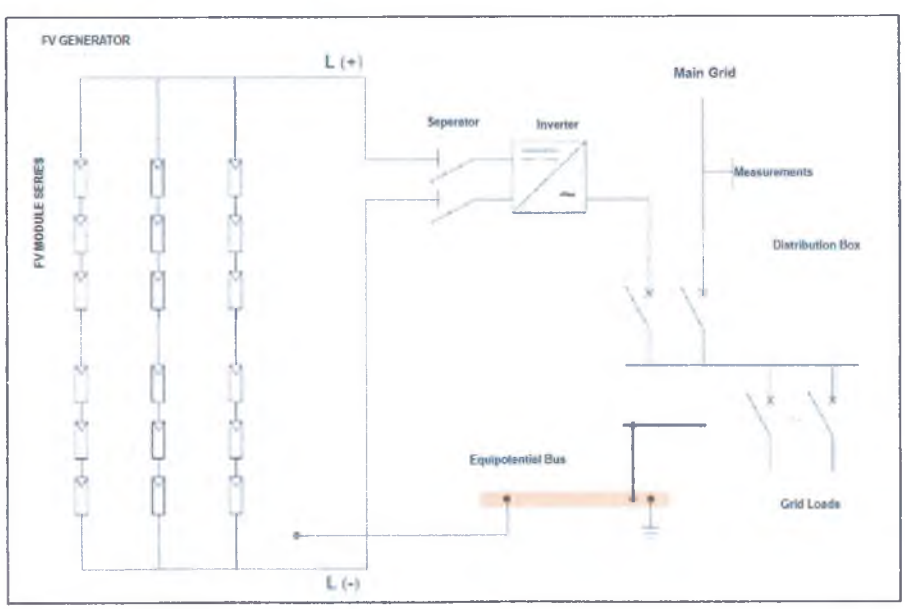

Figure 2.8. The single line diagram of a PV system that is connected to the grid

It is known that the current that one acquires from a PV system is a DC current whereas the energy that is used in the grid is AC in general. That is why the inverters are used to connect the PV units to the grid. This is shown in Figure 2.8. The figure shows that the connection between the invertor and the grid is established with fuses and breakers. And this situation is in a distribution box. In such systems with a grid connection, a ground bus is used to secure the PV system and other equipment. This way the system is grounded. It should not be forgotten that the inverters are made up from electronic devices and just like any other device it may produce harmonics.

2.10. Energy Conversion Systems

The power electronics components are used in the microgrids to control the power flow and to convert the power into the correct AC or the DC form. The schematic representation of a microgrid is shown in Figure 2.9.

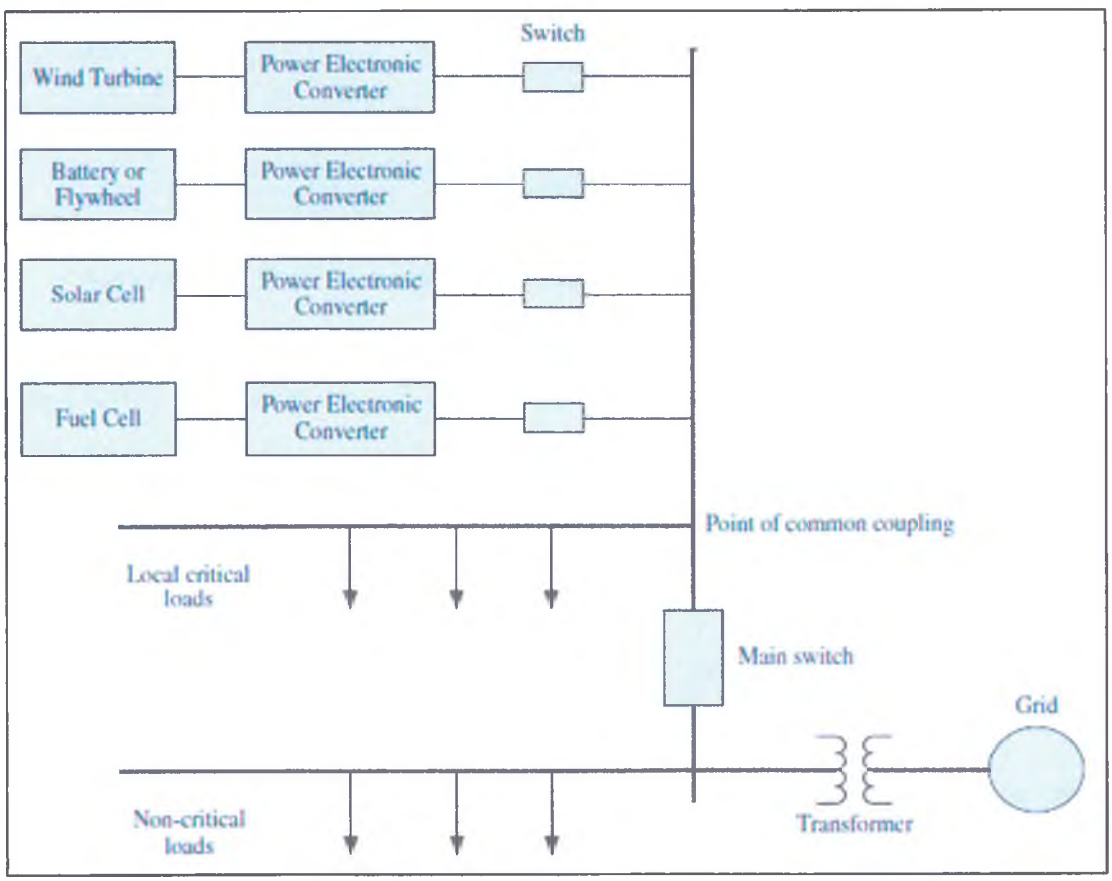

Figure 2.9. The schematic representation of a microgrid

Typically, such converters are in the range of 100 W and 300 W. Depending on the application, they consist of DC-DC or DC-AC conversion units. The output power of the module can increase if a DC-DC conversion unit is connected between the PV and the load. The voltage value of the inverter on the load side is different than the voltage value on the PV side. If the PV is operated under a constant voltage, the output power increase, as it is seen in Figure 2.10, when the previous PV units with an ohmic load are taken as example.

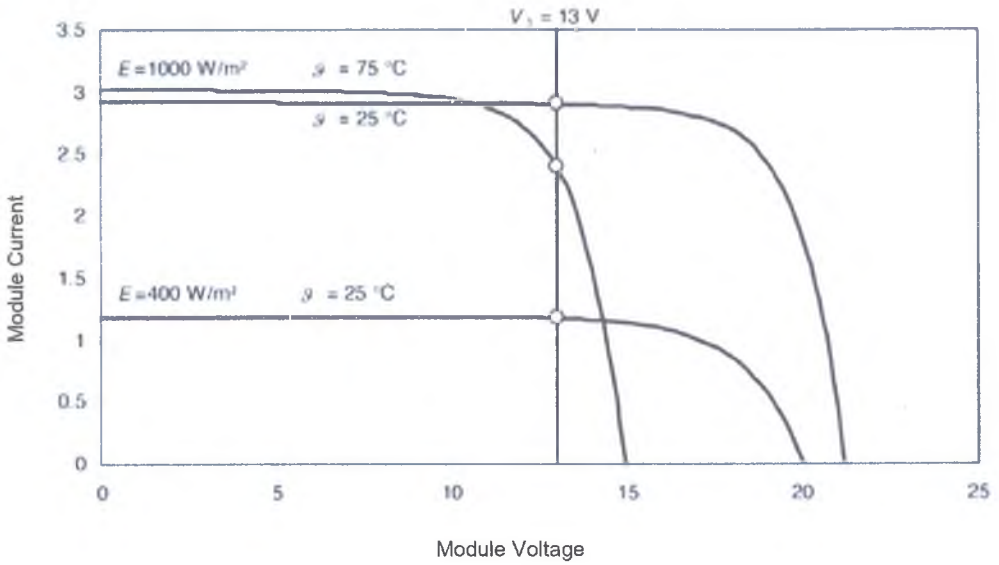

Figure 2.10. The I-V curve of a PV under three different operation points

The DC-DC converters that are produced have the efficiency rate that are more than 90%. Only a small amount of the power that is produced is converted into heat and wasted away. A converter which has the inputs P1 and P2 and the efficiency of 100% can be described as (V. Quaschning, 2016);

$$P_1 = I_1 V_1 = I_2 V_2 = P_2 \tag{2.7}$$

The 3-phase converters are key components in the grid integrations. Aside from classical half bridge and the H bridge topologies, there are many other topologies that are available in the 1-phase systems and some of them are used in the industry. (R. González, et al., 2007). The two levels (2L), three levels (3L), Neutral point

clamp (NPC) and cascading H-bridge (CHB) converter topologies (S.M. Sharkh, et al., 2014).

2.11. Micro-RES Point of Connection with Grid

Electrical energy lines and line equipment have different voltage values, active and reactive power flow. To connect a micro RES system to the grid the critical lines and the line equipment need to be specified. If the micro RES connection is specified with the correct path, the power loss of the grid will be reduced, and the grid stability is increased. In the literature it is shown that the Standard IEEE 30-bus test systems represent the grid. The activity of the micro RES connection should be investigated according to the IEEE 30-bus test systems.

2.12. Summary

In this section, the studies in the literature that are related to our keywords were summarized. The key words are; the PV systems that are connected to grid, the problems in the energy transmission lines and the solutions, microgrid connection points, problems and solutions. Among the problems regarding the operation of the microgrids, there are problems such as; voltage regulation, high power sharing which ensures minimum power losses, harmonic distortions are present.

In the grids where energy sources are many and especially consist of PV systems, the problems regarding the voltage are more serious and sudden. This improves the importance of the grid management.

Also the section above consists of the necessary formulations regarding the PV systems and the components of the PV systems that are connected to the grid. The equations that are defined here will be used in the simulation process.

CHAPTER III

METHODOLOGY

3.1. Introduction

When the most recent studies in the field are investigated, it is realized that many studies that focus on the connection points of the DERs which also include the PV systems to the main grid. The PV systems are produced in either on-grid form or off-grid form. The mathematical equations regarding the PV systems that are connected to the grid and all the components are given below. These equations will be used in the simulation process.

3.2. Reactive Power

The energy system is ever-changing and it has a complex structure. An electrical system is a system that is made of the combination of the subsystems. These subsystems are the generators, transformers, electrical lines and many types of consumers. To investigate the effect of the reactive power in the system one should begin with the power that flows in the transmission and distribution lines. The instantaneous power is the product of the current and the voltage as given in the equation (N.M., Tabatabaei, et al., 2017):

$$p(t) = u(t)i(t) \tag{3.1}$$

Two components can be mentioned here.

- The active power (P), in Watts (W):

$$P = UI\cos\theta[W] \tag{3.2}$$

- The reactive power (Q), in VAr:

$$Q = UI\sin\theta[VAr] \tag{3.3}$$

U and I represent the voltage and the current values in RMS respectively. θ represents the phase angle. The combination of the active and the reactive power gives the apparent power (S) in VA.

$$S = P + jQ[VA] \tag{3.4}$$

In a power system there are electrical components that produce or draw reactive power (F.A. Viawan, and D. Karlsson. 2008) such as synchronous machines, loads, transmission lines etc.

3.3. Voltage and Reactive Power Control Strategy

The traditional transformer voltage and the reactive power control strategy does not put the effect of the load characteristics into consideration. Nine-zone diagram is used widely to establish the voltage regulation and to maintain the balance of the voltage by changing the states of the power balancing equipment (L. Jun-Wei, et al., 2015).

3.3.1. Nine Zone Diagram

The nine-zone diagram is used widely to stabilize the transformer stability and the reactive voltage stability within the transformer's center. The control aim is to adjust the amount of the reactive power compensation device a s shown in Figure 3.1, or to adjust the transformer tap as shown in Figure 3.2.

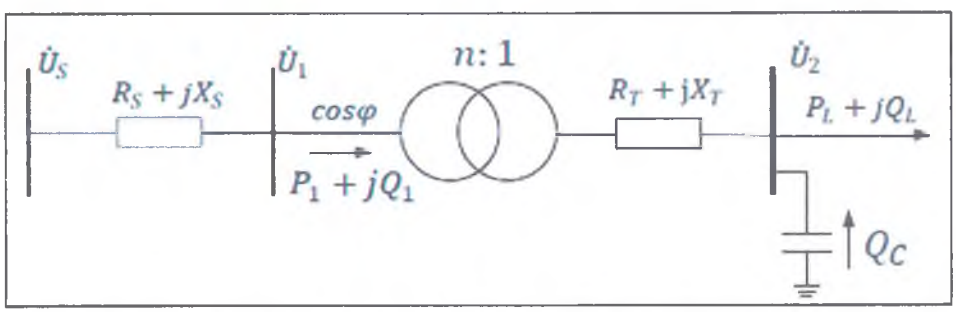

Figure 3.1. The equivalent circuit of the transformer circuit

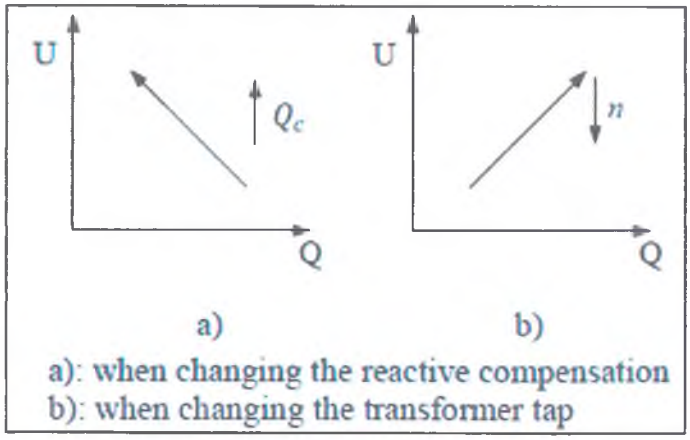

Figure 3.2. The effects of different control equipment

According to the Q1 and U2 data line voltage, the coordinate system is divided into nine zones as shown in Figure 3.3. With this technique, when Q1 and U2 are in undesired regions it is possible to hold them in the desired regions.

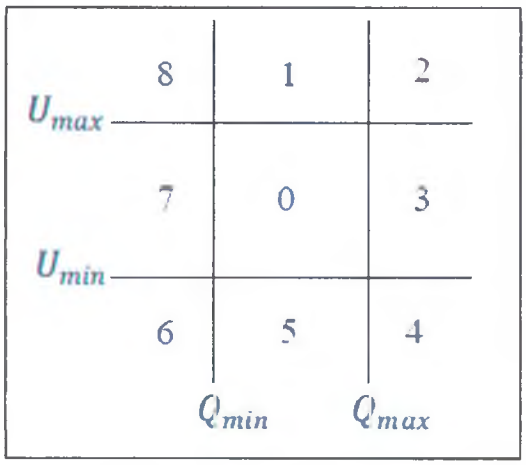

Figure 3.3. Nine zone diagram

The rectifying ways in different zones are given as:

- Zone 0; It is the normal zone and no operations are performed here
- Zone 1; In this zone, the tuning tap adjusting should be done. The capacitors should be deactivated when the voltage is in the upper limit and the tap is not needed.
- Zone 2; In this zone the tap needs to be adjusted to take the voltage to the desired level. If the power factor reaches the limit, the capacitors need to be activated.

- Zone 3; In this zone the capacitors need to be activated. If the reactive power is not within the limits when all the capacitors are activated, the transformer tap needs to be adjusted.
- Zone 4; In this zone to make the power factor more qualified, the capacitors need to be activated. If the voltage reaches the limits, the transformer tap needs to be adjusted.
- Zone 5; In this zone the adjustment reinforcements are performed. If voltage cannot satisfy the need and reaches the limit, the capacitors need to be adjusted.
- Zone 6; In this region the tap needs to be adjusted to make the voltage value reach the desired level. If the power factor reaches the limit, the capacitors need to be deactivated.
- Zone 7; In this zone the capacitors need to be deactivated and if the reactive power doesn't satisfy the needs even after all the capacitors are deactivated, the tap needs to be adjusted.
- Zone 8; The capacitors need to be disconnected to get the power factor in the desired level. If the voltage reaches the limit, tap needs to be adjusted.

3.4. Simulation Progress

The simulation consists of voltage source as generator and PV farm and SVC, OLTC, Loads as residential place, asynchronous motor as fabrication loads, distributions lines and diesel generator, step up and step down transformers and isolating transformers, V-I measurements blocks.

3.4.1. Voltage Source

This block was used to generate a three-phase sinusoidal voltage with time-varying parameters. 120 kV was selected as the voltage level and this block was used in swing mode (Figure 3.4).

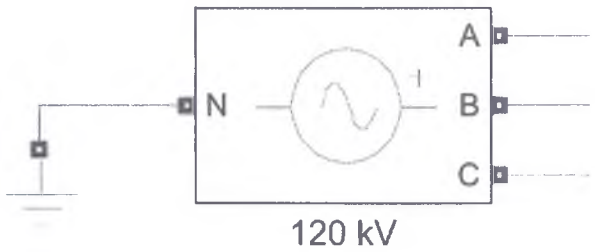

Figure 3.4. Block of voltage source

3.4.2. PV Farm

This block works as a PV farm having %10 efficiency and 80.000 m^2 area. The product of efficiency, the area covered by PV farm and the irradiance in W/m^2 gives the power generated by PV farm. This block was used with 8 MW peak power (Figure 3.5).

Figure 3.5. Block of PV farm

3.4.3. Static Var Compensator

The SVC regulates voltage at its terminals by controlling the amount of reactive power injected into or absorbed from the power system (Figure 3.6). When the system voltage is low, the SVC generates reactive power (SVC capacitive) and when the system voltage is high, it absorbs reactive power (SVC inductive). The variation of reactive power was performed by switching three-phase capacitor banks and inductor banks connected on the secondary side of a coupling transformer. Each

capacitor bank is switched on and off by three thyristor switches (Thyristor Switched Capacitor - TSC). Reactors are either switched on or off.

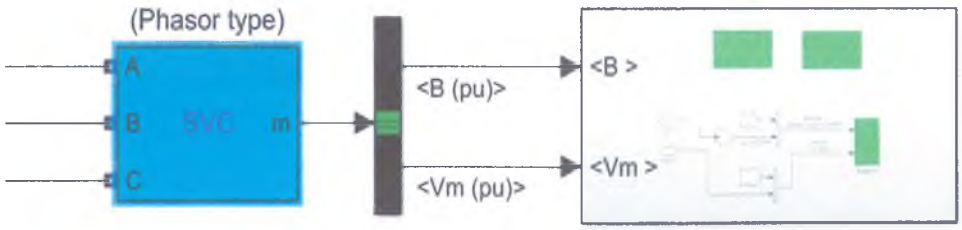

Figure 3.6. Block of SVC

As long as the SVC susceptance B stays within the maximum and minimum susceptance values imposed by the total reactive power of capacitor banks (Bc_{max}) and reactor banks (Bl_{max}), the voltage is regulated at the reference voltage V_{ref}. However, a voltage droop is normally used (usually between 1% and 4% at maximum reactive power output), and the V-I characteristic has the slope indicated in the Figure 3.7.

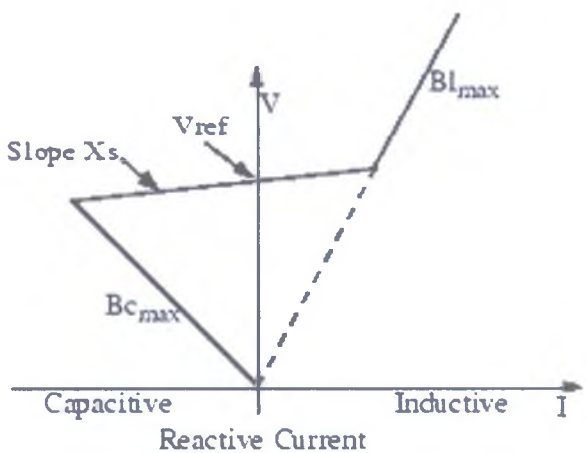

Figure 3.7. V-I characteristic of SVC

The V-I characteristic is described by the following three equations:

$$V = V_{ref} + X_s I \tag{3.5}$$

Equation (3.5) if SVC is in reguletion range ($-Bc_{max} < B < Bl_{max}$)

$$V = -\frac{I}{Bc_{\max}} \tag{3.6}$$

Equation (3.6) if SVC is fully capacitive ($B = Bc_{max}$)

$$V = \frac{I}{Bl_{\max}} \tag{3.7}$$

Equation (3.7) if SVC is fully inductive ($B = Bl_{maz}$)

where

V: Positive sequence voltage (pu)

I: Reactive current (pu/P_{base}) (I > 0 indicates an inductive current)

X_s: Slope or droop reactance (pu/P_{base})

Bc_{max}: Maximum capacitive susceptance (pu/P_{base}) with all TSCs in service, no TSR or TCR

Bl_{max}: Maximum inductive susceptance (pu/P_{base}) with all TSRs in service or TCRs at full conduction, no TSC

P_{base}: Three-phase base power specified in the block dialog box

3.4.4. On Load Tap Changer

This block is used to model a three-phase two-winding transformer or autotransformer using an On-Load Tap Changer (OLTC) for regulating voltage on a transmission or distribution system (Figure 3.8).

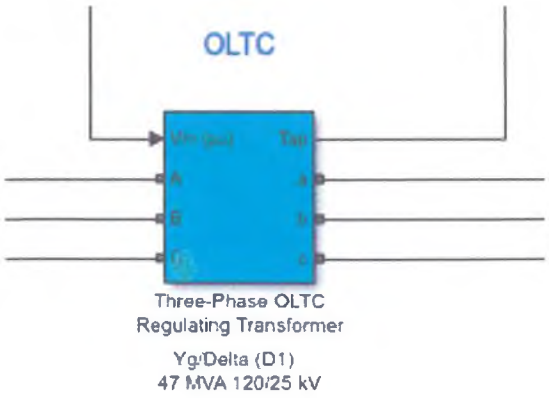

Figure 3.8. Block of 3-phase OLTC

Controlling the voltage in a transmission system mainly affects the reactive power flow, which affects the power transfer limits. Although the regulating transformer does not provide as much flexibility and speed as power-electronics based FACTS, it can be considered as a basic power flow controller. The dynamic performance of the regulating transformer can be enhanced by using a thyristor-based tap changer instead of a mechanical tap changer.

3.4.5. Residental Loads

This block was used as residential loads which allows us to make consumption data changing in every hour. It helps us to make simulation more realistic (Figure 3.9). The 24-hour consumption data graph is given in Figure 3.10.

Figure 3.9. Block of residential loads

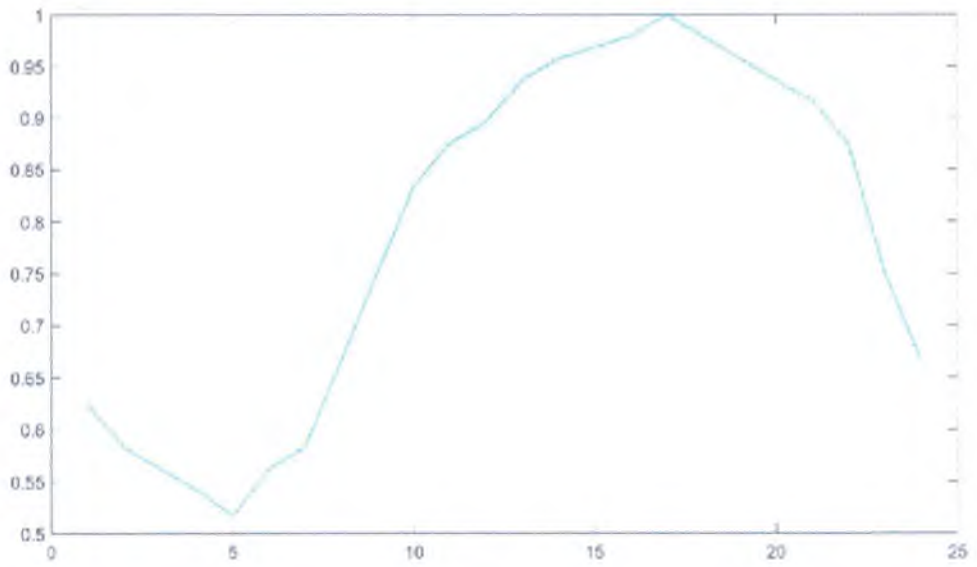

Figure 3.10. 24-hour consumption data

3.4.6. Asynchronous Machine

The ASM block shows a three-phase asynchronous machine (wound rotor, single squirrel-cage, or double squirrel-cage) (Figure 3.11). This block was used to represent the factorial load.

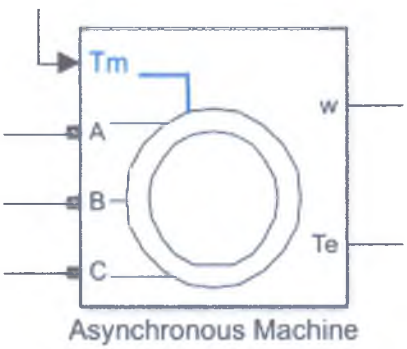

Figure 3.11. Block of ASM

3.4.7. Diesel Generator

In this study, a diesel generator of 15 MW was used as a voltage source. The diesel generator block is shown in Figure 3.12. This block shows the diesel generator, which is a part of the micro grid.

Figure 3.12. Block of diesel generator

3.4.8. Step up-Step Down-Isolating Transformer

25 MVA isolation transformer was used in the study (Figure 3.13). This transformer is used in both isolation and in cases where the voltage must be increased / decreased in the system.

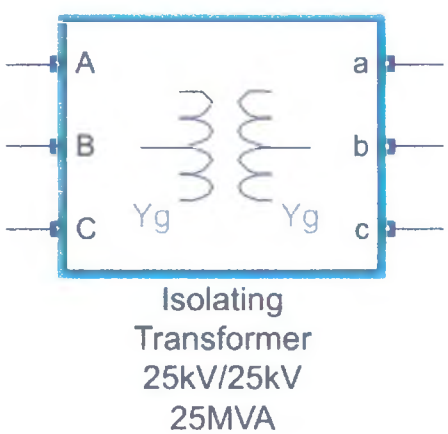

Figure 3.13. Block of 25 MVA Transformer

3.4.9. Lines and Feeders

Mutual Inductance (Z1 – Z0) block representing 3 phases and 30 km was used for lines and the feeders (Figure 3.14). The Three-Phase Mutual Inductance Z1-Z0 block implements a three-phase balanced inductive and resistive impedance with mutual coupling between phases.

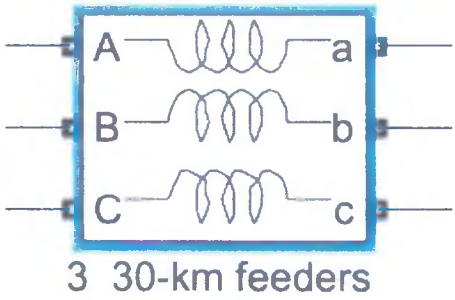

Figure 3.14. Block of 3 phase 30 km feeders

3.4.10. V-I Measurement Blocks

The Three-Phase V-I Measurement block is used to measure instantaneous three-phase voltages and currents in a circuit (Figure 3.15). When connected in series with three-phase elements, it returns the three phase-to-ground or phase-to-phase peak voltages and currents.

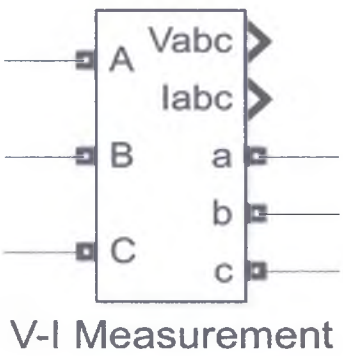

Figure 3.15. V-I measurement block

The block can give output voltages and currents in per unit (pu) values or in volts and amperes. If you choose to measure phase-to-ground voltages in per unit, the block converts the measured voltages based on peak value of nominal phase-to-ground voltage:

$$V_{abc}(pu) = \frac{V_{phase\,to\,ground}(V)}{V_{base}(V)} \tag{3.8}$$

where

$$V_{base} = \frac{V_{nom}(V_{rms})}{\sqrt{3}}\sqrt{2} \tag{3.9}$$

If one chooses to measure currents in per unit, the block converts the measured currents based on the peak value of the nominal current:

$$I_{abc}(pu) = \frac{I_{abc}(A)}{I_{base}(A)} \tag{3.10}$$

where

$$I_{base} = \frac{\sqrt{2}P_{base}}{\sqrt{3}V_{nom}} \tag{3.11}$$

3.4.11. S – P - Q Measurement Block

The Power block outputs total apparent power (S), active power (P) and reactive power (Q) of a three-phase voltage-current phasor signal pair (Figure 3.16).

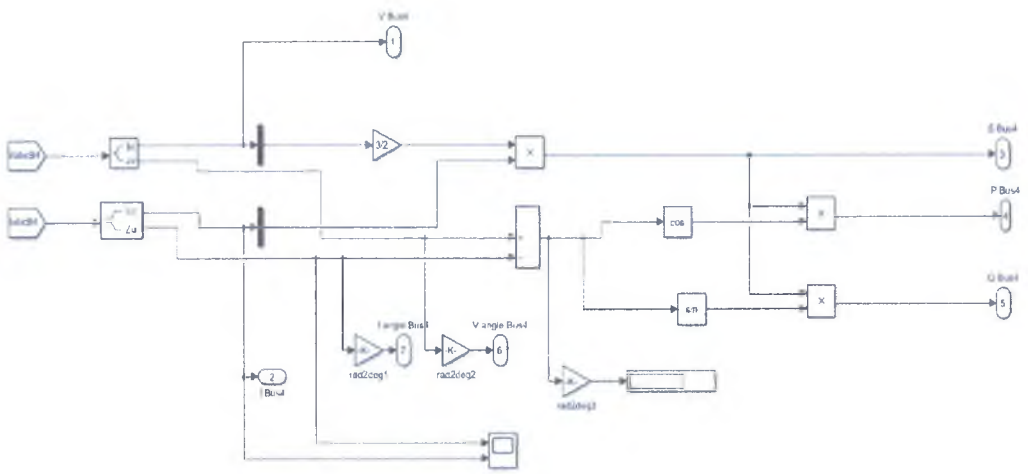

Figure 3.16. S-P-Q measurement block

P and Q are computed as follow

$$P + jQ = \frac{1}{2}\left(V_a I_a^* + V_b I_b^* + V_c I_c^*\right) \tag{3.12}$$

where

I_a^*, I_b^*, I_c^* are the complex conjugates of I_a, I_b and I_c.

The Figure 3.17 shows sign conventions;

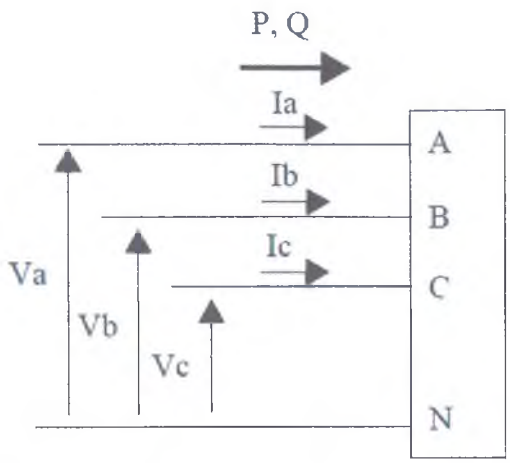

Figure 3.17. Scheme of sign conventions

3.5. Single Line Diagram of Desired system

While the simulation was done, the diagram in Figure 3.18 was followed. According to this diagram, a small scale MG was connected to the 120 kV DG.

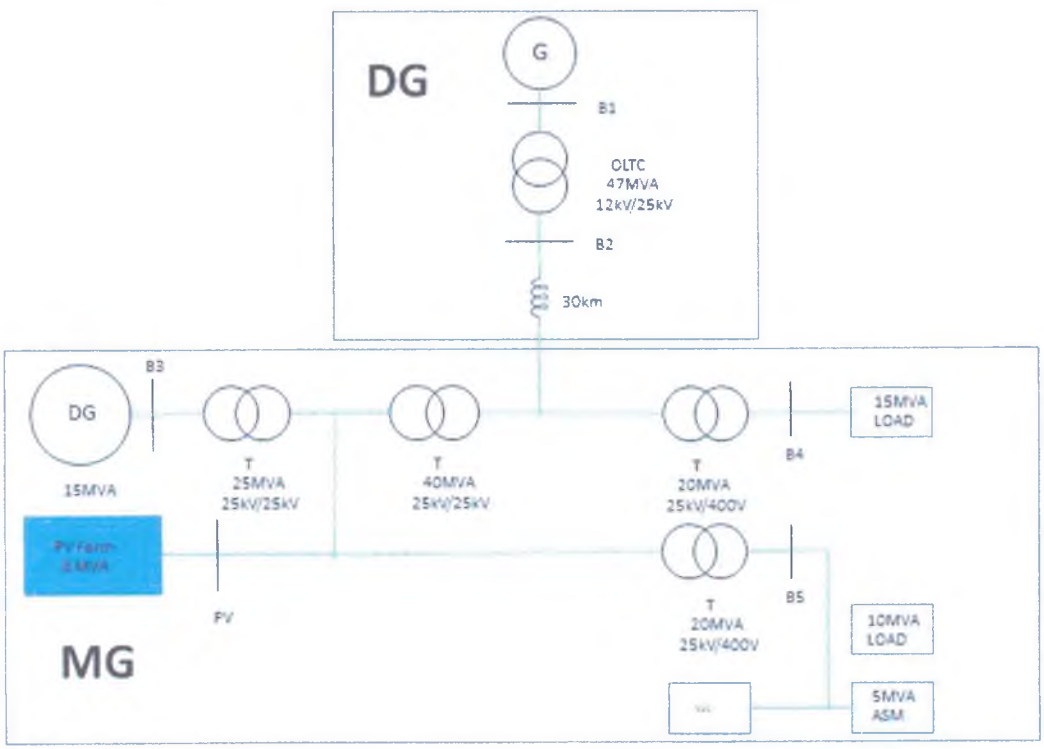

Figure 3.18. Single line diagram of desired system

3.6. Working Principle of Simulation

The basis of the study is based on the following items.

- For simulation of 24 hours, phasor type simulation was used.
- 120 kV and 25 kV distribution lines was used.
- There are 8 buses in simulation and three of them produced energy from which diesel generator (B3), PV Farm (Bus PV), Voltage source (Bus1) and three of them consuming energy which is ASM and residental loads other 2 bus for controlling OLTC and SVC with nine zone diagram.
- The PV farm was also used as a reactive power stabilizer by changing the PV reference voltage.
- For better results, the consumption data was applied to loads for a realistic simulation.
- When the simulation was run for the first time, the checking voltage and reactive power changes had been monitored for 5 hours and this information was used for the controllers on the OLTC and SVC.
- Data were collected from every specific bus to see the changes hourly.
- Two case studies with and without controllers were performed and the results were given in Chapter 4.

The block diagram of the simulation of the study is given in Figure 3.19.

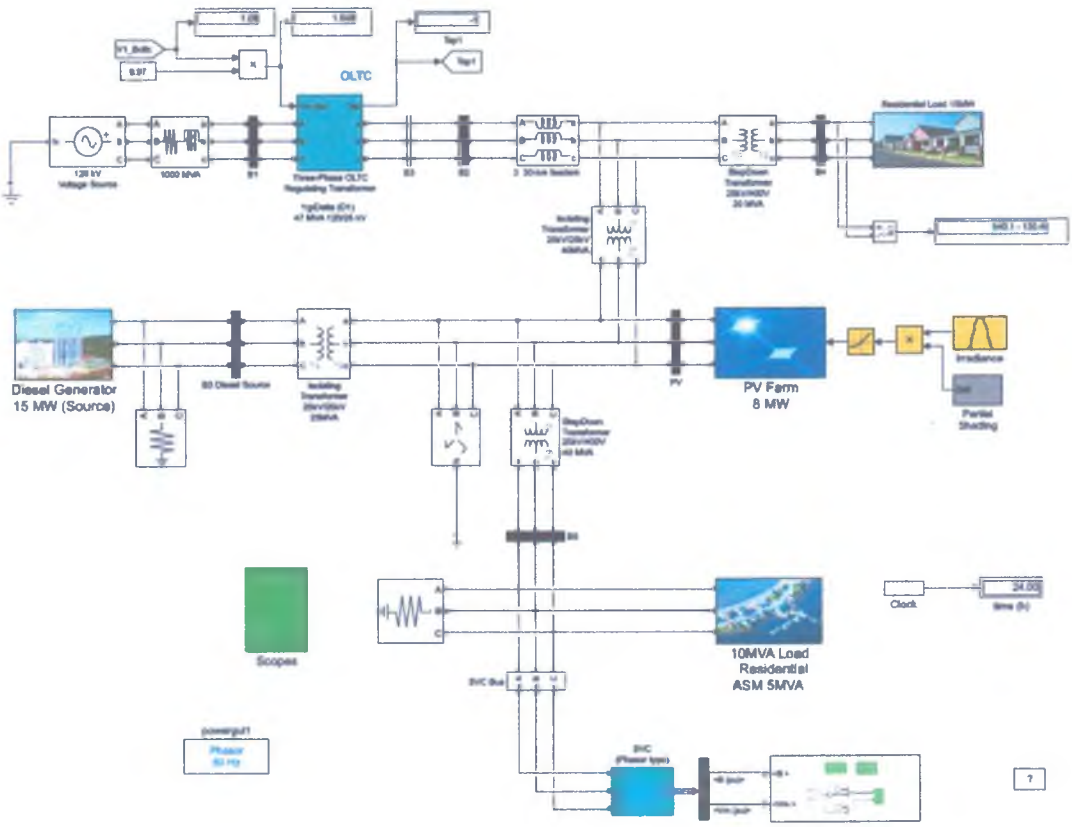

Figure 3.19. Simulation scheme of the study

CHAPTER IV

RESULTS

In this chapter simulation results were presented below in two main cases, one is without control of OLTC and SVC and the other one is effective control of this devices in both cases simulation result extracted in same way for better comparison.

Simulation was run once a day along without any regulation, also we implement consumption data into the simulation to obtain closest value to real life conditions. Consumption data can be seen in every table, on left green section. The following statements may be included regarding the operating status and performance of the system.

For implementing nine zone diagram algorithm there had to be some disturbances on voltage and reactive power. For example on bus 5 at 16:00 voltage was dramatically dropped compared with earlier time day and reactive power was dramatically high at every hour of day which unwanted situation for reliability of grid so we implemented this result to nine zone diagram algorithm which seen on Figure 4.34 and 4.35 and we make a table about what can we do in the second simulation on these specific times and we coded a controller to compensate this reactive power and voltage by tap changes of OLTC and working of SVC, SVC start to work at when reactive power goes higher, both cases can be seen on table 4.10 and 4.26 at voltage drops nearly 360 Vrms levels according to the daily consumption which is the deepest value in day and reactive power is 5.51 Mvar which is the highest value in day, this values can be seen on table 4.10 and when we look into the controlled result we can see changes on bus5 table 4.26 voltage goes up 397.4 Vrms and reactive power decreases to 1.53 Mvar which quite better result compared with first. Also, we can see OLTC tap changes graph all day which is given Figure4

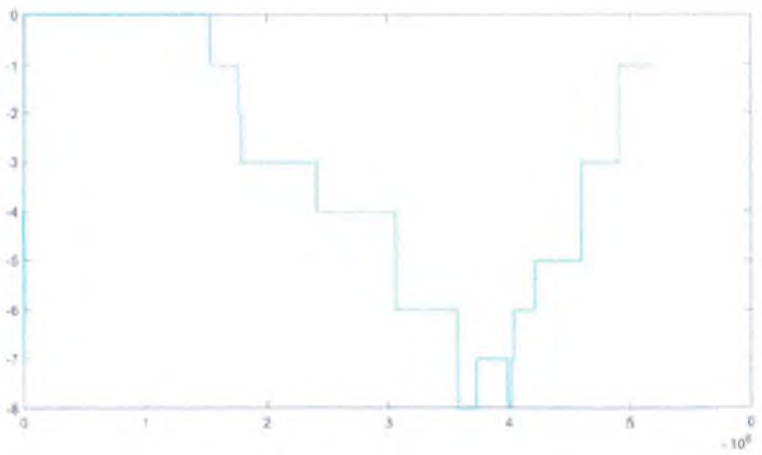

Figure 4.1. OLTC tap changes in one day

24-hour simulation collected 5,185,577 point and if divide this point by 24 we can find specific hour of a day, the calculation for every hour of a day given below Table 4.1.

Table 4.1. The 24 hour data obtained from the simulation

Hour	Data	Hour	Data
01:00	216065	13:00	2808854
02:00	432131	14:00	3024919
03:00	648197	15:00	3240985
04:00	864262	16:00	3457051
05:00	1080328	17:00	3673117
06:00	2196394	18:00	3889182
07:00	1512459	19:00	4105248
08:00	1728525	20:00	4321314
09:00	1944591	21:00	4537379
10:00	2160657	22:00	4753445
11:00	2376722	23:00	4969511
12:00	2592788	00:00	5185577

If we look at 16:00 data is 3,457,051 by this value we can see tap changes at 16:00 on Figure 4.1. At this area tap goes from -4 to -6 and voltage rises nearly 388 to 397, also we can see rises of voltage of bus 5 from Figure 4.53. Also reactive power started to change positive way at 12:00 in first simulation it was nearly 6 MVAr fixed in figure 4.71 we could barely see the injecting of Q by SVC at 12:00. All results obtained in this context will be given below.

4.1. Case 1: All Bus Value without Controller

Table 4.2 presents Bus1 line to neutral voltage, line to line voltage and reactive power, consumption data are shown in green column and given also in Figure 3.10, yellow section shows every hour of the day.

Table 4.2. Bus 1 source values - without controller (V – Q)

Consumption Data	Hour of Day	BUS1 (SOURCE)		
		VOLTAGE (V) L-N	VOLTAGE (V) L-L	REACTİVE P. (Q) Var
0,66667	00:00	106777	130790,50	9,16E+06
0,625	01:00	106777	130790,50	9,15E+06
0,58333	02:00	106802	130821,12	8,90E+06
0,5625	03:00	106917	130961,98	7,73E+06
0,54167	04:00	106945	130996,28	7,51E+06
0,51667	05:00	106892	130931,36	7,96E+06
0,5625	06:00	106868	130901,96	8,17E+06
0,58333	07:00	106776	130789,27	9,04E+06
0,66667	08:00	106704	130701,08	9,70E+06
0,75	09:00	106624	130603,09	1,05E+07
0,83333	10:00	106591	130562,67	1,08E+07
0,875	11:00	106563	130528,37	1,11E+07
0,89583	12:00	106489	130437,73	1,18E+07
0,9375	13:00	106439	130376,48	1,22E+07
0,95833	14:00	106370	130291,97	1,26E+07
0,96875	15:00	106203	130087,41	1,44E+07
0,97917	16:00	106102	129963,69	1,52E+07
1	17:00	106128	129995,54	1,50E+07
0,97917	18:00	106174	130051,89	1,45E+07
0,95833	19:00	106218	130105,78	1,41E+07
0,9375	20:00	106262	130159,68	1,37E+07
0,91667	21:00	106339	130253,99	1,30E+07
0,875	22:00	106553	130516,12	1,10E+07
0,75	23:00	106674	130664,33	1,00E+07
0,66667	00:00	106777	130790,50	9,16E+06

Table 4.3 presents Bus 1 active power, apparent power and current consumption data are shown in green column, also given in Figure 3.10, yellow section shows every hour of the day.

Table 4.3. Bus 1 source values - without controller (P – S – I)

Consumption Data	Hour of Day	BUS1 (SOURCE)		
		ACTİVE P. (P) W	APPARENT P. (S) VA	CURRENT (I) A
0,66666667	00:00	1,83E+07	2,05E+07	128,1
0,625	01:00	1,83E+07	2,04E+07	127,3
0,58333333	02:00	1,77E+07	1,98E+07	124,3
0,5625	03:00	1,72E+07	1,88E+07	117,6
0,54166667	04:00	1,65E+07	1,81E+07	113,5
0,51666667	05:00	1,74E+07	1,91E+07	121,5
0,5625	06:00	1,84E+07	2,01E+07	125
0,58333333	07:00	2,00E+07	2,19E+07	138
0,66666667	08:00	2,08E+07	2,30E+07	143,8
0,75	09:00	2,17E+07	2,41E+07	151,2
0,83333333	10:00	2,19E+07	2,44E+07	152,7
0,875	11:00	2,23E+07	2,49E+07	156
0,89583333	12:00	2,37E+07	2,64E+07	164,9
0,9375	13:00	2,45E+07	2,74E+07	172,1
0,95833333	14:00	2,51E+07	2,80E+07	181,3
0,96875	15:00	2,76E+07	3,11E+07	196
0,97916667	16:00	2,94E+07	3,31E+07	208,5
1	17:00	2,91E+07	3,27E+07	206,5
0,97916667	18:00	2,85E+07	3,20E+07	202,2
0,95833333	19:00	2,80E+07	3,13E+07	197,2
0,9375	20:00	2,73E+07	3,05E+07	192
0,91666667	21:00	2,60E+07	2,91E+07	182,9
0,875	22:00	2,28E+07	2,53E+07	158,8
0,75	23:00	2,06E+07	2,29E+07	143,1
0,66666667	00:00	1,83E+07	2,05E+07	128,1

Table 4.4 presents Bus 2 line to neutral voltage, line to line voltage and reactive power, consumption data are shown in green column, given also given in Figure 3.10, yellow section shows every hour of the day.

Table 4.4. Bus 2 values - without controller (V – P)

Consumption Data	Hour of Day	BUS2		
		VOLTAGE (V) L-N	VOLTAGE (V) L-L	REACTİVE P. (Q) Var
0,666667	00:00	21583	26436,88543	7,80E+06
0,625	01:00	21602	26460,15842	7,79E+06
0,583333	02:00	21302	26092,69024	7,66E+06
0,5625	03:00	21324	26119,63791	6,56E+06
0,541667	04:00	21324	26119,63791	6,44E+06
0,516667	05:00	21283	26069,41726	6,71E+06
0,5625	06:00	21262	26043,69448	6,84E+06
0,583333	07:00	21189	25954,27723	7,44E+06
0,666667	08:00	21127	25878,3338	7,97E+06
0,75	09:00	21056	25791,36634	8,56E+06
0,833333	10:00	21025	25753,39463	8,83E+06
0,875	11:00	21001	25723,99717	9,00E+06
0,895833	12:00	20904	25605,18246	9,46E+06
0,9375	13:00	20900	25600,28289	9,74E+06
0,958333	14:00	20852	25541,48798	9,98E+06
0,96875	15:00	21112	25859,9604	1,12E+07
0,979167	16:00	21037	25768,09335	1,16E+07
1	17:00	21061	25797,49081	1,14E+07
0,979167	18:00	21099	25844,03678	1,12E+07
0,958333	19:00	21140	25894,25743	1,09E+07
0,9375	20:00	21170	25931,00424	1,07E+07
0,916667	21:00	21230	26004,49788	1,02E+07
0,875	22:00	21410	26224,97878	9,03E+06
0,75	23:00	21500	26335,21924	8,32E+06
0,666667	00:00	21583	26436,88543	7,80E+06

Table 4.5 presents Bus 2 active power, apparent power and current and consumption data are shown in green column, also given in Figure 3.10, yellow section shows every hour of the day.

Table 4.5. Bus 2 values - without controller (P – S – I)

Consumption Data	Hour of Day	BUS2		
		ACTİVE P. (P) W	APPARENT P. (S) VA	CURRENT (I) A
0,6666667	00:00	1,83E+07	1,99E+07	614,2
0,625	01:00	1,83E+07	1,99E+07	614,6
0,5833333	02:00	1,77E+07	1,93E+07	595,8
0,5625	03:00	1,72E+07	1,84E+07	575,5
0,5416667	04:00	1,65E+07	1,77E+07	554
0,5166667	05:00	1,74E+07	1,86E+07	592
0,5625	06:00	1,84E+07	1,96E+07	610,9
0,5833333	07:00	2,00E+07	2,13E+07	669,8
0,6666667	08:00	2,08E+07	2,23E+07	706,3
0,75	09:00	2,17E+07	2,33E+07	736,7
0,8333333	10:00	2,19E+07	2,36E+07	746,9
0,875	11:00	2,23E+07	2,40E+07	761,6
0,8958333	12:00	2,37E+07	2,55E+07	802
0,9375	13:00	2,45E+07	2,63E+07	844,5
0,9583333	14:00	2,51E+07	2,70E+07	886,6
0,96875	15:00	2,76E+07	2,98E+07	949,3
0,9791667	16:00	2,94E+07	3,16E+07	1001
1	17:00	2,91E+07	3,13E+07	985,8
0,9791667	18:00	2,85E+07	3,06E+07	969
0,9583333	19:00	2,80E+07	3,00E+07	946,3
0,9375	20:00	2,73E+07	2,93E+07	926
0,9166667	21:00	2,60E+07	2,79E+07	883,7
0,875	22:00	2,28E+07	2,45E+07	764,3
0,75	23:00	2,06E+07	2,22E+07	690,1
0,6666667	00:00	1,83E+07	1,99E+07	614,2

Table 4.6 presents Bus 3 line to neutral voltage, line to line voltage and reactive power and consumption data are shown in green column, also given in Figure 3.10, yellow section shows every hour of the day.

Table 4.6. Bus 3 DG values - without controller (V – Q)

Consumption Data	Hour of Day	B3 SOURCE(DG)		
		VOLTAGE (V)L-N	VOLTAGE (V)L-L	REACTİVE P. (Q)VAr
0,66667	00:00	20410	25000,08487	3,74E+06
0,625	01:00	20410	25000,08487	3,71E+06
0,58333	02:00	20410	25000,08487	3,44E+06
0,5625	03:00	20400	24987,83593	4,19E+06
0,54167	04:00	20410	25000,08487	3,92E+06
0,51667	05:00	20410	25000,08487	4,48E+06
0,5625	06:00	20410	25000,08487	4,96E+06
0,58333	07:00	20390	24975,58699	5,75E+06
0,66667	08:00	20390	24975,58699	6,78E+06
0,75	09:00	20380	24963,33805	7,61E+06
0,83333	10:00	20380	24963,33805	8,01E+06
0,875	11:00	20380	24963,33805	8,32E+06
0,89583	12:00	20330	24902,09335	9,03E+06
0,9375	13:00	20370	24951,08911	9,55E+06
0,95833	14:00	20370	24951,08911	9,14E+06
0,96875	15:00	20370	24951,08911	9,81E+06
0,97917	16:00	20370	24951,08911	1,06E+07
1	17:00	20370	24951,08911	1,03E+07
0,97917	18:00	20370	24951,08911	9,83E+06
0,95833	19:00	20370	24951,08911	9,40E+06
0,9375	20:00	20380	24963,33805	8,93E+06
0,91667	21:00	20380	24963,33805	8,27E+06
0,875	22:00	20390	24975,58699	6,02E+06
0,75	23:00	20390	24975,58699	4,87E+06
0,66667	00:00	20410	25000,08487	3,74E+06

Table 4.7 presents Bus 3 active power, apparent power, current and consumption data are shown in green column, also given in Figure 3.10, yellow section shows every hour of the day.

Table 4.7. Bus 3 DG values - without controller (P – S – I)

Consumption Data	Hour of Day	B3 SOURCE(DG)		
		ACTIVE P. (P) W	APPARENT P. (S) VA	CURRENT (I) A
0,66666667	00:00	2,80E+06	4,67E+06	153,3
0,625	01:00	2,80E+06	4,64E+06	153,1
0,58333333	02:00	2,80E+06	4,43E+06	145,8
0,5625	03:00	2,80E+06	5,04E+06	164,3
0,54166667	04:00	2,80E+06	4,81E+06	156,9
0,51666667	05:00	2,80E+06	5,28E+06	173,5
0,5625	06:00	2,80E+06	5,69E+06	180,6
0,58333333	07:00	2,80E+06	6,39E+06	212,5
0,66666667	08:00	2,80E+06	7,34E+06	239,7
0,75	09:00	2,80E+06	8,11E+06	267,5
0,83333333	10:00	2,80E+06	8,49E+06	276
0,875	11:00	2,80E+06	8,78E+06	285,9
0,89583333	12:00	2,80E+06	9,45E+06	311,7
0,9375	13:00	2,90E+06	9,98E+06	327,3
0,95833333	14:00	2,90E+06	9,59E+06	349,8
0,96875	15:00	2,90E+06	1,02E+07	332,7
0,97916667	16:00	2,90E+06	1,10E+07	360,9
1	17:00	2,90E+06	1,07E+07	351
0,97916667	18:00	2,90E+06	1,02E+07	335,6
0,95833333	19:00	2,90E+06	9,83E+06	324,5
0,9375	20:00	2,90E+06	9,39E+06	307,7
0,91666667	21:00	2,90E+06	8,76E+06	277
0,875	22:00	2,90E+06	6,68E+06	227,1
0,75	23:00	2,80E+06	5,62E+06	190
0,66666667	00:00	2,80E+06	4,67E+06	153,3

Table 4.8 presents Bus 4 (load) line to neutral voltage, line to line voltage and reactive power and consumption data are shown in green column, also given in Figure 3.10, yellow section shows every hour of the day.

Table 4.8. Bus 4 load values - without controller (V – Q)

Consumption Data	Hour of Day	BUS4 (LOAD)		
		VOLTAGE (V)L-N	VOLTAGE (V)L-L	REACTİVE P. (Q)VAr
0,666667	00:00	311,4	381,4319661	-2,88E+06
0,625	01:00	311,7	381,7994342	-2,88E+06
0,583333	02:00	313	383,3917963	-2,77E+06
0,5625	03:00	310,6	380,4520509	-2,67E+06
0,541667	04:00	312	382,1669024	-2,56E+06
0,516667	05:00	309,6	379,227157	-2,78E+06
0,5625	06:00	308	377,2673267	-2,89E+06
0,583333	07:00	303,5	371,7553041	-3,29E+06
0,666667	08:00	298,9	366,1207921	-3,76E+06
0,75	09:00	294,3	360,4862801	-4,12E+06
0,833333	10:00	292,4	358,1589816	-4,32E+06
0,875	11:00	290,5	355,8316832	-4,42E+06
0,895833	12:00	287,5	352,1570014	-4,62E+06
0,9375	13:00	284,9	348,9722772	-4,73E+06
0,958333	14:00	283,1	346,7674682	-4,78E+06
0,96875	15:00	284,5	348,4823197	-4,84E+06
0,979167	16:00	281,4	344,6851485	-4,92E+06
1	17:00	282,7	346,2775106	-4,83E+06
0,979167	18:00	284,5	348,4823197	-4,72E+06
0,958333	19:00	286,6	351,0545969	-4,62E+06
0,9375	20:00	288,3	353,1369165	-4,48E+06
0,916667	21:00	292,3	358,0364922	-4,28E+06
0,875	22:00	301,1	368,8155587	-3,63E+06
0,75	23:00	306,6	375,5524752	-3,25E+06
0,666667	00:00	311,4	381,4319661	-2,88E+06

Table 4.9 presents Bus 4 (load) active power, apparent power, current and consumption data are shown in green column, also given in Figure 3.10, yellow section shows every hour of the day.

Table 4.9. Bus 4 load values - without controller (P – S – I)

Consumption Data	Hour of Day	BUS4(LOAD)		
		ACTİVE P. (P) W	APPARENT P. (S) VA	CURRENT (I) A
0,6666667	00:00	-8,75E+06	9,21E+06	1,97E+04
0,625	01:00	-8,73E+06	9,19E+06	1,96E+04
0,5833333	02:00	-8,44E+06	8,88E+06	1,90E+04
0,5625	03:00	-8,11E+06	8,53E+06	1,84E+04
0,5416667	04:00	-7,78E+06	8,19E+06	1,75E+04
0,5166667	05:00	-8,44E+06	8,89E+06	1,92E+04
0,5625	06:00	-8,89E+06	9,35E+06	1,99E+04
0,5833333	07:00	-1,00E+07	1,05E+07	2,43E+04
0,6666667	08:00	-1,12E+07	1,19E+07	2,67E+04
0,75	09:00	-1,25E+07	1,32E+07	3,01E+04
0,8333333	10:00	-1,31E+07	1,38E+07	3,18E+04
0,875	11:00	-1,34E+07	1,41E+07	3,25E+04
0,8958333	12:00	-1,41E+07	1,48E+07	3,43E+04
0,9375	13:00	-1,44E+07	1,51E+07	3,55E+04
0,9583333	14:00	-1,45E+07	1,53E+07	3,60E+04
0,96875	15:00	-1,47E+07	1,55E+07	3,67E+04
0,9791667	16:00	-1,50E+07	1,58E+07	3,74E+04
1	17:00	-1,47E+07	1,54E+07	3,65E+04
0,9791667	18:00	-1,44E+07	1,51E+07	3,55E+04
0,9583333	19:00	-1,40E+07	1,48E+07	3,43E+04
0,9375	20:00	-1,37E+07	1,45E+07	3,35E+04
0,9166667	21:00	-1,31E+07	1,38E+07	3,16E+04
0,875	22:00	-1,13E+07	1,18E+07	2,62E+04
0,75	23:00	-1,00E+07	1,05E+07	2,32E+04
0,6666667	00:00	-8,75E+06	9,21E+06	1,97E+04

Table 4.10 presents Bus 5 line to neutral voltage, line to line voltage and reactive power and consumption data are shown in green column, also given in Figure 3.10, yellow section shows every hour of the day.

Table 4.10. Bus 5 value - without controller (V – Q)

Consumption Data	Hour of Day	BUS5		
		VOLTAGE (V)L-N	VOLTAGE (V)L-L	REACTİVE P. (Q)VAr
0,66667	00:00	312	382,1669024	-4,26E+06
0,625	01:00	312	382,1669024	-4,26E+06
0,58333	02:00	312,8	383,1468175	-4,18E+06
0,5625	03:00	311,2	381,1869873	-4,11E+06
0,54167	04:00	312	382,1669024	-4,05E+06
0,51667	05:00	310,5	380,3295615	-4,19E+06
0,5625	06:00	309,5	379,1046676	-4,25E+06
0,58333	07:00	306,9	375,9199434	-4,59E+06
0,66667	08:00	304,5	372,980198	-4,79E+06
0,75	09:00	302	369,9179632	-5,04E+06
0,83333	10:00	300,9	368,5705799	-5,15E+06
0,875	11:00	300,1	367,5906648	-5,21E+06
0,89583	12:00	298,1	365,1408769	-5,34E+06
0,9375	13:00	296,6	363,3035361	-5,41E+06
0,95833	14:00	295,3	361,711174	-5,43E+06
0,96875	15:00	295,8	362,3236209	-5,46E+06
0,97917	16:00	294,1	360,2413013	-5,51E+06
1	17:00	295	361,3437058	-5,46E+06
0,97917	18:00	296,1	362,6910891	-5,39E+06
0,95833	19:00	297,3	364,1609618	-5,31E+06
0,9375	20:00	298,2	365,2633663	-5,25E+06
0,91667	21:00	299,4	366,733239	-5,15E+06
0,875	22:00	305,9	374,6950495	-4,74E+06
0,75	23:00	309,3	378,8596888	-4,52E+06
0,66667	00:00	312	382,1669024	-4,26E+06

Table 4.11 presents Bus 5 active power, apparent power and current are shown in green column consumption data is also given in Figure 3.10, yellow section shows every hour of the day.

Table 4.11. Bus 5 value - without controller (P – S – I)

Consumption Data	Hour of Day	BUS5		
		ACTİVE P. (P) W	APPARENT P. (S) VA	CURRENT (I) A
0,66666667	00:00	-1,14E+07	1,22E+07	2,61E+04
0,625	01:00	-1,14E+07	1,22E+07	2,61E+04
0,58333333	02:00	-1,12E+07	1,20E+07	2,56E+04
0,5625	03:00	-1,10E+07	1,18E+07	2,52E+04
0,54166667	04:00	-1,08E+07	1,15E+07	2,46E+04
0,51666667	05:00	-1,12E+07	1,20E+07	2,57E+04
0,5625	06:00	-1,15E+07	1,23E+07	2,64E+04
0,58333333	07:00	-1,31E+07	1,39E+07	2,84E+04
0,66666667	08:00	-1,40E+07	1,48E+07	3,06E+04
0,75	09:00	-1,44E+07	1,52E+07	3,27E+04
0,83333333	10:00	-1,46E+07	1,55E+07	3,39E+04
0,875	11:00	-1,49E+07	1,58E+07	3,44E+04
0,89583333	12:00	-1,50E+07	1,59E+07	3,55E+04
0,9375	13:00	-1,53E+07	1,62E+07	3,63E+04
0,95833333	14:00	-1,54E+07	1,63E+07	3,67E+04
0,96875	15:00	-1,55E+07	1,64E+07	3,70E+04
0,97916667	16:00	-1,57E+07	1,66E+07	3,75E+04
1	17:00	-1,54E+07	1,64E+07	3,69E+04
0,97916667	18:00	-1,52E+07	1,61E+07	3,63E+04
0,95833333	19:00	-1,50E+07	1,59E+07	3,57E+04
0,9375	20:00	-1,48E+07	1,57E+07	3,49E+04
0,91666667	21:00	-1,45E+07	1,54E+07	3,39E+04
0,875	22:00	-1,33E+07	1,41E+07	3,04E+04
0,75	23:00	-1,24E+07	1,32E+07	2,85E+04
0,66666667	00:00	-1,14E+07	1,22E+07	2,61E+04

Table 4.12 presents Bus load line to neutral voltage, line to line voltage, reactive power and consumption data are shown in green column, also given in Figure 3.10, yellow section shows every hour of the day.

Table 4.12. Bus load values - without controller (V – Q)

Cons. Data	Hour of Day	LOAD		
		VOLTAGE (V)L-N	VOLTAGE (V)L-L	REACTIVE P. (Q)VAr
0,666667	00:00	312	382,1669024	-1,92E+06
0,625	01:00	312	382,1669024	-1,91E+06
0,583333	02:00	312,8	383,1468175	-1,84E+06
0,5625	03:00	311,2	381,1869873	-1,78E+06
0,541667	04:00	312	382,1669024	-1,71E+06
0,516667	05:00	310,5	380,3295615	-1,85E+06
0,5625	06:00	309,5	379,1046676	-1,91E+06
0,583333	07:00	306,9	375,9199434	-2,21E+06
0,666667	08:00	304,5	372,980198	-2,51E+06
0,75	09:00	302	369,9179632	-2,74E+06
0,833333	10:00	300,9	368,5705799	-2,89E+06
0,875	11:00	300,1	367,5906648	-2,95E+06
0,895833	12:00	298,1	365,1408769	-3,08E+06
0,9375	13:00	296,6	363,3035361	-3,15E+06
0,958333	14:00	295,3	361,711174	-3,19E+06
0,96875	15:00	295,8	362,3236209	-3,22E+06
0,979167	16:00	294,1	360,2413013	-3,28E+06
1	17:00	295	361,3437058	-3,22E+06
0,979167	18:00	296,1	362,6910891	-3,15E+06
0,958333	19:00	297,3	364,1609618	-3,07E+06
0,9375	20:00	298,2	365,2633663	-3,00E+06
0,916667	21:00	299,4	366,733239	-2,88E+06
0,875	22:00	305,9	374,6950495	-2,45E+06
0,75	23:00	309,3	378,8596888	-2,16E+06
0,666667	00:00	312	382,1669024	-1,92E+06

Table 4.13 presents Bus load active power, apparent power and current and consumption data are shown in green column, also given in Figure 3.10, yellow section shows every hour of the day.

Table 4.13. Bus load values - without controller (P – S – I)

Cons. Data	Hour of Day	LOAD		
		ACTIVE P. (P) W	APPARENT P. (S) VA	CURRENT (I) A
0,6666667	00:00	-5,84E+06	6,15E+06	1,31E+04
0,625	01:00	-5,83E+06	6,14E+06	1,31E+04
0,5833333	02:00	-5,61E+06	5,90E+06	1,26E+04
0,5625	03:00	-5,42E+06	5,70E+06	1,22E+04
0,5416667	04:00	-5,18E+06	5,45E+06	1,17E+04
0,5166667	05:00	-5,64E+06	5,94E+06	1,27E+04
0,5625	06:00	-5,90E+06	6,20E+06	1,32E+04
0,5833333	07:00	-7,54E+06	7,86E+06	1,54E+04
0,6666667	08:00	-8,39E+06	8,76E+06	1,73E+04
0,75	09:00	-8,77E+06	9,19E+06	1,94E+04
0,8333333	10:00	-9,04E+06	9,49E+06	2,04E+04
0,875	11:00	-9,30E+06	9,76E+06	2,09E+04
0,8958333	12:00	-9,40E+06	9,89E+06	2,21E+04
0,9375	13:00	-9,65E+06	1,02E+07	2,27E+04
0,9583333	14:00	-9,80E+06	1,03E+07	2,28E+04
0,96875	15:00	-9,89E+06	1,04E+07	2,34E+04
0,9791667	16:00	-1,01E+07	1,06E+07	2,36E+04
1	17:00	-9,82E+06	1,03E+07	2,33E+04
0,9791667	18:00	-9,61E+06	1,01E+07	2,27E+04
0,9583333	19:00	-9,41E+06	9,90E+06	2,21E+04
0,9375	20:00	-9,18E+06	9,66E+06	2,17E+04
0,9166667	21:00	-8,88E+06	9,33E+06	2,09E+04
0,875	22:00	-7,70E+06	8,08E+06	1,77E+04
0,75	23:00	-6,75E+06	7,09E+06	1,53E+04
0,6666667	00:00	-5,84E+06	6,15E+06	1,31E+04

Table 4.14 presents Bus PV line to neutral voltage, line to line voltage and reactive power and consumption data are shown in green column, also given in Figure 3.10, yellow section shows every hour of the day.

Table 4.14. Bus PV farm values - without controller (V – Q)

Cons. Data	Hour of Day	PV FARM		
		VOLTAGE (V)L-N	VOLTAGE (V)L-L	REACTIVE P. (Q)VAr
0,66667	00:00	19910	24387,63791	-4,49E+04
0,625	01:00	19920	24399,88685	-4,49E+04
0,58333	02:00	19950	24436,63366	-4,49E+04
0,5625	03:00	19850	24314,14427	-4,49E+04
0,54167	04:00	19890	24363,14003	-4,49E+04
0,51667	05:00	19820	24277,39745	-4,49E+04
0,5625	06:00	19780	24228,4017	-4,49E+04
0,58333	07:00	19640	24056,91655	-4,49E+04
0,66667	08:00	19510	23897,68034	-4,49E+04
0,75	09:00	19390	23750,69307	-4,49E+04
0,83333	10:00	19340	23689,44837	-4,49E+04
0,875	11:00	19290	23628,20368	-4,49E+04
0,89583	12:00	19190	23505,71429	-4,49E+04
0,9375	13:00	19110	23407,72277	-4,49E+04
0,95833	14:00	19050	23334,22914	-4,49E+04
0,96875	15:00	19100	23395,47383	-4,49E+04
0,97917	16:00	18970	23236,23762	-4,49E+04
1	17:00	19010	23285,23338	-4,49E+04
0,97917	18:00	19070	23358,72702	-4,49E+04
0,95833	19:00	19140	23444,46959	-4,49E+04
0,9375	20:00	19190	23505,71429	-4,49E+04
0,91667	21:00	19310	23652,70156	-4,49E+04
0,875	22:00	19630	24044,66761	-4,49E+04
0,75	23:00	19760	24203,90382	-4,49E+04
0,66667	00:00	19910	24387,63791	-4,49E+04

Table 4.15 presents Bus PV active power, apparent power and current and consumption data are shown in green column, also given in Figure 3.10, yellow section shows every hour of the day.

Table 4.15. Bus PV farm values - without controller (P – S – I)

Cons. Data	Hour of Day	PV FARM		
		ACTIVE P. (P) W	APPARENT P. (S) VA	CURRENT (I) A
0,66666667	00:00	-892	4,49E+04	1,506
0,625	01:00	-892	4,49E+04	1,506
0,58333333	02:00	-896	4,49E+04	1,503
0,5625	03:00	-888	4,49E+04	1,511
0,54166667	04:00	-889	4,49E+04	1,508
0,51666667	05:00	2686	4,50E+04	1,513
0,5625	06:00	2,29E+04	5,04E+04	1,642
0,58333333	07:00	5,99E+05	6,01E+05	18,77
0,66666667	08:00	1,99E+06	1,99E+06	63,56
0,75	09:00	3,13E+06	3,13E+06	106,1
0,83333333	10:00	4,09E+06	4,09E+06	141,4
0,875	11:00	4,19E+06	4,19E+06	145,3
0,89583333	12:00	4,00E+06	4,00E+06	143,4
0,9375	13:00	3,70E+06	3,70E+06	131,3
0,95833333	14:00	2,88E+06	2,88E+06	101,4
0,96875	15:00	1,64E+06	1,64E+06	52,85
0,97916667	16:00	1,84E+05	1,90E+05	13,19
1	17:00	4774	4,52E+04	1,579
0,97916667	18:00	-818	4,49E+04	1,574
0,95833333	19:00	-823	4,49E+04	1,567
0,9375	20:00	-828	4,49E+04	1,565
0,91666667	21:00	-851	4,49E+04	1,549
0,875	22:00	-872	4,49E+04	1,534
0,75	23:00	-877	4,49E+04	1,519
0,66666667	00:00	-892	4,49E+04	1,506

Table 4.16 presents Bus ASM line to neutral voltage, line to line voltage and reactive power and consumption data are shown in green column, also given in Figure 3.10, yellow section shows every hour of the day.

Table 4.16. Bus ASM values - without controller (V – Q)

Cons. Data	Hour of Day	BUS ASM		
		VOLTAGE (V)L-N	VOLTAGE (V)L-L	REACTIVE P. (Q)VAr
0,666667	00:00	312	382,1669024	-2,30E+06
0,625	01:00	311,9	382,044413	-2,30E+06
0,583333	02:00	312,71	383,0409867	-2,30E+06
0,5625	03:00	311,22	381,2114851	-2,30E+06
0,541667	04:00	312	382,1669024	-2,30E+06
0,516667	05:00	310,512	380,3442603	-2,30E+06
0,5625	06:00	309,79	379,4598868	-2,30E+06
0,583333	07:00	307,06	376,1159264	-2,30E+06
0,666667	08:00	304,6	373,1026874	-2,20E+06
0,75	09:00	302,07	370,0037058	-2,20E+06
0,833333	10:00	300,8	368,4480905	-2,20E+06
0,875	11:00	300,1	367,5906648	-2,20E+06
0,895833	12:00	298,07	365,1041301	-2,20E+06
0,9375	13:00	296,8	363,5485149	-2,20E+06
0,958333	14:00	295,4	361,8336634	-2,20E+06
0,96875	15:00	296,25	362,8748232	-2,20E+06
0,979167	16:00	294,12	360,2657992	-2,20E+06
1	17:00	294,88	361,1967185	-2,20E+06
0,979167	18:00	296	362,5685997	-2,20E+06
0,958333	19:00	297,1	363,915983	-2,20E+06
0,9375	20:00	298,2	365,2633663	-2,20E+06
0,916667	21:00	300,3	367,8356436	-2,20E+06
0,875	22:00	305,8	374,5725601	-2,20E+06
0,75	23:00	308,8	378,2472419	-2,20E+06
0,666667	00:00	312	382,1669024	-2,20E+06

Table 4.17 presents Bus ASM active power, apparent power and current and consumption data are shown in green column, also given in Figure 3.10, yellow section shows every hour of the day.

Table 4.17. Bus ASM values - without controller

Cons. Data	Hour of Day	BUS ASM		
		ACTIVE P. (P) W	APPARENT P. (S) VA	CURRENT (I) A
0,6666667	00:00	-5,60E+06	6,05E+06	1,30E+04
0,625	01:00	-5,60E+06	6,05E+06	1,30E+04
0,5833333	02:00	-5,60E+06	6,05E+06	1,30E+04
0,5625	03:00	-5,60E+06	6,05E+06	1,30E+04
0,5416667	04:00	-5,60E+06	6,05E+06	1,30E+04
0,5166667	05:00	-5,60E+06	6,05E+06	1,30E+04
0,5625	06:00	-5,60E+06	6,05E+06	1,30E+04
0,5833333	07:00	-5,60E+06	6,05E+06	1,30E+04
0,6666667	08:00	-5,60E+06	6,02E+06	1,30E+04
0,75	09:00	-5,60E+06	6,02E+06	1,30E+04
0,8333333	10:00	-5,60E+06	6,02E+06	1,30E+04
0,875	11:00	-5,60E+06	6,02E+06	1,30E+04
0,8958333	12:00	-5,60E+06	6,02E+06	1,30E+04
0,9375	13:00	-5,60E+06	6,02E+06	1,30E+04
0,9583333	14:00	-5,60E+06	6,02E+06	1,30E+04
0,96875	15:00	-5,60E+06	6,02E+06	1,30E+04
0,9791667	16:00	-5,60E+06	6,02E+06	1,30E+04
1	17:00	-5,60E+06	6,02E+06	1,30E+04
0,9791667	18:00	-5,60E+06	6,02E+06	1,30E+04
0,9583333	19:00	-5,60E+06	6,02E+06	1,30E+04
0,9375	20:00	-5,60E+06	6,02E+06	1,30E+04
0,9166667	21:00	-5,60E+06	6,02E+06	1,30E+04
0,875	22:00	-5,60E+06	6,02E+06	1,30E+04
0,75	23:00	-5,60E+06	6,02E+06	1,30E+04
0,6666667	00:00	-5,60E+06	6,02E+06	1,30E+04

4.2. Case 2: All Bus Value with Controller

Table 4.18 presents Bus 1 line to neutral voltage, line to line voltage, reactive power and consumption data are shown in green column, also given in Figure 3.10, yellow section shows every hour of the day.

Table 4.18. Bus 1 source values - with controller (V – Q)

Consumption Data	Hour of Day	BUS1 (SOURCE)		
		VOLTAGE (V)L-N	VOLTAGE (V)L-L	REACTIVE P. (Q)VAr
0,66667	00:00	1,07E+05	130941,16	8,70E+06
0,625	01:00	1,07E+05	130941,16	8,24E+06
0,58333	02:00	1,07E+05	130941,16	8,09E+06
0,5625	03:00	1,07E+05	130941,16	7,91E+06
0,54167	04:00	1,07E+05	130941,16	7,70E+06
0,51667	05:00	1,07E+05	130941,16	8,09E+06
0,5625	06:00	1,07E+05	130818,67	8,25E+06
0,58333	07:00	1,07E+05	130573,69	9,07E+06
0,66667	08:00	1,06E+05	130206,22	9,60E+06
0,75	09:00	1,06E+05	130206,22	1,38E+07
0,83333	10:00	1,06E+05	130206,22	1,40E+07
0,875	11:00	1,06E+05	130206,22	1,43E+07
0,89583	12:00	1,06E+05	130206,22	1,49E+07
0,9375	13:00	1,06E+05	130206,22	1,61E+07
0,95833	14:00	1,06E+05	130206,22	1,91E+07
0,96875	15:00	1,06E+05	129593,78	1,95E+07
0,97917	16:00	1,06E+05	129593,78	1,99E+07
1	17:00	1,05E+05	129103,82	2,10E+07
0,97917	18:00	1,06E+05	129593,78	2,09E+07
0,95833	19:00	1,06E+05	129593,78	1,92E+07
0,9375	20:00	1,06E+05	129593,78	1,75E+07
0,91667	21:00	1,06E+05	129593,78	1,69E+07
0,875	22:00	1,06E+05	129593,78	1,28E+07
0,75	23:00	1,07E+05	106700,00	9,46E+06
0,66667	00:00	1,07E+05	130818,67	8,70E+06

In Table 4.19 Bus1 active power, apparent power and current and consumption data are shown in green column, also given in Figure 3.10, yellow section shows every hour of the day.

Table 4.19. Bus1 source values - with controller (P – S – I)

Consumption Data	Hour of Day	BUS1 (SOURCE)		
		ACTIVE P. (P) W	APPARENT P. (S) VA	CURRENT (I) A
0,666667	00:00	1,83E+07	2,03E+07	126
0,625	01:00	1,83E+07	2,01E+07	125
0,583333	02:00	1,78E+07	1,95E+07	121,7
0,5625	03:00	1,72E+07	1,89E+07	118,2
0,541667	04:00	1,66E+07	1,83E+07	114
0,516667	05:00	1,77E+07	1,95E+07	122
0,5625	06:00	1,83E+07	2,01E+07	125
0,583333	07:00	2,01E+07	2,20E+07	135
0,666667	08:00	2,08E+07	2,29E+07	146
0,75	09:00	2,18E+07	2,58E+07	160
0,833333	10:00	2,20E+07	2,61E+07	163,4
0,875	11:00	2,33E+07	2,73E+07	166,4
0,895833	12:00	2,34E+07	2,77E+07	178
0,9375	13:00	2,45E+07	2,93E+07	182
0,958333	14:00	2,58E+07	3,21E+07	192,7
0,96875	15:00	2,75E+07	3,37E+07	212,6
0,979167	16:00	2,92E+07	3,53E+07	223,8
1	17:00	2,86E+07	3,55E+07	233,9
0,979167	18:00	2,87E+07	3,55E+07	224,5
0,958333	19:00	2,80E+07	3,39E+07	213,7
0,9375	20:00	2,74E+07	3,24E+07	203,8
0,916667	21:00	2,59E+07	3,10E+07	196,8
0.875	22:00	2,27E+07	2,60E+07	163,6
0,75	23:00	2,05E+07	2,25E+07	142
0,666667	00:00	1,83E+07	2,03E+07	126

In Table 4.20 Bus 2 line to neutral voltage, line to line voltage and reactive power and consumption data are shown in green column, also given in Figure 3.10, yellow section shows every hour of the day.

Table 4.20. Bus 2 values - with controller (V – Q)

Cons. Data	Hour of Day	BUS2		
		VOLTAGE (V)L-N	VOLTAGE (V)L-L	REACTIVE P. (Q)VAr
0,666667	00:00	2,16E+04	26494,45545	7,40E+06
0,625	01:00	2,16E+04	26494,45545	6,98E+06
0,583333	02:00	2,16E+04	26494,45545	6,86E+06
0,5625	03:00	2,16E+04	26494,45545	6,72E+06
0,541667	04:00	2,16E+04	26494,45545	6,59E+06
0,516667	05:00	2,16E+04	26494,45545	6,86E+06
0,5625	06:00	2,16E+04	26494,45545	6,97E+06
0,583333	07:00	2,19E+04	26776,18105	7,45E+06
0,666667	08:00	2,25E+04	27523,36634	9,04E+06
0,75	09:00	2,25E+04	27498,86846	1,17E+07
0,833333	10:00	2,25E+04	27498,86846	1,20E+07
0,875	11:00	2,24E+04	27474,37058	1,11E+07
0,895833	12:00	2,27E+04	27805,09194	1,35E+07
0,9375	13:00	2,27E+04	27805,09194	1,31E+07
0,958333	14:00	2,27E+04	27805,09194	1,33E+07
0,96875	15:00	2,34E+04	28674,76662	1,59E+07
0,979167	16:00	2,33E+04	28540,02829	1,62E+07
1	17:00	2,42E+04	29605,686	1,87E+07
0,979167	18:00	2,38E+04	29152,47525	1,72E+07
0,958333	19:00	2,34E+04	28662,51768	1,57E+07
0,9375	20:00	2,31E+04	28270,55163	1,42E+07
0,916667	21:00	2,31E+04	28344,04526	1,38E+07
0,875	22:00	2,26E+04	27658,10467	1,06E+07
0,75	23:00	2,20E+04	26898,67044	7,98E+06
0,666667	00:00	2,21E+04	27008,91089	7,40E+06

In Table 4.21 Bus 2 active power, apparent power and current and consumption data are shown in green column, also given in Figure 3.10, yellow section shows every hour of the day.

Table 4.21. Bus 2 values - with controller (P – S – I)

Consumption Data	Hour of Day	BUS2		
		ACTIVE P. (P) W	APPARENT P. (S) VA	CURRENT (I) A
0,66666667	00:00	1,83E+07	1,97E+07	595,5
0,625	01:00	1,83E+07	1,96E+07	601,8
0,58333333	02:00	1,78E+07	1,90E+07	583,6
0,5625	03:00	1,72E+07	1,85E+07	566,3
0,54166667	04:00	1,66E+07	1,79E+07	546,5
0,51666667	05:00	1,77E+07	1,90E+07	582,9
0,5625	06:00	1,83E+07	1,96E+07	603
0,58333333	07:00	2,01E+07	2,14E+07	651,5
0,66666667	08:00	2,08E+07	2,27E+07	689,5
0,75	09:00	2,18E+07	2,47E+07	731,1
0,83333333	10:00	2,96E+07	3,19E+07	739,4
0,875	11:00	2,33E+07	2,58E+07	753,5
0,89583333	12:00	2,34E+07	2,70E+07	792,4
0,9375	13:00	2,45E+07	2,78E+07	811
0,95833333	14:00	2,58E+07	2,90E+07	847,2
0,96875	15:00	2,75E+07	3,18E+07	915,2
0,97916667	16:00	2,92E+07	3,34E+07	951,1
1	17:00	2,86E+07	3,42E+07	955
0,97916667	18:00	2,87E+07	3,35E+07	931,9
0,95833333	19:00	2,80E+07	3,21E+07	911,5
0,9375	20:00	2,74E+07	3,08E+07	890
0,91666667	21:00	2,59E+07	2,94E+07	858,1
0,875	22:00	2,27E+07	2,50E+07	749,5
0,75	23:00	2,05E+07	2,20E+07	668,4
0,66666667	00:00	1,83E+07	1,97E+07	595,5

In Table 4.22 Bus 3 line to neutral voltage, line to line voltage and reactive power and consumption data are shown in green column, also given in Figure 3.10, yellow section shows every hour of the day.

Table 4.22. Bus 3 DG values - with controller (V – Q)

Cons. Data	Hour of Day	B3 SOURCE(DG)		
		VOLTAGE (V)L-N	VOLTAGE (V)L-L	REACTIVE P. (Q)VAr
0,66667	00:00	2,04E+04	25012,3338	-4,06E+05
0,625	01:00	2,04E+04	25012,3338	1,95E+06
0,58333	02:00	2,04E+04	25012,3338	1,66E+06
0,5625	03:00	2,04E+04	25012,3338	1,41E+06
0,54167	04:00	2,04E+04	25012,3338	1,17E+06
0,51667	05:00	2,04E+04	25012,3338	1,69E+06
0,5625	06:00	2,04E+04	25012,3338	1,93E+06
0,58333	07:00	2,04E+04	25012,3338	3,16E+06
0,66667	08:00	2,04E+04	25012,3338	2,67E+06
0,75	09:00	2,04E+04	25012,3338	1,41E+06
0,83333	10:00	2,04E+04	25012,3338	1,72E+06
0,875	11:00	2,04E+04	25012,3338	1,97E+06
0,89583	12:00	2,04E+04	25012,3338	1,32E+06
0,9375	13:00	2,04E+04	25012,3338	5,64E+06
0,95833	14:00	2,04E+04	25012,3338	1,05E+06
0,96875	15:00	2,04E+04	25012,3338	-9,29E+05
0,97917	16:00	2,04E+04	25012,3338	-2,22E+05
1	17:00	2,04E+04	25012,3338	-3,13E+06
0,97917	18:00	2,04E+04	25012,3338	-2,03E+06
0,95833	19:00	2,04E+04	25012,3338	-1,16E+06
0,9375	20:00	2,04E+04	25012,3338	-2,27E+05
0,91667	21:00	2,04E+04	25012,3338	-8,20E+05
0,875	22:00	2,04E+04	25012,3338	-3,49E+05
0,75	23:00	2,04E+04	25012,3338	6,72E+05
0,66667	00:00	2,04E+04	25012,3338	-4,06E+05

In Table 4.23 Bus 3 active power, apparent power and current and consumption data are shown in green column, also given in Figure 3.10, yellow section shows every hour of the day.

Table 4.23. Bus 3 DG values - with controller (P – S – I)

Cons. Data	Hour of Day	B3 SOURCE(DG)		
		ACTIVE P. (P) W	APPARENT P. (S) VA	CURRENT (I) A
0,666667	00:00	2,80E+06	2,83E+06	93,7
0,625	01:00	2,80E+06	3,41E+06	112,5
0,583333	02:00	2,80E+06	3,26E+06	107,2
0,5625	03:00	2,80E+06	3,13E+06	102,7
0,541667	04:00	2,80E+06	3,03E+06	98,35
0,516667	05:00	2,80E+06	3,27E+06	106,5
0,5625	06:00	2,80E+06	3,40E+06	112,7
0,583333	07:00	2,80E+06	4,22E+06	139,1
0,666667	08:00	2,80E+06	3,87E+06	126
0,75	09:00	2,80E+06	3,13E+06	102
0,833333	10:00	2,80E+06	3,29E+06	108,5
0,875	11:00	2,80E+06	3,42E+06	113,2
0,895833	12:00	2,80E+06	3,10E+06	104,2
0,9375	13:00	2,90E+06	6,34E+06	96,13
0,958333	14:00	2,90E+06	3,08E+06	96,72
0,96875	15:00	2,90E+06	3,05E+06	99,25
0,979167	16:00	2,90E+06	2,91E+06	95,72
1	17:00	2,90E+06	4,27E+06	141
0,979167	18:00	2,90E+06	3,54E+06	116
0,958333	19:00	2,90E+06	3,12E+06	101,9
0,9375	20:00	2,90E+06	2,91E+06	95,38
0,916667	21:00	2,90E+06	3,01E+06	99,48
0,875	22:00	2,90E+06	2,92E+06	94,55
0,75	23:00	2,80E+06	2,88E+06	94,02
0,666667	00:00	2,80E+06	2,83E+06	93,7

In Table 4.24 Bus 4 load line to neutral voltage, line to line voltage and reactive power and consumption data are shown in green column, also given in Figure 3.10, yellow section shows every hour of the day.

Table 4.24. Bus 4 load values - with controller (V – Q)

Cons. Data	Hour of Day	BUS 4 (LOAD)		
		VOLTAGE (V)L-N	VOLTAGE (V)L-L	REACTIVE P. (Q)VAr
0,666667	00:00	320,8	392,9459689	-2,88E+06
0,625	01:00	315	385,8415842	-2,87E+06
0,583333	02:00	316,1	387,1889675	-2,78E+06
0,5625	03:00	317,4	388,7813296	-2,67E+06
0,541667	04:00	318,6	390,2512023	-2,55E+06
0,516667	05:00	316	387,0664781	-2,72E+06
0,5625	06:00	314,9	385,7190948	-2,92E+06
0,583333	07:00	310	379,7171146	-3,37E+06
0,666667	08:00	310,3	380,0845827	-3,68E+06
0,75	09:00	313,8	384,3717115	-4,13E+06
0,833333	10:00	311,9	382,044413	-4,34E+06
0,875	11:00	310,9	380,8195191	-4,43E+06
0,895833	12:00	310,7	380,5745403	-4,56E+06
0,9375	13:00	312,5	382,7793494	-4,72E+06
0,958333	14:00	310,3	380,0845827	-4,78E+06
0,96875	15:00	317,7	389,1487977	-4,84E+06
0,979167	16:00	315,1	385,9640736	-4,93E+06
1	17:00	326,1	399,4379066	-4,83E+06
0,979167	18:00	322,5	395,0282885	-4,72E+06
0,958333	19:00	319,4	391,2311174	-4,62E+06
0,9375	20:00	316	387,0664781	-4,52E+06
0,916667	21:00	318,7	390,3736917	-4,29E+06
0,875	22:00	319,2	390,9861386	-3,67E+06
0,75	23:00	317,5	388,903819	-3,32E+06
0,666667	00:00	320,8	392,9459689	-2,88E+06

In Table 4.25 Bus shows 4 load line active power, apparent power and current and consumption data are shown in green column, also given in Figure 3.10, yellow section shows every hour of the day.

Table 4.25. Bus 4 load values - with controller (P – S – I)

Cons. Data	Hour of Day	BUS4(LOAD)		
		ACTIVE P. (P) W	APPARENT P. (S) VA	CURRENT (I) A
0,66666667	00:00	-8,75E+06	9,21E+06	1,91E+04
0,625	01:00	-8,73E+06	9,19E+06	1,95E+04
0,58333333	02:00	-8,44E+06	8,88E+06	1,87E+04
0,5625	03:00	-8,11E+06	8,53E+06	1,80E+04
0,54166667	04:00	-7,78E+06	8,19E+06	1,71E+04
0,51666667	05:00	-8,44E+06	8,87E+06	1,86E+04
0,5625	06:00	-8,89E+06	9,36E+06	1,98E+04
0,58333333	07:00	-1,00E+07	1,06E+07	2,29E+04
0,66666667	08:00	-1,12E+07	1,18E+07	2,56E+04
0,75	09:00	-1,25E+07	1,32E+07	2,83E+04
0,83333333	10:00	-1,31E+07	1,38E+07	2,93E+04
0,875	11:00	-1,34E+07	1,42E+07	3,01E+04
0,89583333	12:00	-1,41E+07	1,48E+07	3,13E+04
0,9375	13:00	-1,44E+07	1,51E+07	3,22E+04
0,95833333	14:00	-1,45E+07	1,53E+07	3,28E+04
0,96875	15:00	-1,47E+07	1,55E+07	3,24E+04
0,97916667	16:00	-1,50E+07	1,58E+07	3,34E+04
1	17:00	-1,47E+07	1,54E+07	3,18E+04
0,97916667	18:00	-1,44E+07	1,51E+07	3,13E+04
0,95833333	19:00	-1,40E+07	1,48E+07	3,04E+04
0,9375	20:00	-1,37E+07	1,45E+07	3,04E+04
0,91666667	21:00	-1,31E+07	1,38E+07	2,86E+04
0,875	22:00	-1,13E+07	1,19E+07	2,56E+04
0,75	23:00	-1,00E+07	1,05E+07	2,29E+04
0,66666667	00:00	-8,75E+06	9,21E+06	1,91E+04

In Table 4.26 shows Bus 5 line to neutral voltage, line to line voltage and reactive power and consumption data are shown in green column, also given in Figure 3.10, yellow section shows every hour of the day.

Table 4.26. Bus 5 value - with controller (V – Q)

Cons. Data	Hour of Day	BUS5		
		VOLTAGE (V)L-N	VOLTAGE (V)L-L	REACTIVE P. (Q)VAr
0,66667	00:00	326,8	400,2953324	-1,18E+05
0,625	01:00	319,2	390,9861386	-1,91E+06
0,58333	02:00	319,9	391,8435644	-1,85E+06
0,5625	03:00	320,7	392,8234795	-1,78E+06
0,54167	04:00	321,3	393,5584158	-1,69E+06
0,51667	05:00	319,8	391,721075	-1,86E+06
0,5625	06:00	319,3	391,108628	-1,99E+06
0,58333	07:00	316,6	387,8014144	-2,25E+06
0,66667	08:00	316,4	387,5564356	-2,49E+06
0,75	09:00	319,1	390,8636492	-2,78E+06
0,83333	10:00	318,1	389,6387553	-2,91E+06
0,875	11:00	317,5	388,903819	-3,00E+06
0,89583	12:00	318,9	390,6186704	-3,08E+06
0,9375	13:00	322,4	394,9057992	-1,43E+06
0,95833	14:00	321,1	393,3134371	-1,48E+06
0,96875	15:00	325,7	398,9479491	-1,46E+06
0,97917	16:00	324,5	397,4780764	-1,53E+06
1	17:00	330,7	405,0724187	-1,34E+06
0,97917	18:00	328,3	402,1326733	-1,33E+06
0,95833	19:00	326,5	399,9278642	-1,27E+06
0,9375	20:00	324,4	397,355587	-1,16E+06
0,91667	21:00	326,2	399,560396	-1,05E+06
0,875	22:00	325,7	398,9479491	-8,10E+05
0,75	23:00	324,2	397,1106082	-4,43E+05
0,66667	00:00	326,8	400,2953324	-1,18E+05

In Table 4.27 Bus 5 active power, apparent power and current and consumption data are shown in green column, also given in Figure 3.10, yellow section shows every hour of the day.

Table 4.27. Bus 5 values - with controller (P – S – I)

Cons. Data	Hour of Day	BUS5		
		ACTIVE P. (P) W	APPARENT P. (S) VA	CURRENT (I) A
0,666667	00:00	-1,14E+07	1,14E+07	2,33E+04
0,625	01:00	-1,14E+07	1,16E+07	2,43E+04
0,583333	02:00	-1,12E+07	1,14E+07	2,36E+04
0,5625	03:00	-1,10E+07	1,12E+07	2,29E+04
0,541667	04:00	-1,08E+07	1,09E+07	2,27E+04
0,516667	05:00	-1,12E+07	1,14E+07	2,36E+04
0,5625	06:00	-1,15E+07	1,17E+07	2,42E+04
0,583333	07:00	-1,31E+07	1,33E+07	2,60E+04
0,666667	08:00	-1,40E+07	1,42E+07	2,82E+04
0,75	09:00	-1,44E+07	1,46E+07	2,95E+04
0,833333	10:00	-1,46E+07	1,49E+07	3,07E+04
0,875	11:00	-1,49E+07	1,52E+07	3,12E+04
0,895833	12:00	-1,50E+07	1,53E+07	3,19E+04
0,9375	13:00	-1,53E+07	1,53E+07	3,15E+04
0,958333	14:00	-1,54E+07	1,55E+07	3,18E+04
0,96875	15:00	-1,55E+07	1,56E+07	3,16E+04
0,979167	16:00	-1,57E+07	1,57E+07	3,22E+04
1	17:00	-1,54E+07	1,55E+07	3,11E+04
0,979167	18:00	-1,52E+07	1,53E+07	3,10E+04
0,958333	19:00	-1,50E+07	1,51E+07	3,06E+04
0,9375	20:00	-1,48E+07	1,48E+07	3,05E+04
0,916667	21:00	-1,45E+07	1,45E+07	2,89E+04
0,875	22:00	-1,33E+07	1,33E+07	2,70E+04
0,75	23:00	-1,24E+07	1,24E+07	2,57E+04
0,666667	00:00	-1,14E+07	1,14E+07	2,33E+04

In Table 4.28 Bus load line to neutral voltage, line to line voltage and reactive power and consumption data are shown in green column, also given in Figure 3.10, yellow section shows every hour of the day.

Table 4.28. Bus load values - with controller (V – Q)

Cons. Data	Hour of Day	LOAD		
		VOLTAGE (V)L-N	VOLTAGE (V)L-L	REACTIVE P. (Q)VAr
0,666667	00:00	326,8	400,2953324	-1,92E+06
0,625	01:00	319,2	390,9861386	-1,91E+06
0,583333	02:00	319,9	391,8435644	-1,84E+06
0,5625	03:00	320,7	392,8234795	-1,78E+06
0,541667	04:00	321,3	393,5584158	-1,72E+06
0,516667	05:00	319,8	391,721075	-1,85E+06
0,5625	06:00	319,3	391,108628	-1,92E+06
0,583333	07:00	316,6	387,8014144	-2,22E+06
0,666667	08:00	316,4	387,5564356	-2,47E+06
0,75	09:00	319,1	390,8636492	-2,74E+06
0,833333	10:00	318,1	389,6387553	-2,88E+06
0,875	11:00	317,5	388,903819	-2,95E+06
0,895833	12:00	318,9	390,6186704	-3,07E+06
0,9375	13:00	322,4	394,9057992	-3,15E+06
0,958333	14:00	321,1	393,3134371	-3,18E+06
0,96875	15:00	325,7	398,9479491	-3,23E+06
0,979167	16:00	324,5	397,4780764	-3,28E+06
1	17:00	330,7	405,0724187	-3,21E+06
0,979167	18:00	328,3	402,1326733	-3,15E+06
0,958333	19:00	326,5	399,9278642	-3,08E+06
0,9375	20:00	324,4	397,355587	-3,02E+06
0,916667	21:00	326,2	399,560396	-2,85E+06
0,875	22:00	325,7	398,9479491	-2,43E+06
0,75	23:00	324,2	397,1106082	-2,17E+06
0,666667	00:00	326,8	400,2953324	-1,92E+06

In Table 4.29 Bus load active power, apparent power and current and consumption data are shown in green column, also given in Figure 3.10, yellow section shows every hour of the day.

Table 4.29. Bus load values - with controller (P – S – I)

Cons. Data	Hour of Day	LOAD		
		ACTIVE P. (P) W	APPARENT P. (S) VA	CURRENT (I) A
0,66666667	00:00	-5,88E+06	6,18E+06	1,25E+04
0,625	01:00	-5,82E+06	6,13E+06	1,29E+04
0,58333333	02:00	-5,61E+06	5,90E+06	1,23E+04
0,5625	03:00	-5,39E+06	5,68E+06	1,19E+04
0,54166667	04:00	-5,19E+06	5,46E+06	1,14E+04
0,51666667	05:00	-5,49E+06	5,79E+06	1,25E+04
0,5625	06:00	-5,76E+06	6,07E+06	1,28E+04
0,58333333	07:00	-6,80E+06	7,15E+06	1,48E+04
0,66666667	08:00	-7,51E+06	7,91E+06	1,69E+04
0,75	09:00	-8,37E+06	8,80E+06	1,85E+04
0,83333333	10:00	-8,78E+06	9,24E+06	1,94E+04
0,875	11:00	-8,97E+06	9,44E+06	1,97E+04
0,89583333	12:00	-9,32E+06	9,81E+06	2,04E+04
0,9375	13:00	-9,61E+06	1,01E+07	2,09E+04
0,95833333	14:00	-9,69E+06	1,02E+07	2,11E+04
0,96875	15:00	-9,82E+06	1,03E+07	2,11E+04
0,97916667	16:00	-1,00E+07	1,05E+07	2,16E+04
1	17:00	-9,77E+06	1,03E+07	2,07E+04
0,97916667	18:00	-9,63E+06	1,01E+07	2,04E+04
0,95833333	19:00	-9,35E+06	9,84E+06	2,01E+04
0,9375	20:00	-9,10E+06	9,59E+06	1,99E+04
0,91666667	21:00	-8,60E+06	9,06E+06	1,90E+04
0,875	22:00	-7,63E+06	8,01E+06	1,77E+04
0,75	23:00	-6,78E+06	7,12E+06	1,45E+04
0,66666667	00:00	-5,88E+06	6,18E+06	1,25E+04

In Table 4.30 Bus PV line to neutral voltage, line to line voltage and reactive power and consumption data are shown in green column, also given in Figure 3.10, yellow section shows every hour of the day.

Table 4.30. Bus PV farm values - with controller (V – Q)

Cons. Data	Hour of Day	PV FARM		
		VOLTAGE (V)L-N	VOLTAGE (V)L-L	REACTIVE P. (Q)VAr
0,66667	00:00	2,06E+04	25171,57001	-4,50E+04
0,625	01:00	2,02E+04	24779,60396	-4,51E+04
0,58333	02:00	2,03E+04	24828,59972	-4,51E+04
0,5625	03:00	2,03E+04	24914,34229	-4,51E+04
0,54167	04:00	2,03E+04	24816,35078	-4,51E+04
0,51667	05:00	2,02E+04	24742,85714	-4,51E+04
0,5625	06:00	2,01E+04	24620,36775	-4,51E+04
0,58333	07:00	2,02E+04	24693,86139	-4,51E+04
0,66667	08:00	2,03E+04	24914,34229	-4,63E+04
0,75	09:00	2,03E+04	24853,0976	-4,69E+04
0,83333	10:00	2,03E+04	24828,59972	-4,76E+04
0,875	11:00	2,04E+04	24938,84017	-4,76E+04
0,89583	12:00	2,05E+04	25061,32956	-4,65E+04
0,9375	13:00	2,04E+04	24987,83593	-4,77E+04
0,95833	14:00	2,04E+04	24987,83593	-4,67E+04
0,96875	15:00	2,07E+04	25294,05941	-4,58E+04
0,97917	16:00	2,06E+04	25196,06789	-4,50E+04
1	17:00	2,06E+04	25183,81895	-4,50E+04
0,97917	18:00	2,08E+04	25502,29137	-4,50E+04
0,95833	19:00	2,07E+04	25343,05516	-4,50E+04
0,9375	20:00	2,06E+04	25196,06789	-4,50E+04
0,91667	21:00	2,05E+04	25061,32956	-4,50E+04
0,875	22:00	2,06E+04	25171,57001	-4,50E+04
0,75	23:00	2,04E+04	25024,58274	-4,50E+04
0,66667	00:00	2,06E+04	25171,57001	-4,50E+04

In Table 4.31 Bus PV active power, apparent power and current and consumption data are shown in green column, also given in Figure 3.10, yellow section shows every hour of the day.

Table 4.31. Bus PV farm values - with controller (P – S – I)

Cons. Data	Hour of Day	PV FARM		
		ACTIVE P. (P) W	APPARENT P. (S) VA	CURRENT (I) A
0,666667	00:00	-964,2	4,50E+04	1,497
0,625	01:00	-935	4,51E+04	1,521
0,583333	02:00	-938	4,51E+04	1,517
0,5625	03:00	-940	4,51E+04	1,514
0,541667	04:00	-943	4,51E+04	1,513
0,516667	05:00	605	4,51E+04	1,529
0,5625	06:00	3,40E+04	5,65E+04	2,33
0,583333	07:00	5,60E+05	5,62E+05	18,37
0,666667	08:00	1,95E+06	1,95E+06	61,61
0,75	09:00	3,11E+06	3,11E+06	104,7
0,833333	10:00	4,09E+06	4,09E+06	130,1
0,875	11:00	4,21E+06	4,21E+06	137,7
0,895833	12:00	4,13E+06	4,13E+06	135,7
0,9375	13:00	3,78E+06	3,78E+06	121,6
0,958333	14:00	2,73E+06	2,73E+06	91,18
0,96875	15:00	1,51E+06	1,51E+06	49,08
0,979167	16:00	3,46E+05	3,49E+05	16,53
1	17:00	-1016	4,50E+04	1,723
0,979167	18:00	-1003	4,50E+04	1,479
0,958333	19:00	-989,8	4,50E+04	1,487
0,9375	20:00	-977,5	4,50E+04	1,492
0,916667	21:00	-981,3	4,50E+04	1,506
0,875	22:00	-972	4,50E+04	1,491
0,75	23:00	-954	4,50E+04	1,502
0,666667	00:00	-964,2	4,50E+04	1,497

In Table 4.32 Bus ASM line to neutral voltage, line to line voltage and reactive power and consumption data are shown in green column, also given in Figure 3.10, yellow section shows every hour of the day.

Table 4.32. Bus ASM values - with controller (V – Q)

Cons. Data	Hour of Day	ASM		
		VOLTAGE (V)L-N	VOLTAGE (V)L-L	REACTIVE P. (Q)VAr
0,666667	00:00	326,8	400,2953324	-4,50E+04
0,625	01:00	319,2	390,9861386	-4,50E+04
0,583333	02:00	319,9	391,8435644	-4,50E+04
0,5625	03:00	320,7	392,8234795	-4,50E+04
0,541667	04:00	321,3	393,5584158	-4,50E+04
0,516667	05:00	319,8	391,721075	-4,50E+04
0,5625	06:00	319,3	391,108628	-4,50E+04
0,583333	07:00	316,6	387,8014144	-4,50E+04
0,666667	08:00	316,4	387,5564356	-4,50E+04
0,75	09:00	319,1	390,8636492	-4,60E+04
0,833333	10:00	318,1	389,6387553	-4,60E+04
0,875	11:00	317,5	388,903819	-4,60E+04
0,895833	12:00	318,9	390,6186704	-4,60E+04
0,9375	13:00	322,4	394,9057992	-4,60E+04
0,958333	14:00	321,1	393,3134371	-4,60E+04
0,96875	15:00	325,7	398,9479491	-4,50E+04
0,979167	16:00	324,5	397,4780764	-4,50E+04
1	17:00	330,7	405,0724187	-4,50E+04
0,979167	18:00	328,3	402,1326733	-4,50E+04
0,958333	19:00	326,5	399,9278642	-4,50E+04
0,9375	20:00	324,4	397,355587	-4,50E+04
0,916667	21:00	326,2	399,560396	-4,50E+04
0,875	22:00	325,7	398,9479491	-4,50E+04
0,75	23:00	324,2	397,1106082	-4,50E+04
0,666667	00:00	326,8	400,2953324	-4,50E+04

In Table 4.33 Bus ASM active power, apparent power and current and consumption data are shown in green column, also given in Figure 3.10, yellow section shows every hour of the day.

Table 4.33. Bus ASM values - with controller (P – S – I)

Cons. Data	Hour of Day	ASM		
		ACTIVE P. (P) W	APPARENT P. (S) VA	CURRENT (I) A
0,66666667	00:00	-5,60E+06	5,50E+06	1,25E+04
0,625	01:00	-5,60E+06	5,50E+06	1,27E+04
0,58333333	02:00	-5,60E+06	5,50E+06	1,27E+04
0,5625	03:00	-5,60E+06	5,50E+06	1,27E+04
0,54166667	04:00	-5,60E+06	5,50E+06	1,27E+04
0,51666667	05:00	-5,60E+06	5,50E+06	1,27E+04
0,5625	06:00	-5,60E+06	5,50E+06	1,27E+04
0,58333333	07:00	-5,60E+06	5,50E+06	1,28E+04
0,66666667	08:00	-5,60E+06	5,50E+06	1,28E+04
0,75	09:00	-5,60E+06	5,50E+06	1,27E+04
0,83333333	10:00	-5,60E+06	5,50E+06	1,27E+04
0,875	11:00	-5,60E+06	5,50E+06	1,28E+04
0,89583333	12:00	-5,60E+06	5,50E+06	1,27E+04
0,9375	13:00	-5,60E+06	5,50E+06	1,26E+04
0,95833333	14:00	-5,60E+06	5,50E+06	1,25E+04
0,96875	15:00	-5,60E+06	5,50E+06	1,25E+04
0,97916667	16:00	-5,60E+06	5,50E+06	1,25E+04
1	17:00	-5,60E+06	5,50E+06	1,23E+04
0,97916667	18:00	-5,60E+06	5,50E+06	1,24E+04
0,95833333	19:00	-5,60E+06	5,50E+06	1,25E+04
0,9375	20:00	-5,60E+06	5,50E+06	1,25E+04
0,91666667	21:00	-5,60E+06	5,50E+06	1,25E+04
0,875	22:00	-5,60E+06	5,50E+06	1,25E+04
0,75	23:00	-5,60E+06	5,50E+06	1,25E+04
0,66666667	00:00	-5,60E+06	5,50E+06	1,25E+04

4.3. Case 1: All Graph without Controller

Figure 4.2 shows us voltage on bus 1 which belongs to voltage source block before the OLTC voltage change slightly with usage of system in first simulation there is no control so this curve shape with consumption data.

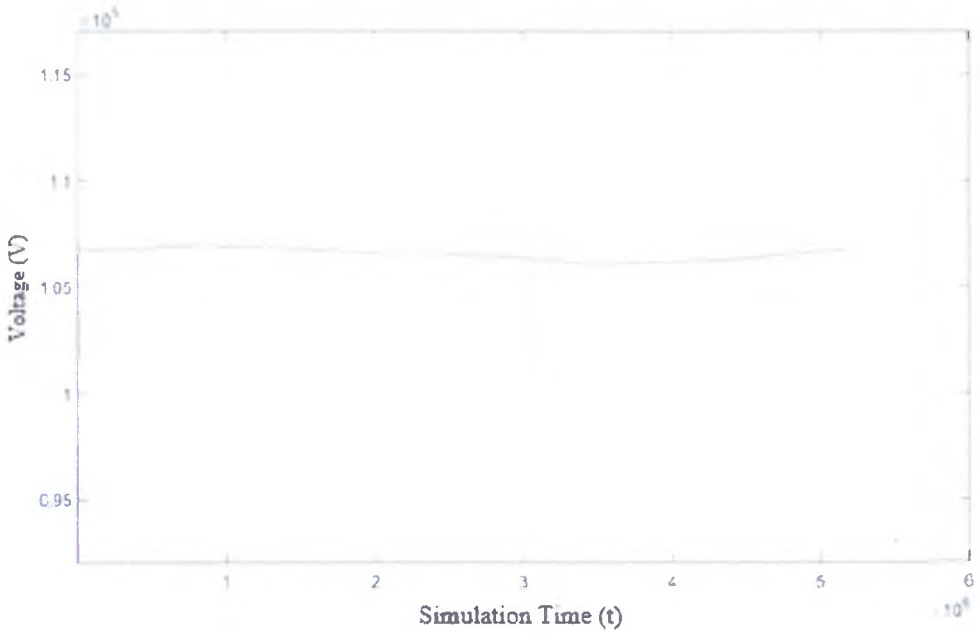

Figure 4.2. Voltage graph of bus 1 (V_{bus1})

Figure 4.3 shows us voltage on bus 2 which also measures feedback for OLTC and it is placed after the OLTC voltage change slightly with usage of system in first simulation there is no control so this curve shape with consumption data.

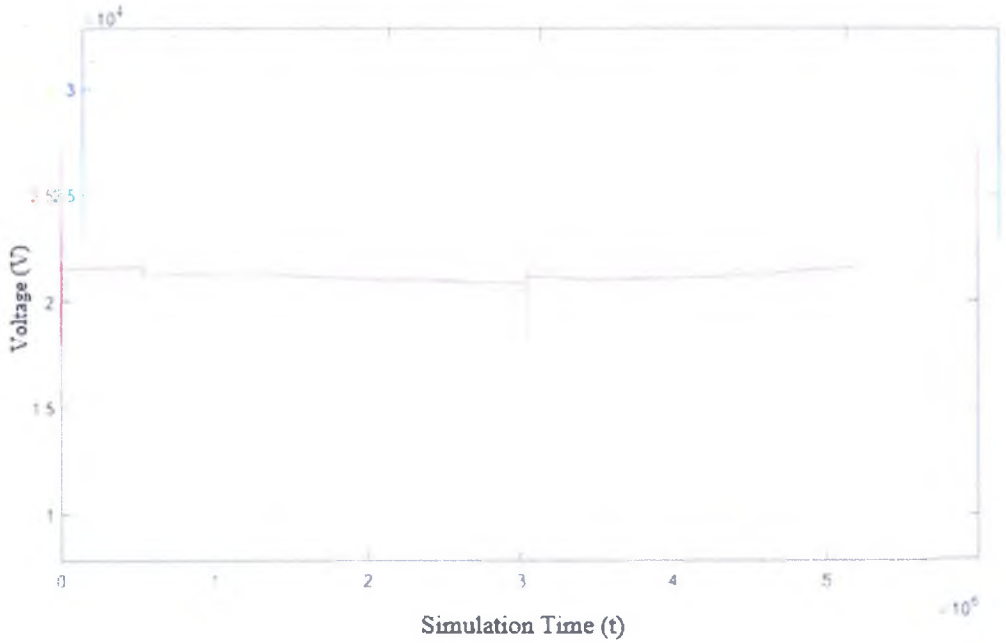

Figure 4.3. Voltage graph of bus 2 (V_{bus2})

Figure 4.4 shows us voltage on bus 3 which measures voltage of diesel generator, voltage change slightly with usage of system in first simulation there is no control so this curve shape with consumption data.

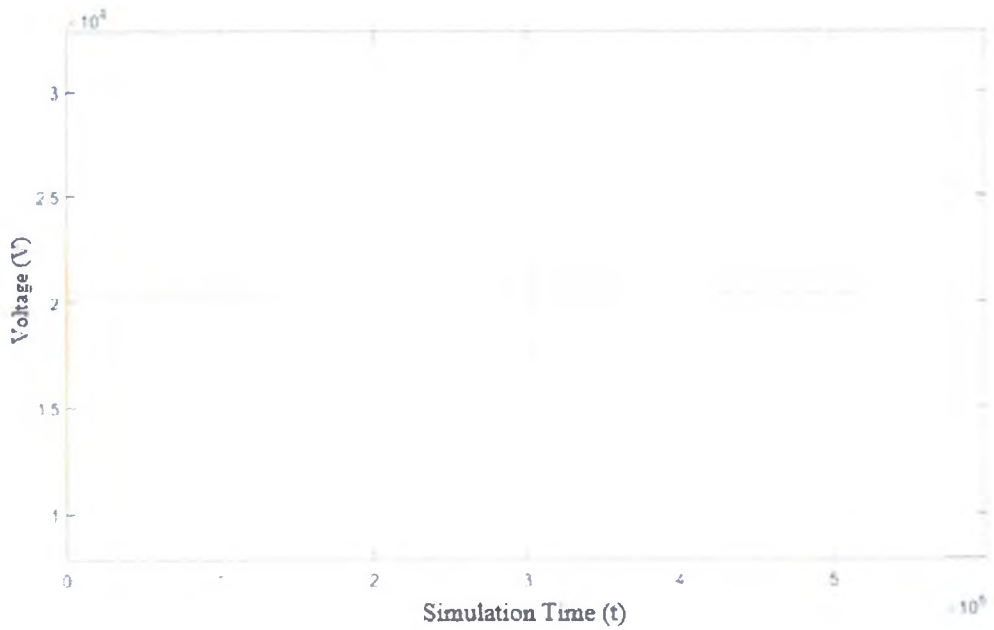

Figure 4.4. Voltage graph of bus 3 (V_{bus3})

Figure 4.5 shows us voltage on bus4 which measures the voltage of 15 MW residential load voltage change slightly with usage of system in first simulation there is no control so this curve shape with consumption data.

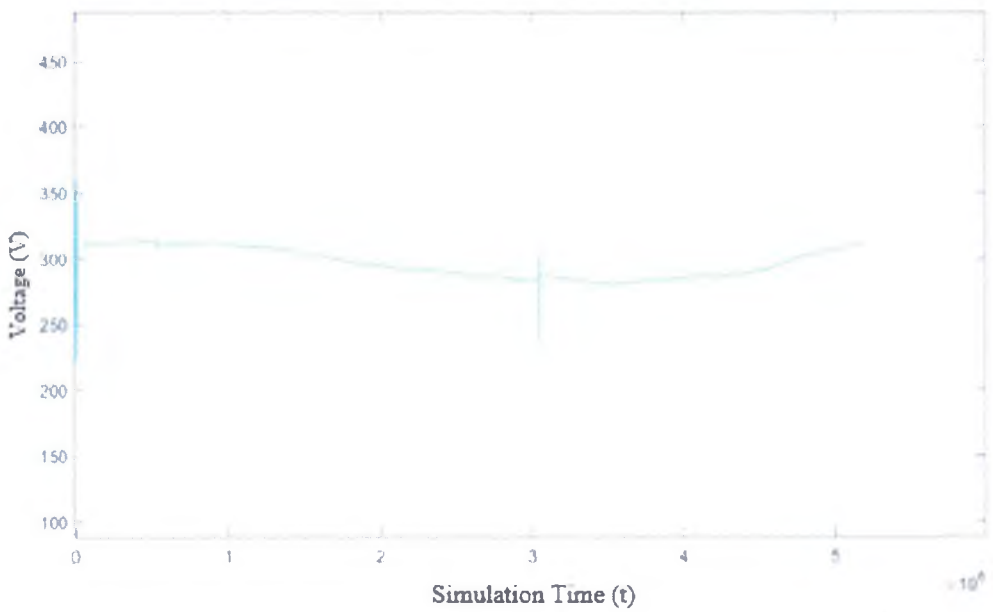

Figure 4.5. Voltage graph of bus 4 (V_{bus4})

Figure 4.6 shows us voltage on bus5 which measures voltage of 10MW residential load and ASM, voltage change slightly with usage of system in first simulation there is no control so this curve shape with consumption data.

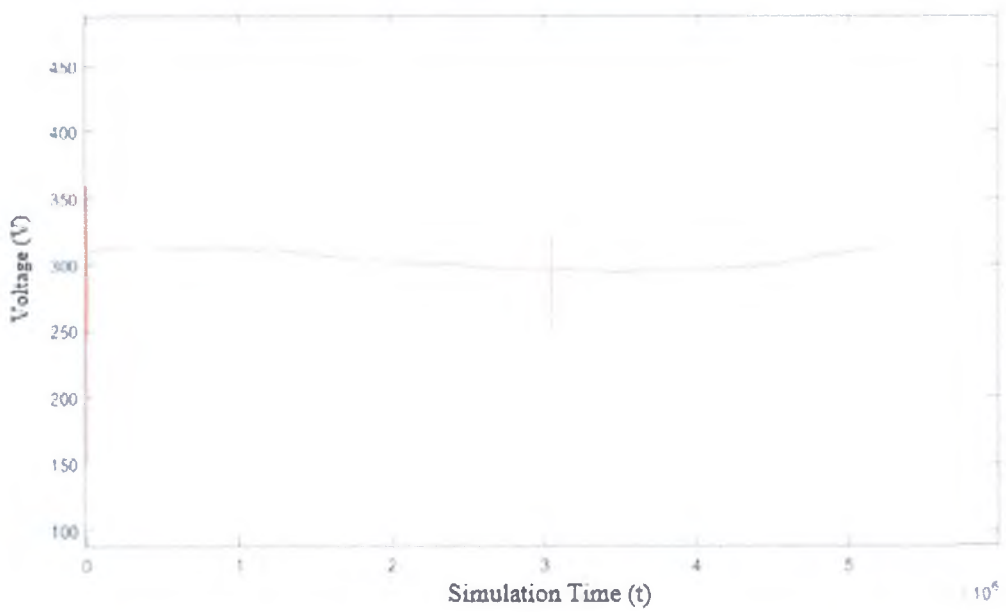

Figure 4.6. Voltage graph of bus 5 (V_{bus5})

This graph Figure 4.7 shows us voltage on load bus which also inside of bus5 represents residential loads, voltage change slightly with usage of system in first simulation there is no control so this curve shape with consumption data.

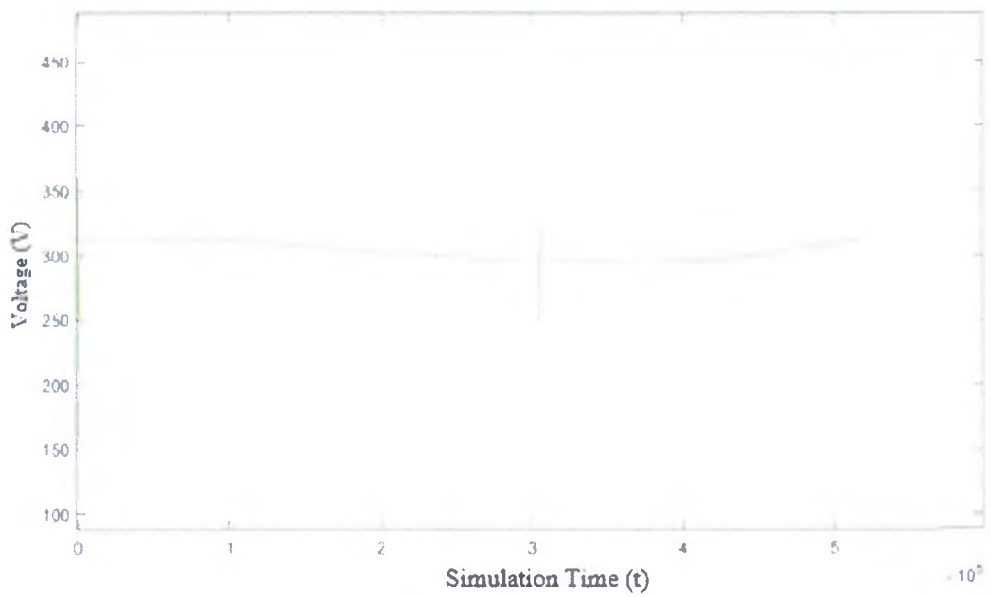

Figure 4.7. Voltage graph of load (V_{load})

Figure 4.8 shows us voltage on PV bus, actually voltage on this bus is the same as line voltage which 25kV, PV's are not producing any voltage in night time, also it can be seen on radiation data.

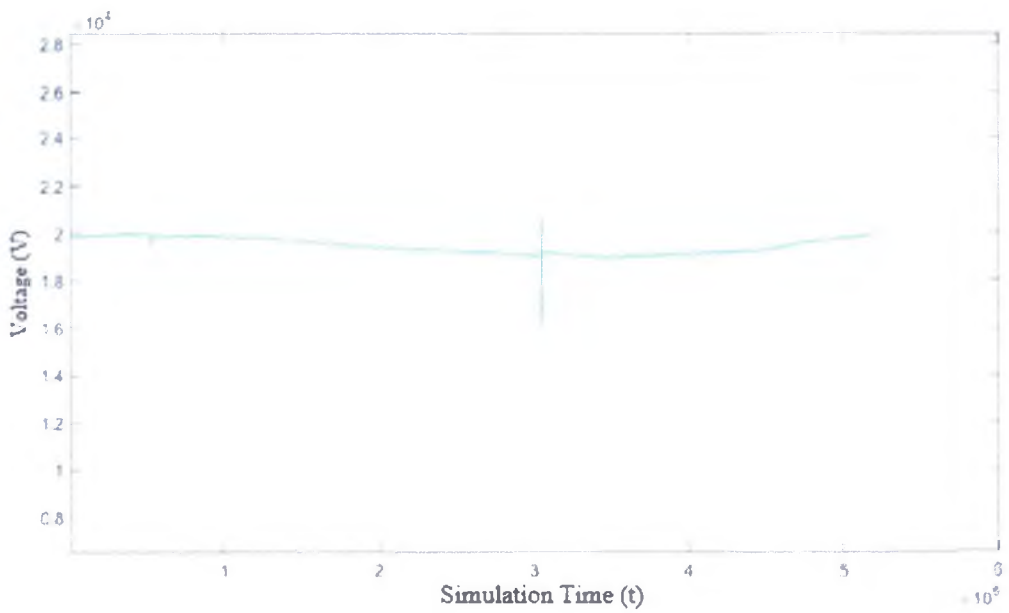

Figure 4.8. Voltage graph of PV (V_{PV})

Figure 4.9 shows us voltage on ASM bus which is also inside of bus5, voltage change slightly with usage of system in first simulation there is no control so this curve shape with consumption data.

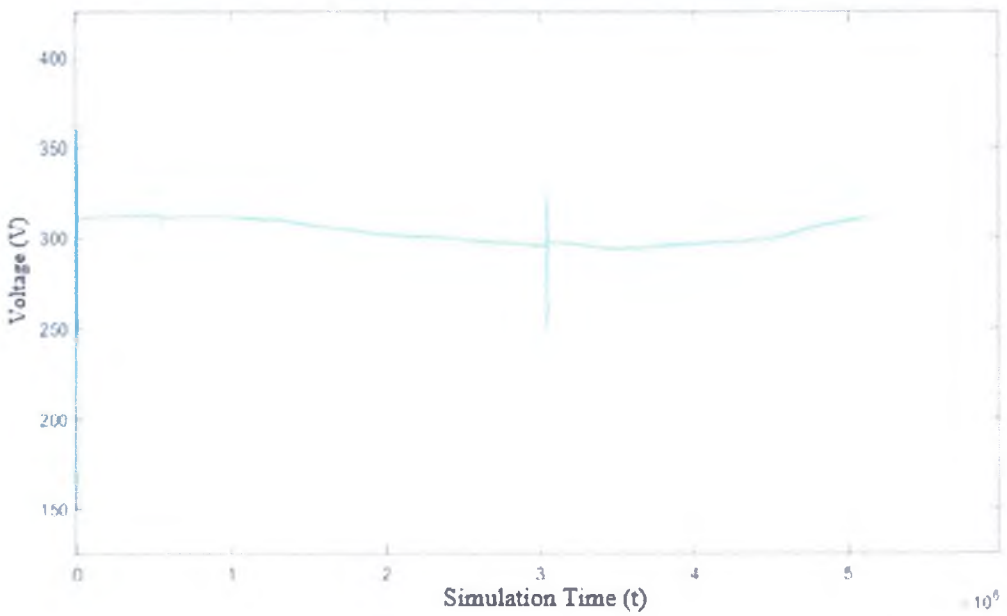

Figure 4.9. Voltage graph of ASM (V_{ASM})

This graph Figure 4.10 shows us all voltages on all buses,

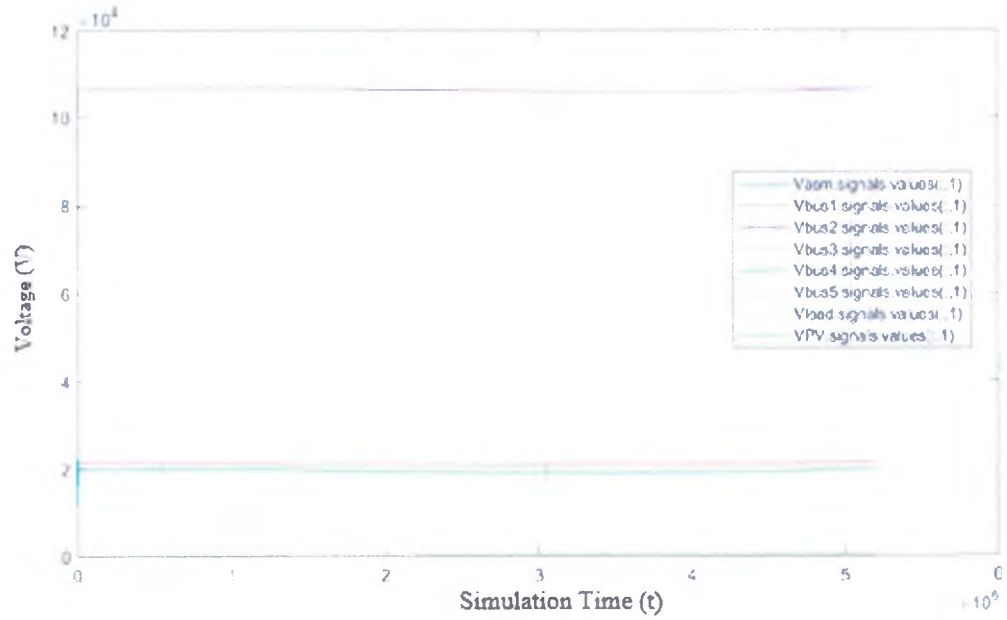

Figure 4.10. Voltage graphs of all (V_{all})

Figure 4.11 shows us active power on bus1 which belongs to voltage source block before the OLTC, active power change with usage of system in first simulation there is no control so this curve shape with consumption data.

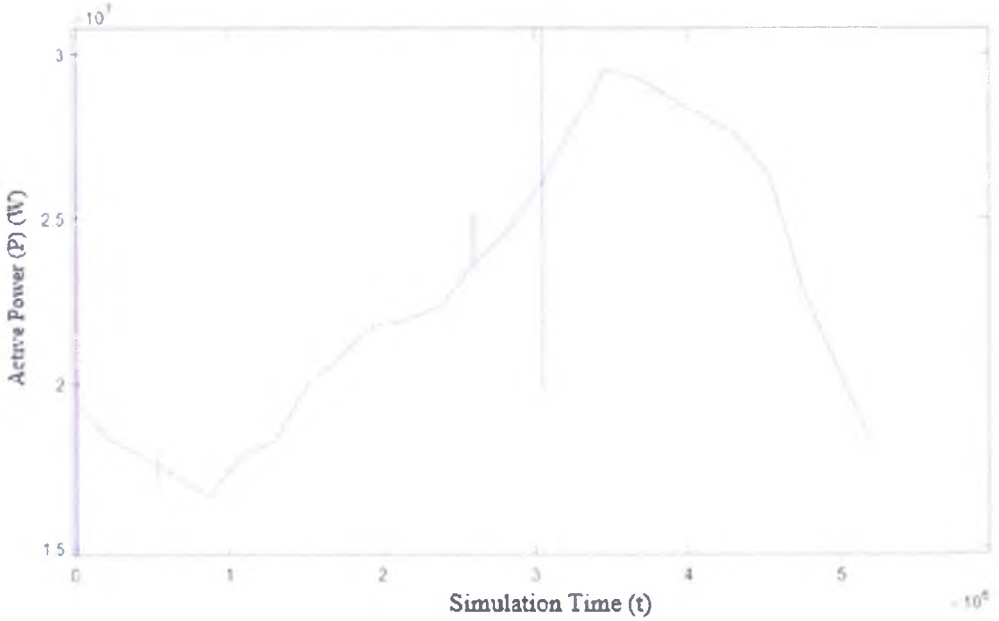

Figure 4.11. Active power graph of bus 1 (P_{bus1})

Figure 4.12 shows us active power on bus2 which also measures feedback for OLTC and it is placed after the OLTC active power change with usage of system in first simulation there is no control so this curve shape with consumption data.

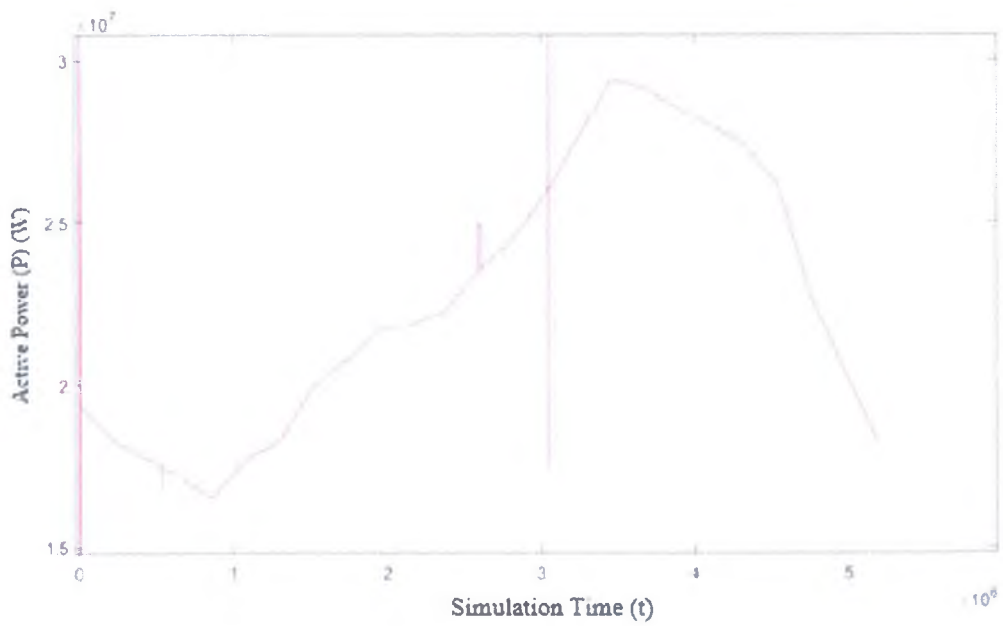

Figure 4.12. Active power graph of bus 2 (P_{bus2})

Figure 4.13 shows us active power on bus3. This block measures voltage and current of diesel generator, active power change slightly with usage of system in first simulation there is no control so this curve shape with consumption data.

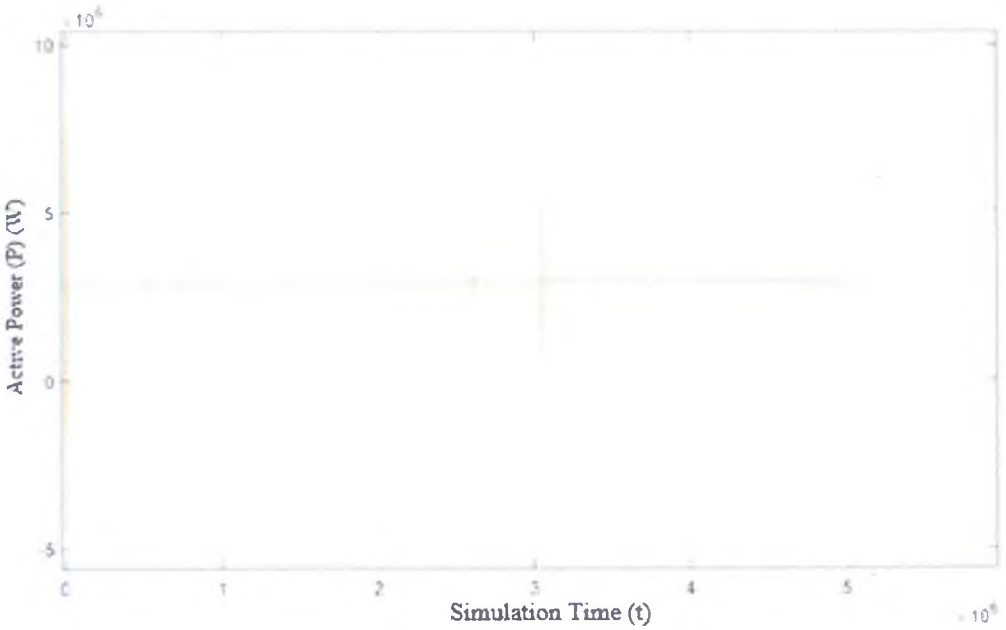

Figure 4.13. Active power graph of bus 3 (P_{bus3})

Figure 4.14 shows us active power on bus4 which measures the active power of 15 MW residential load active power change with usage of system in first simulation there is no control so this curve shape with consumption data.

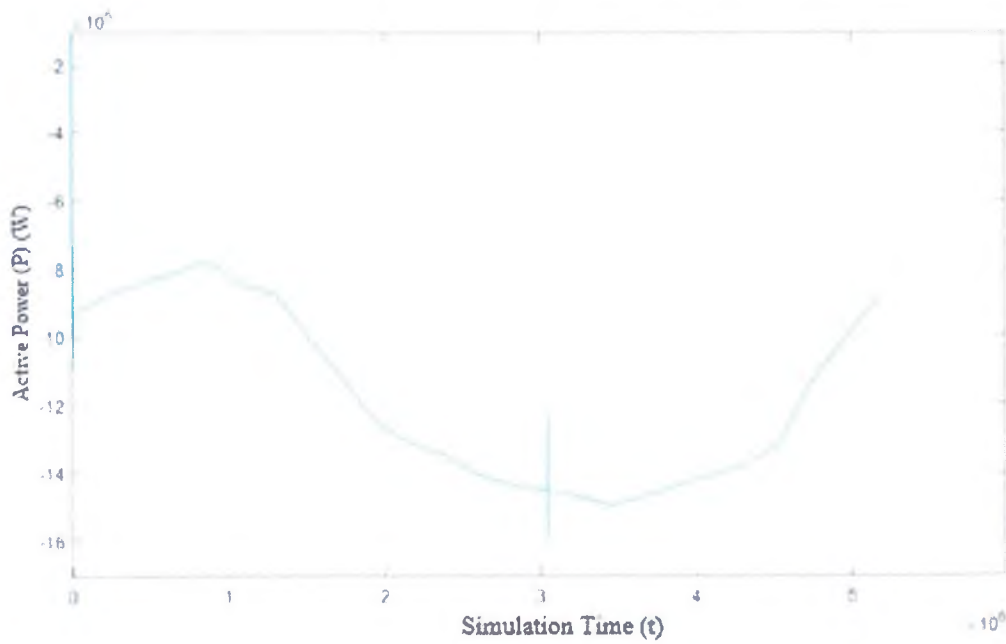

Figure 4.14. Active power graph of bus 4 (P_{bus4})

Figure 4.15 shows us active power on bus5 which measures voltage and current of 10MW residential load and ASM, active power change with usage of system in first simulation there is no control so this curve shape with consumption data.

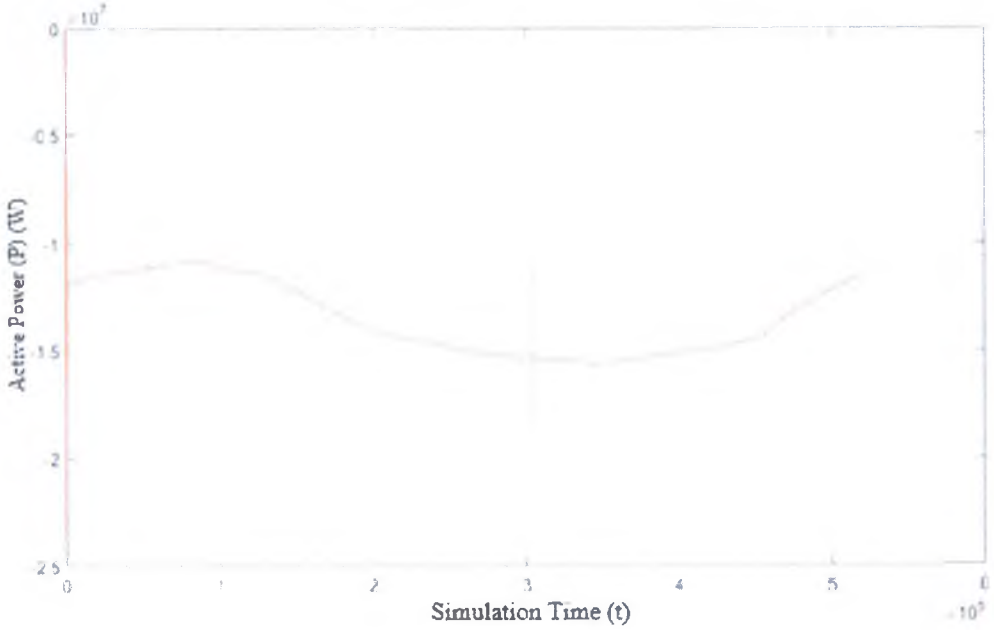

Figure 4.15. Active power graph of bus 5 (P_{bus5})

Figure 4.16 shows us active power on load bus which also inside of bus5 represent residential loads, active power change with usage of system in first simulation there is no control so this curve shape with consumption data.

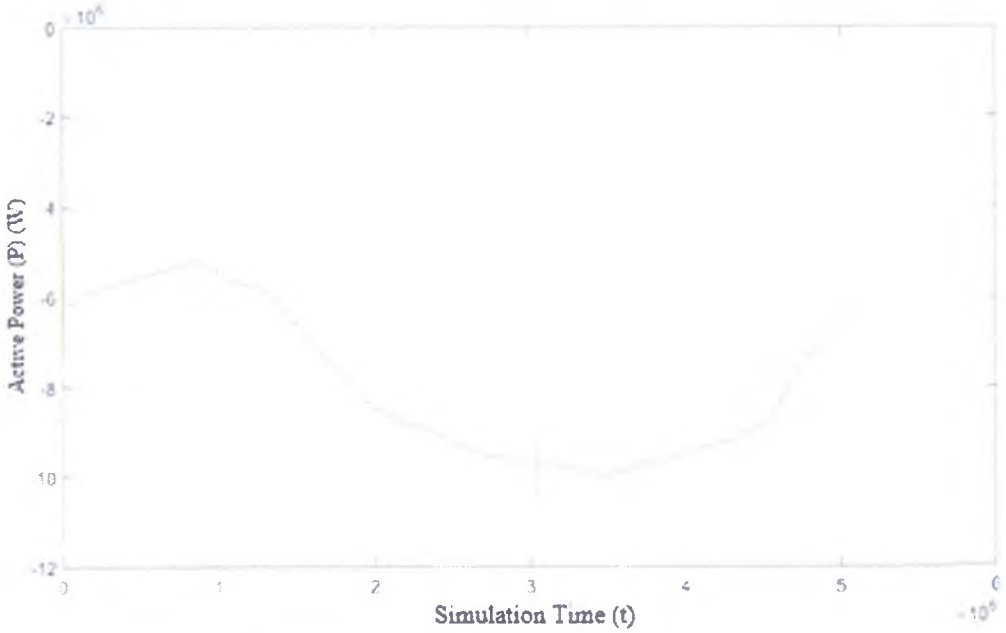

Figure 4.16. Active power graph of load (P_{load})

Figure 4.17 shows us active power on PV bus which changes parallel with irradiance data and PV system block produce maximum energy at 13:00-14:00.

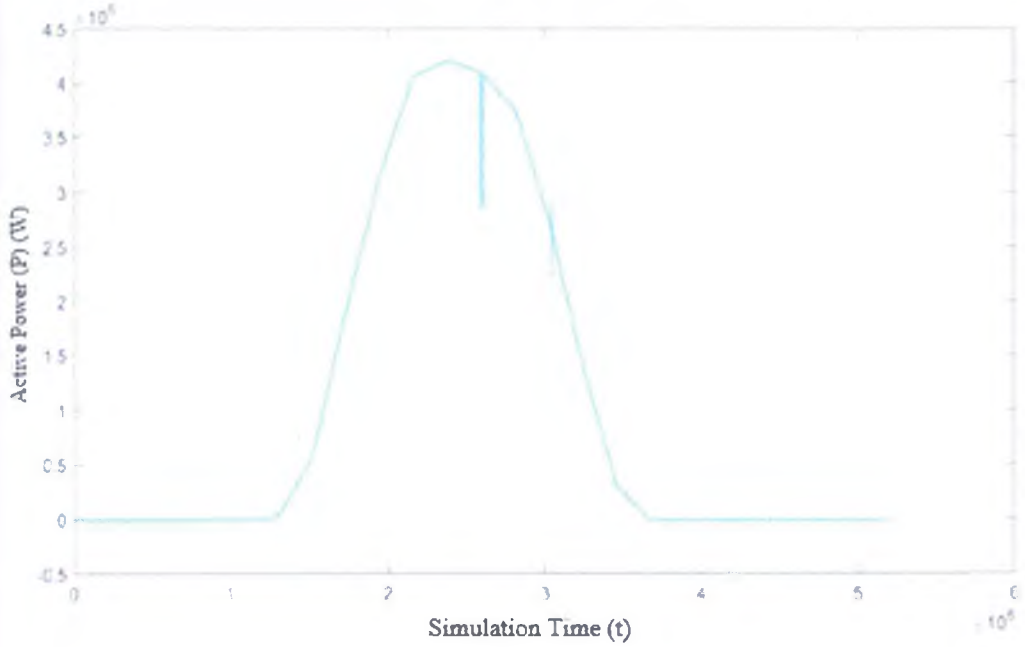

Figure 4.17. Active power graph of PV (P_{PV})

Figure 4.18 shows us active power on ASM bus which is also inside of bus5, voltage change with usage of system in first simulation there is no control so this curve shape with consumption data.

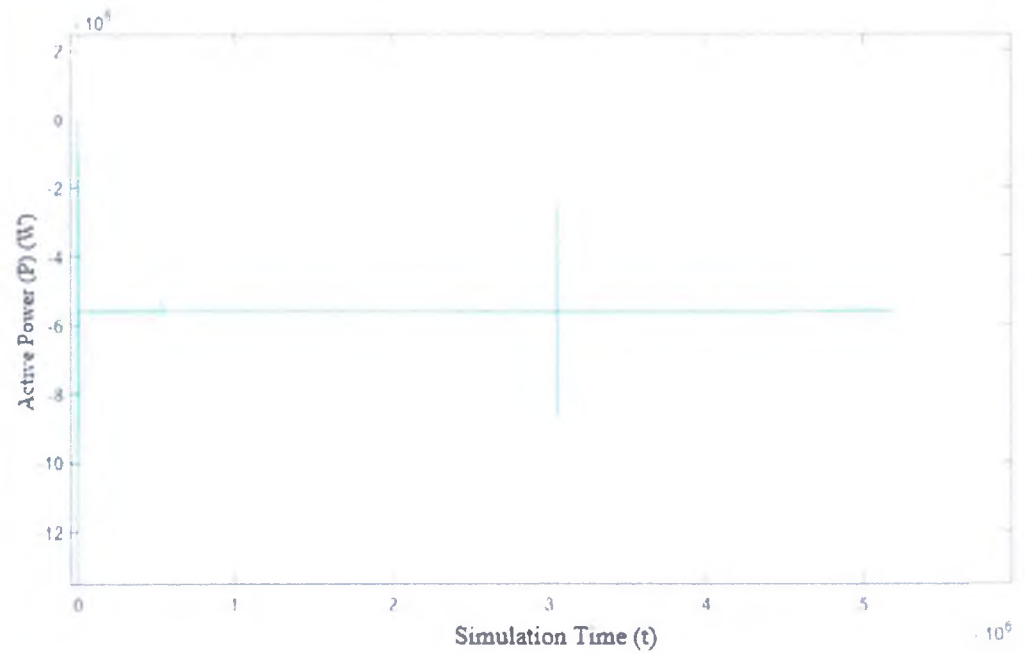

Figure 4.18. Active power graph of ASM (P_{ASM})

Figure 4.19 shows us all active power on all buses.

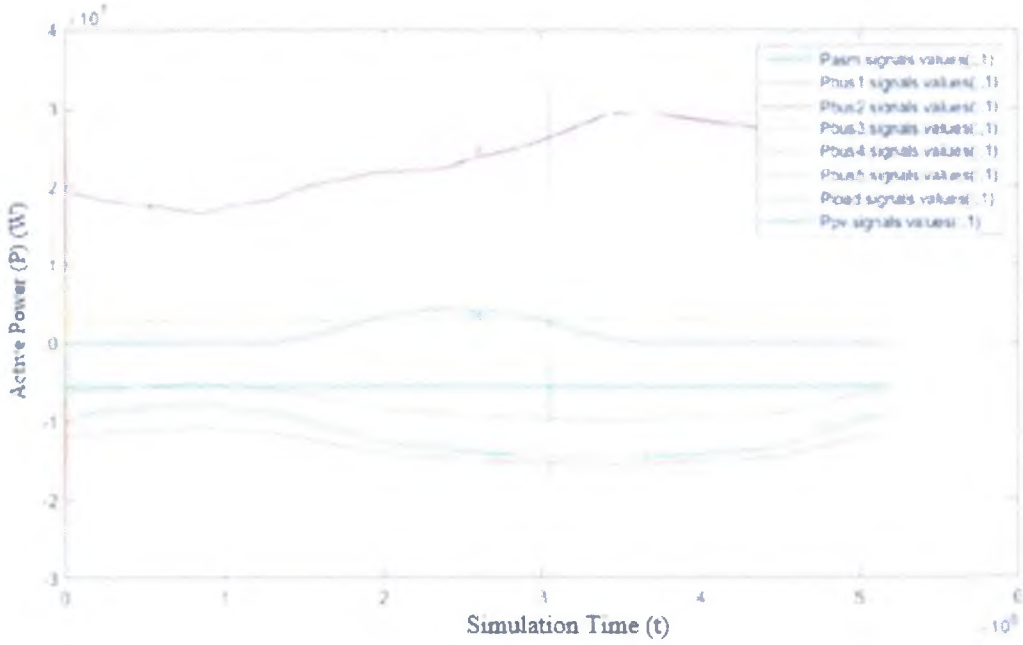

Figure 4.19. Active power graphs of all (P_{all})

Figure 4.11 shows us reactive power on bus1. This bus belongs to voltage source block before the OLTC, reactive power change with usage of system in first simulation there is no control so this curve shape with consumption data.

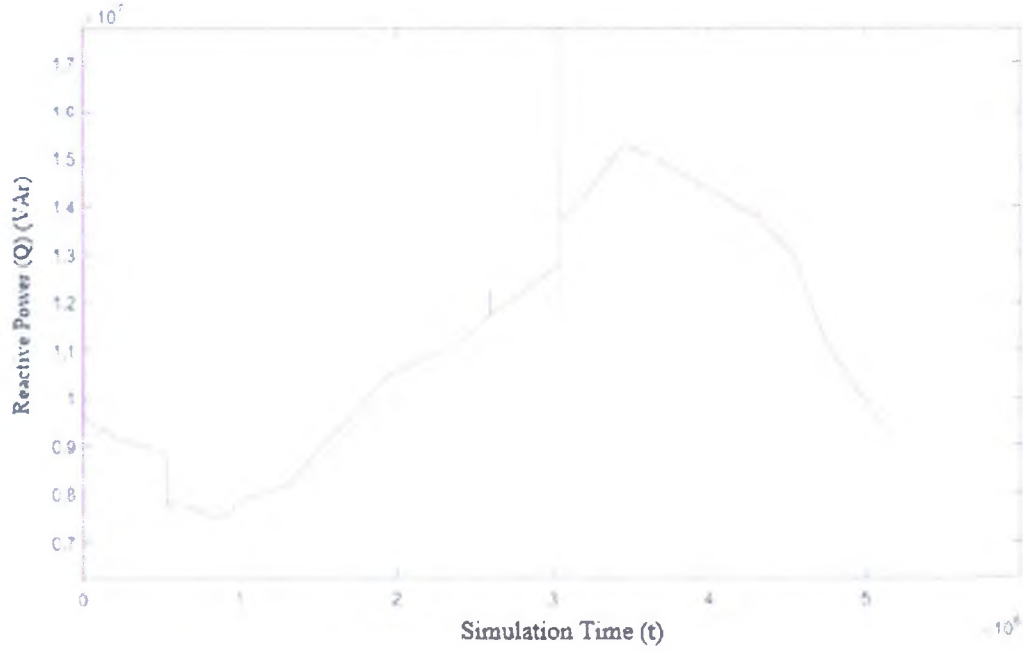

Figure 4.20. Reactive power graph of bus 1 (Q_{bus1})

Figure 4.21 shows us reactive power on bus2, this bus also measures feedback for OLTC and it is placed after the OLTC active power change with usage of system in first simulation there is no control so this curve shape with consumption data.

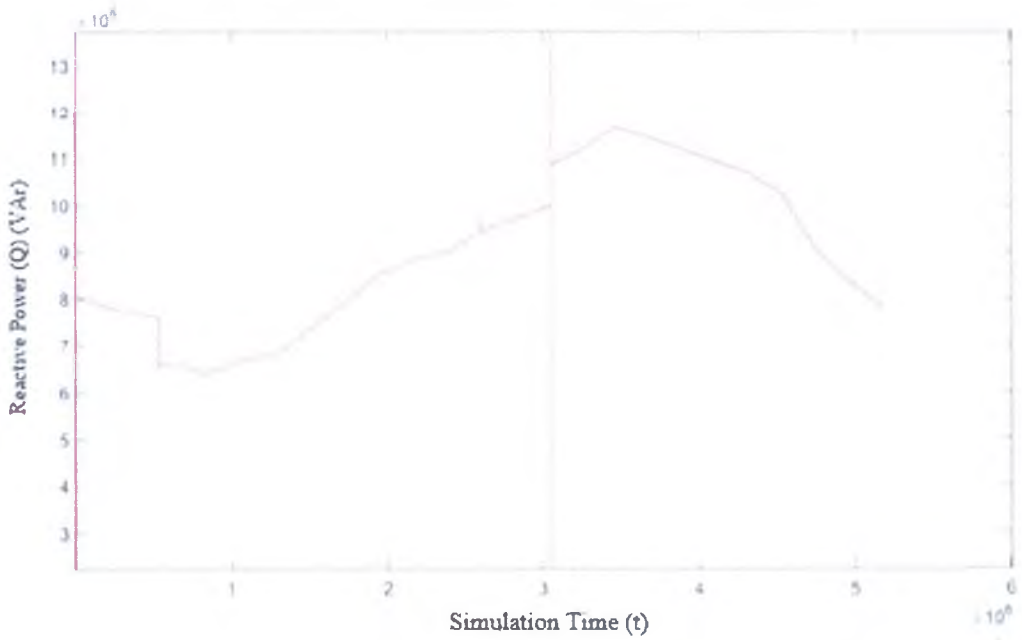

Figure 4.21. Reactive power graph of bus 2 (Q_{bus2})

Figure 4.22 shows us reactive power on bus3, this block measures voltage and current of diesel generator, reactive power change slightly with usage of system in first simulation there is no control so this curve shape with consumption data.

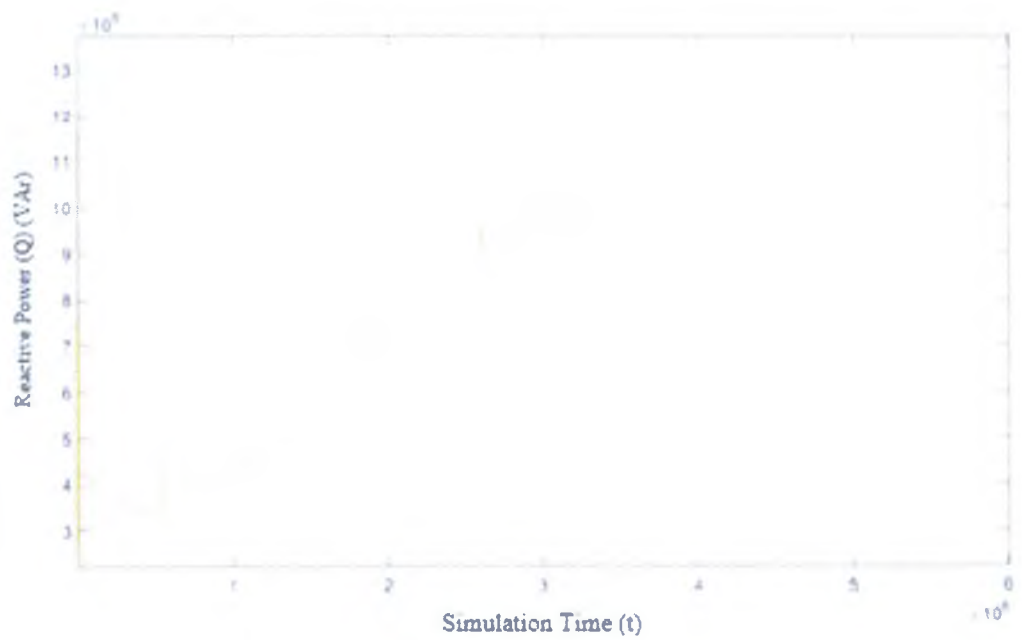

Figure 4.22. Reactive power graph of bus 3 (Q_{bus3})

Figure 4.23 shows us reactive power on bus4, which measures the reactive power of 15 MW residential load active power change with usage of system in first simulation there is no control so this curve shape with consumption data.

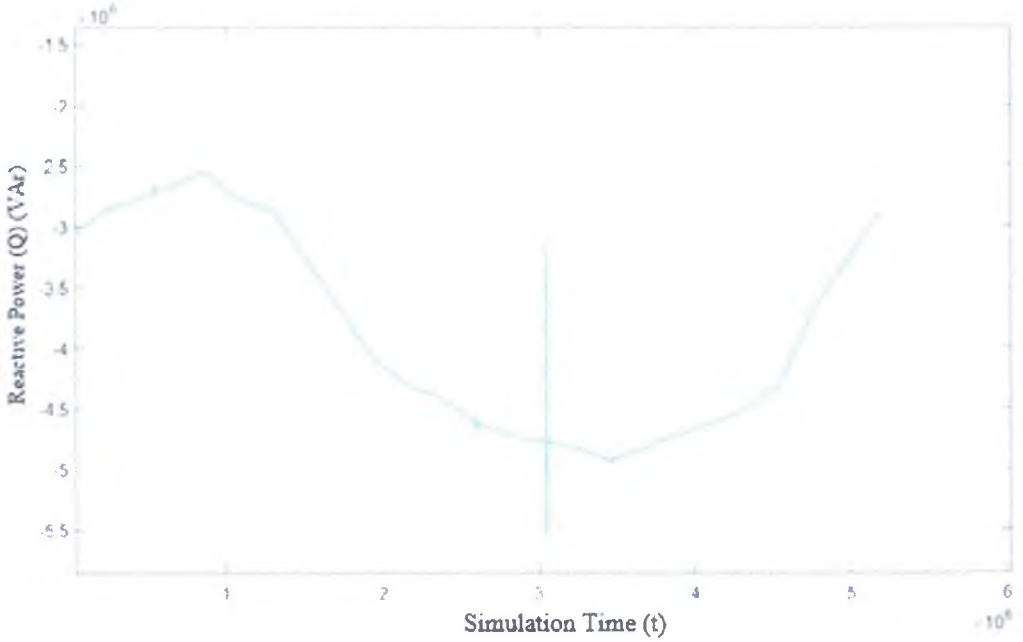

Figure 4.23. Reactive power graph of bus 4 (Q_{bus4})

Figure 4.24 shows us reactive power on bus5, which measures voltage and current of 10MW residential load and ASM, reactive power change with usage of system in first simulation there is no control so this curve shape with consumption data.

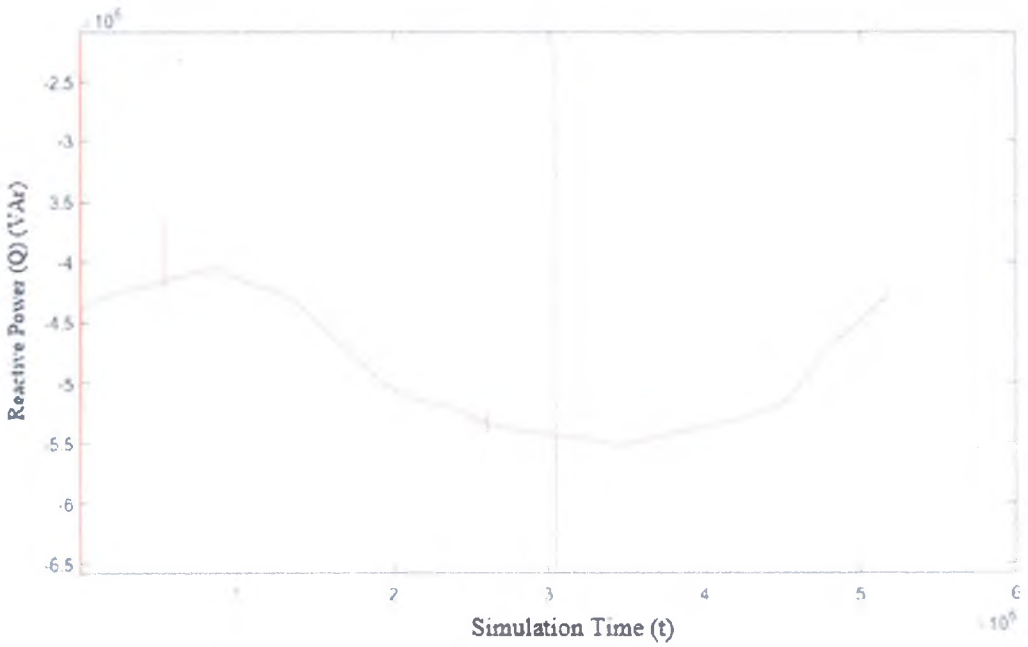

Figure 4.24. Reactive power graph of bus 5 (Q_{bus5})

Figure 4.25 shows us reactive power on load bus which is also inside of bus5 representing residential loads, reactive power change with usage of system in first simulation there is no control so this curve shape with consumption data.

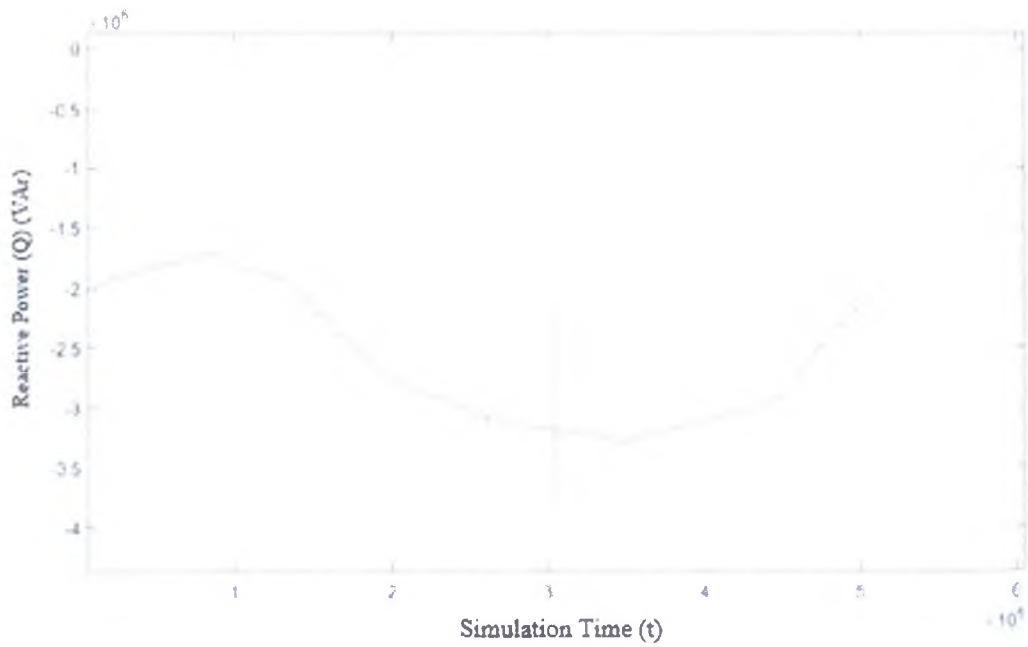

Figure 4.25. Reactive power graph of load (Q_{load})

Figure 4.26 shows us reactive power on PV bus which changes parallel with irradiance data and PV system block produce maximum energy at 13:00-14:00.

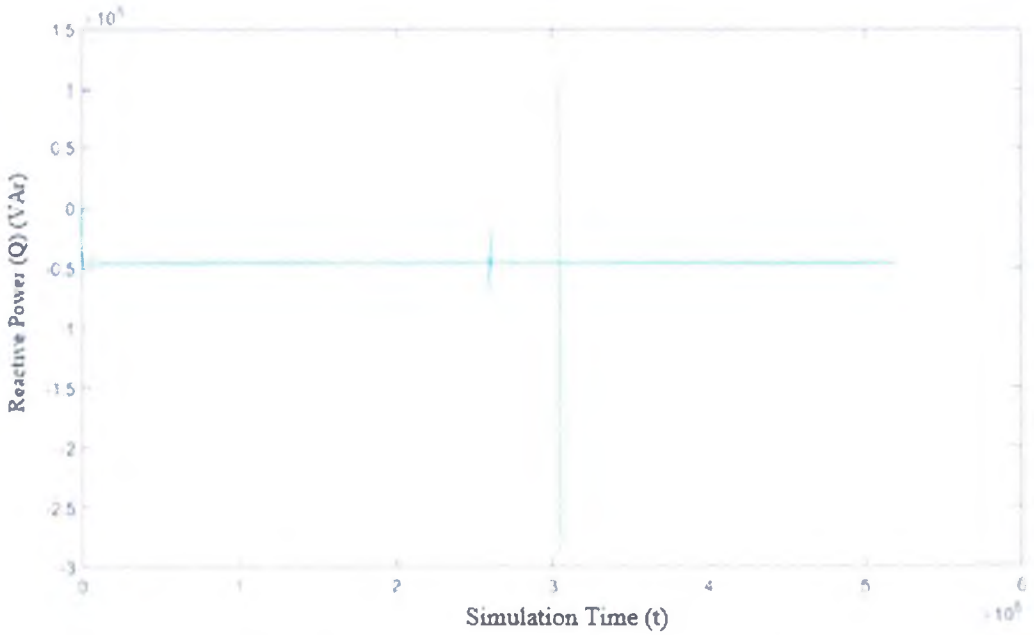

Figure 4.26. Reactive power graph of PV (Q_{PV})

Figure 4.27 shows us reactive power on ASM bus, which is also inside of bus5, reactive power change with usage of system in first simulation there is no control so this curve shape with consumption data.

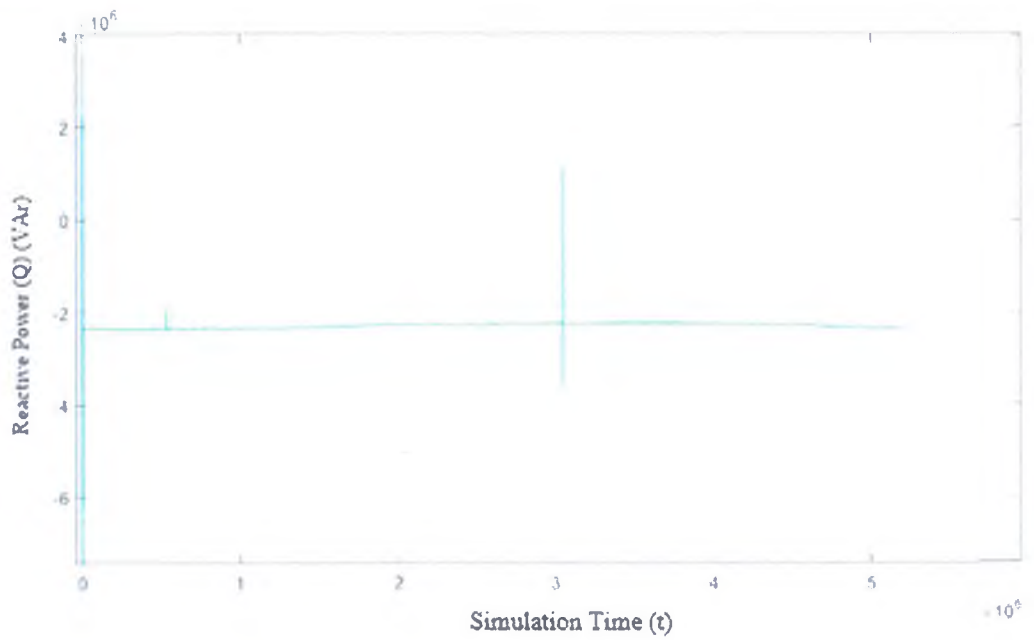

Figure 4.27. Reactive power graph of ASM (Q_{ASM})

Figure 4.28 shows us reactive power on all buses,

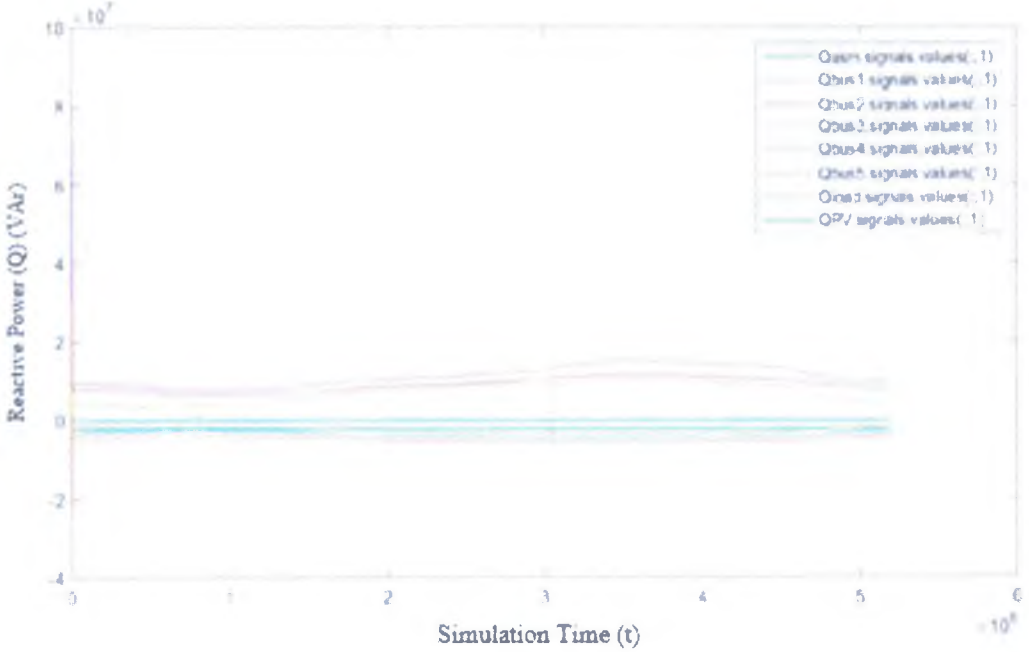

Figure 4.28. Reactive power graphs of all (Q_{all})

Figure 4.29 shows us apparent power on bus1 which belongs to voltage source block before the OLTC, apparent power change with usage of system in first simulation there is no control so this curve shape with consumption data.

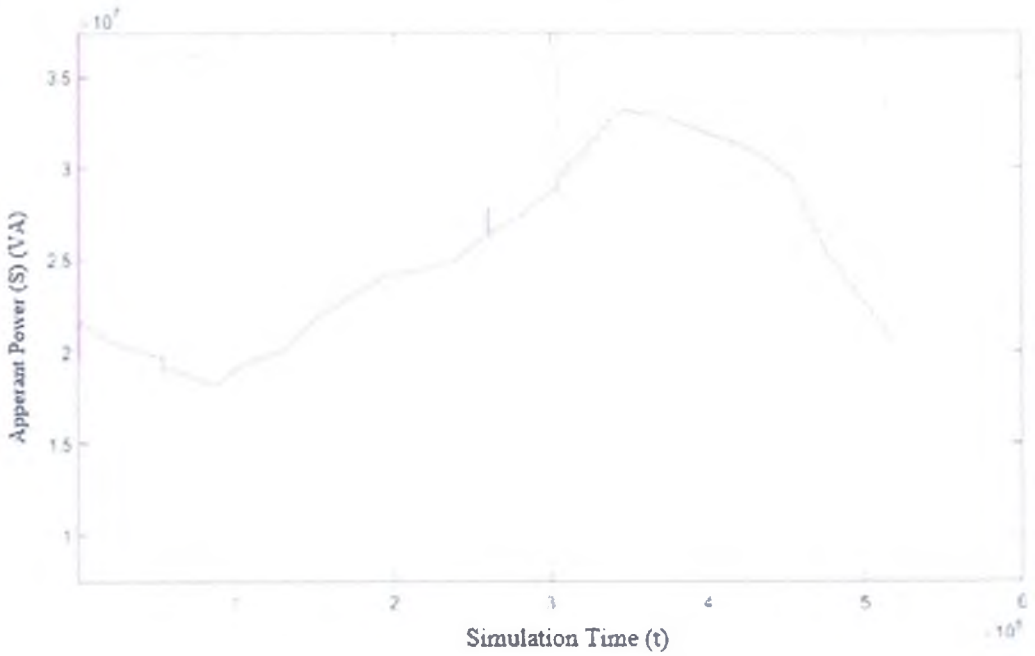

Figure 4.29. Apparent power graph of bus 1 (S_{bus1})

Figure 4.30 shows us apparent power on bus2. This bus also measures feedback for OLTC and it is placed after the OLTC apparent power change with usage of system in first simulation there is no control so this curve shape with consumption data.

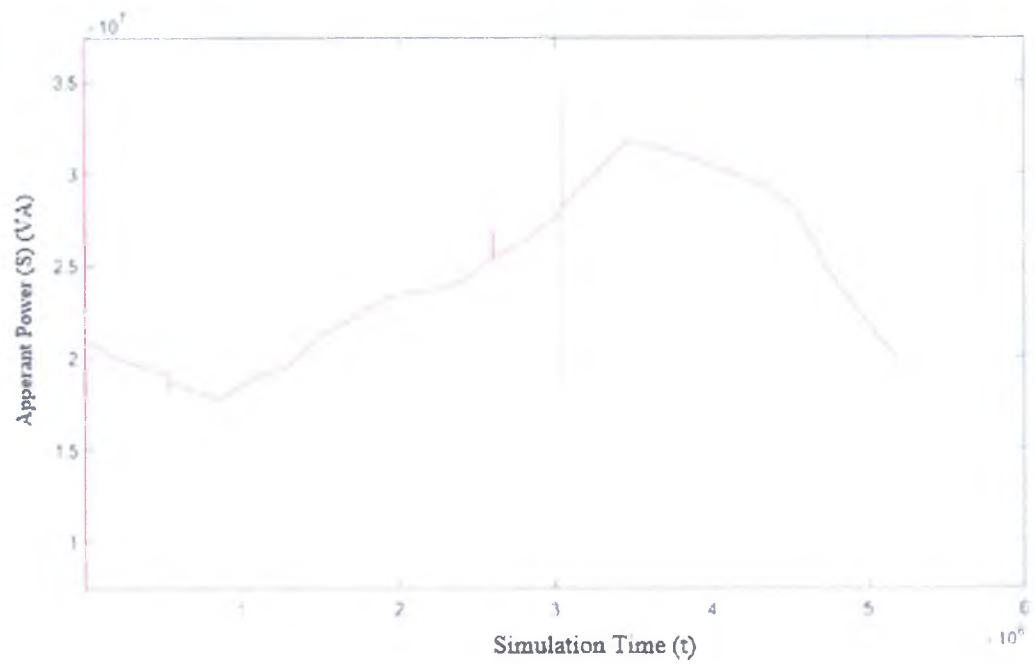

Figure 4.30. Apparent power graph of bus 2 (S_{bus2})

Figure 4.31 shows us reactive power on bus3. This block measures voltage and current of diesel generator, reactive power change slightly with usage of system in first simulation there is no control so this curve shape with consumption data.

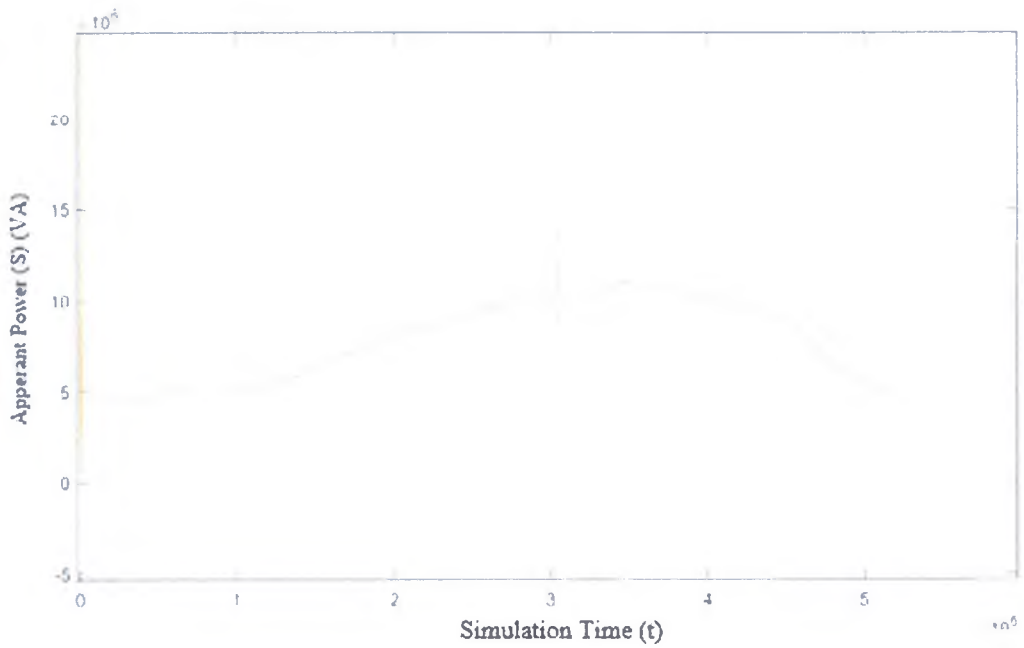

Figure 4.31. Apparent power graph of bus 3 (S_{bus3})

Figure 4.32 shows us apparent power on bus4 which measures the apparent power of 15 MW residential load active power change with usage of system in first simulation there is no control so this curve shape with consumption data.

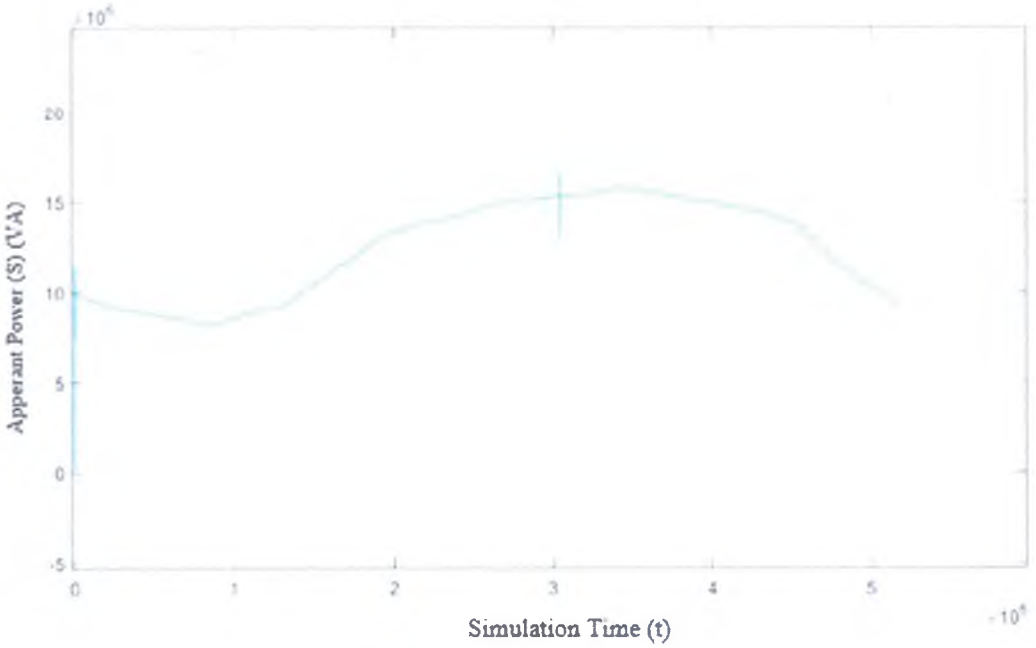

Figure 4.32. Apparent power graph of bus 4 (S_{bus4})

Figure 4.33 shows us apparent power on bus5 which measures voltage and current of 10MW residential load and ASM, apparent power change with usage of system in first simulation there is no control so this curve shape with consumption data.

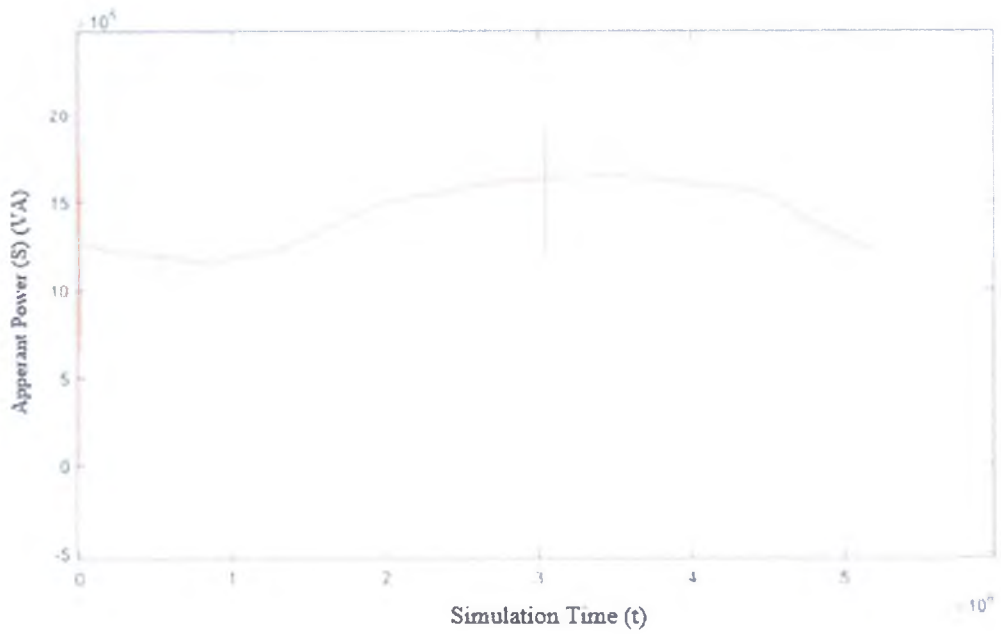

Figure 4.33. Apparent power graph of bus 5 (S_{bus5})

Figure 4.34 shows us apparent power on load bus which is also inside of bus5 represent residential loads, apparent power change with usage of system in first simulation there is no control so this curve shape with consumption data.

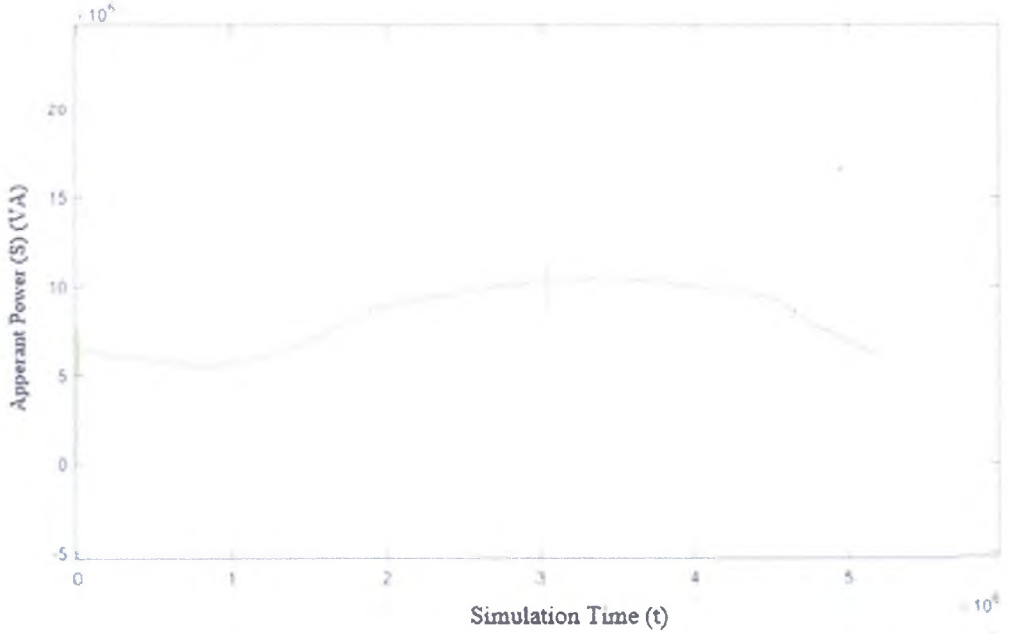

Figure 4.34. Apparent power graph of load (S_{load})

Figure 4.35 shows us apparent power on PV bus, it changes parallel with irradiance data and PV system block produce maximum energy at 13:00-14:00.

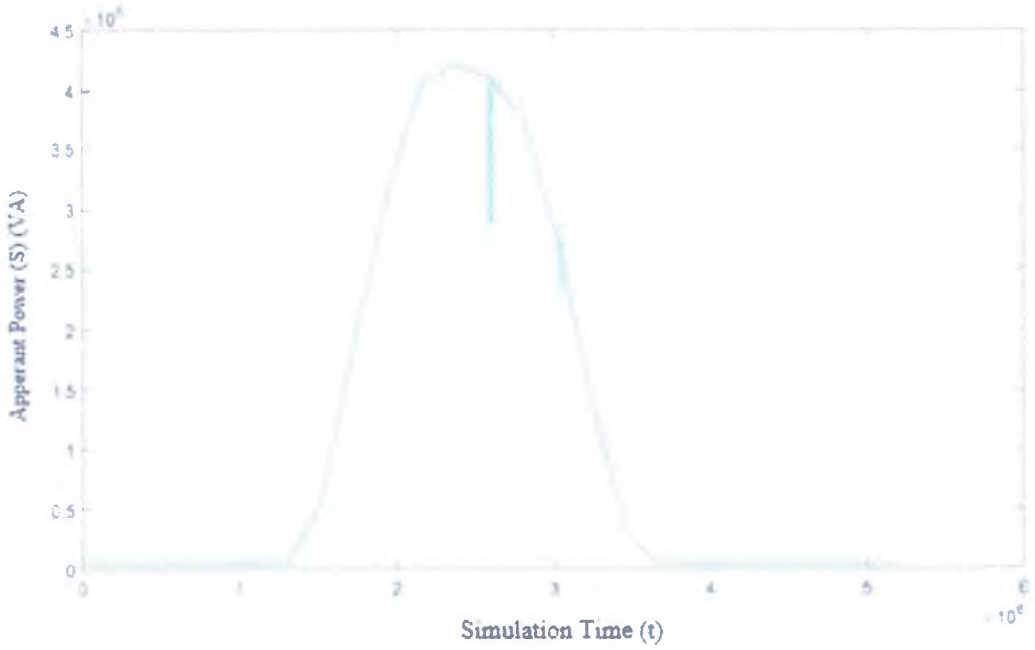

Figure 4.35. Apparent power graph of PV (S_{PV})

Figure 4.36 shows us apparent power on ASM bus which is also inside of bus5, apparent power change with usage of system in first simulation there is no control so this curve shape with consumption data.

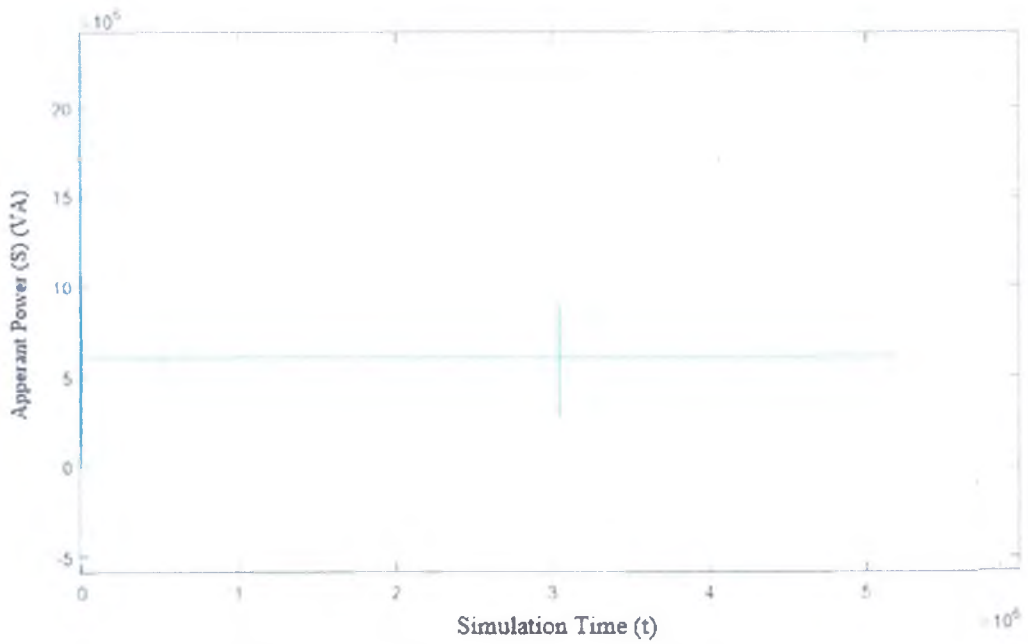

Figure 4.36. Apparent power graph of ASM (S_{ASM})

Figure 4.37 shows us apparent power on all buses.

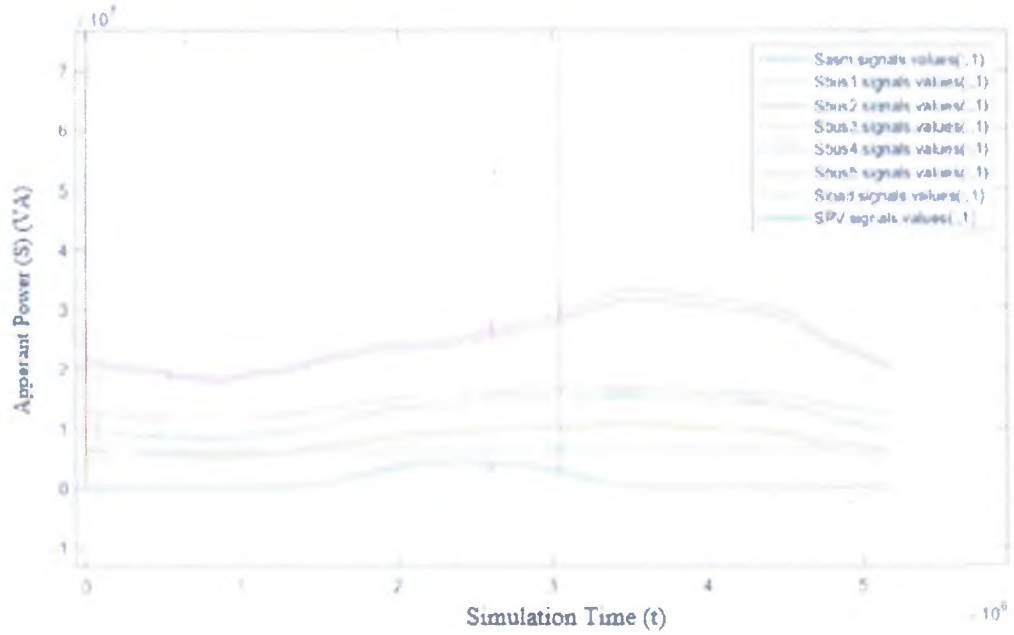

Figure 4.37. Apparent power graphs of all (S_{all})

Figure 4.38 shows us current flowing on bus1 which belongs to voltage source block before the OLTC, current flowing change with usage of system in first simulation there is no control so this curve shape with consumption data.

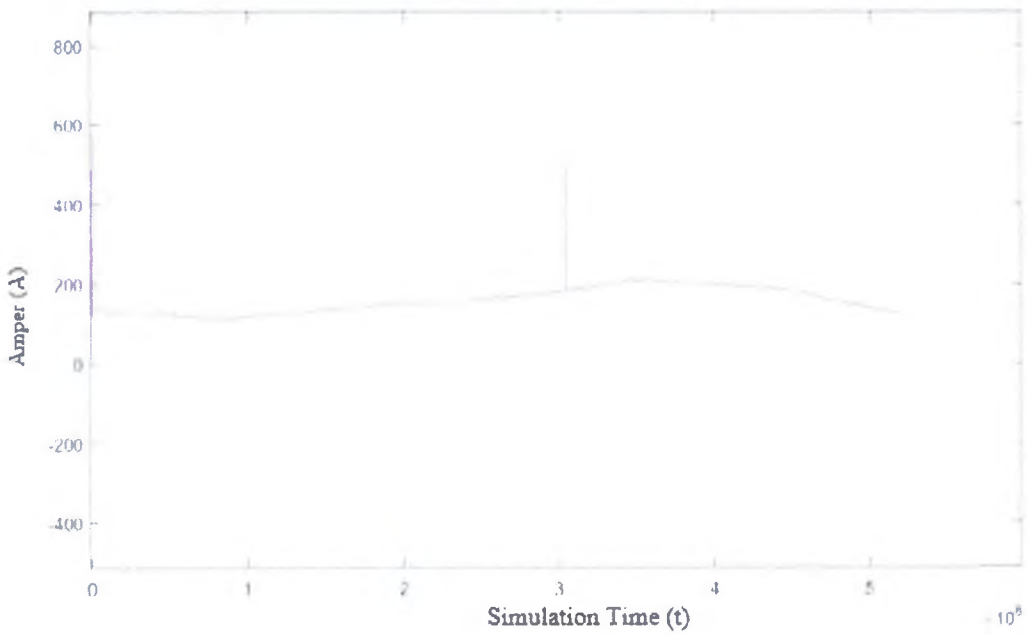

Figure 4.38. Current graph of bus 1 (I_{bus1})

This graph Figure 4.39 shows us current flowing on bus2, this bus also measure feedback for OLTC and it is placed after the OLTC current flowing change with

usage of system in first simulation there is no control so this curve shape with consumption data.

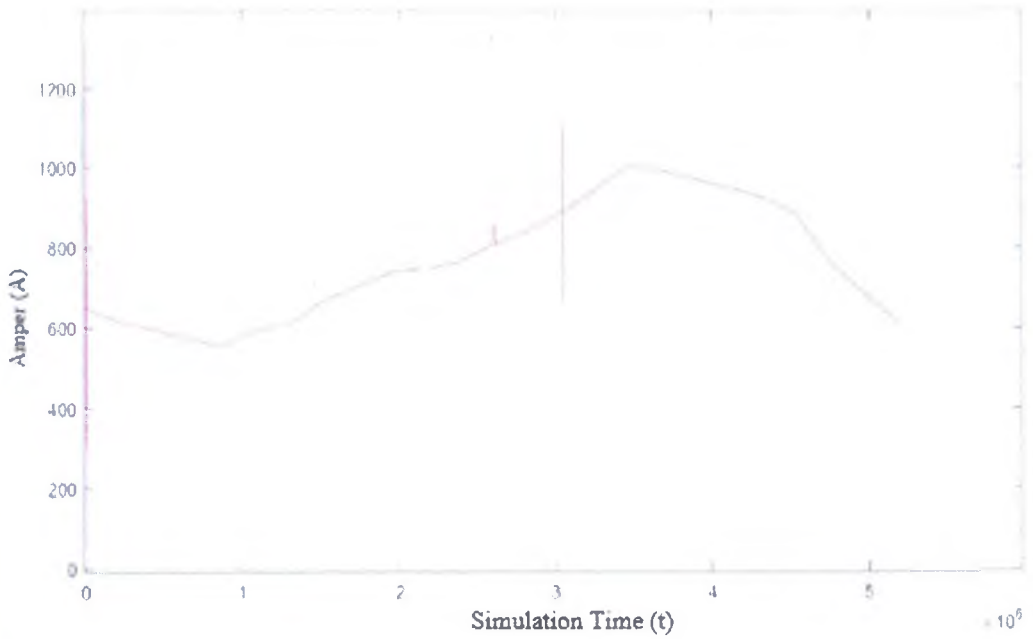

Figure 4.39. Current graph of bus 2 (I_{bus2})

Figure 4.40 shows us current flowing on bus3. This block measures voltage and current of diesel generator, current flowing change slightly with usage of system in first simulation there is no control so this curve shape with consumption data.

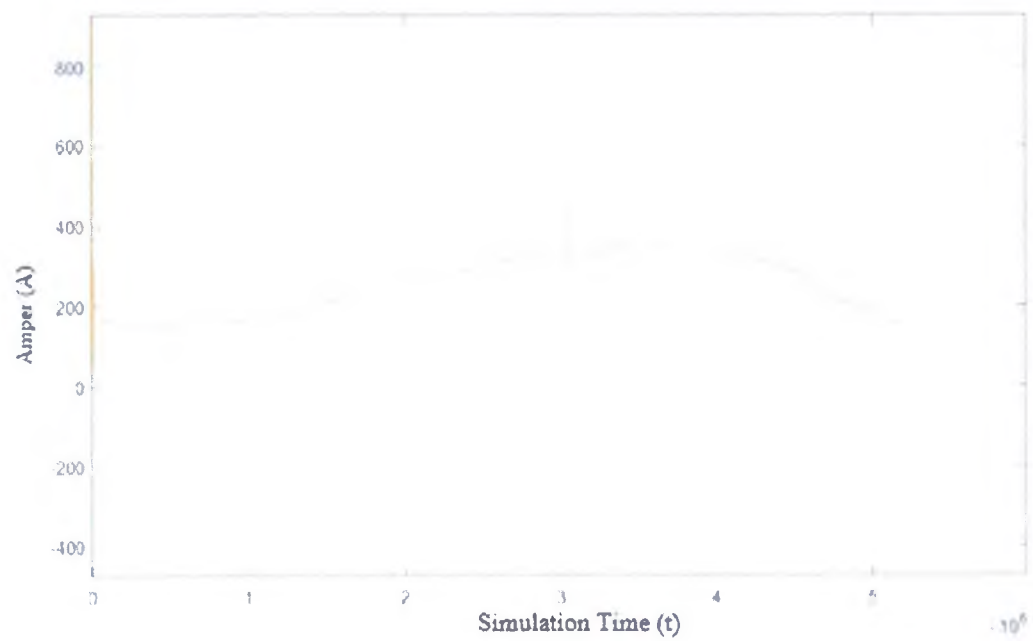

Figure 4.40. Current graph of bus 3 (I_{bus3})

Figure 4.41 shows us current flowing on bus4 which measures the apparent power of 15 MW residential load current flowing change with usage of system in first simulation there is no control so this curve shape with consumption data.

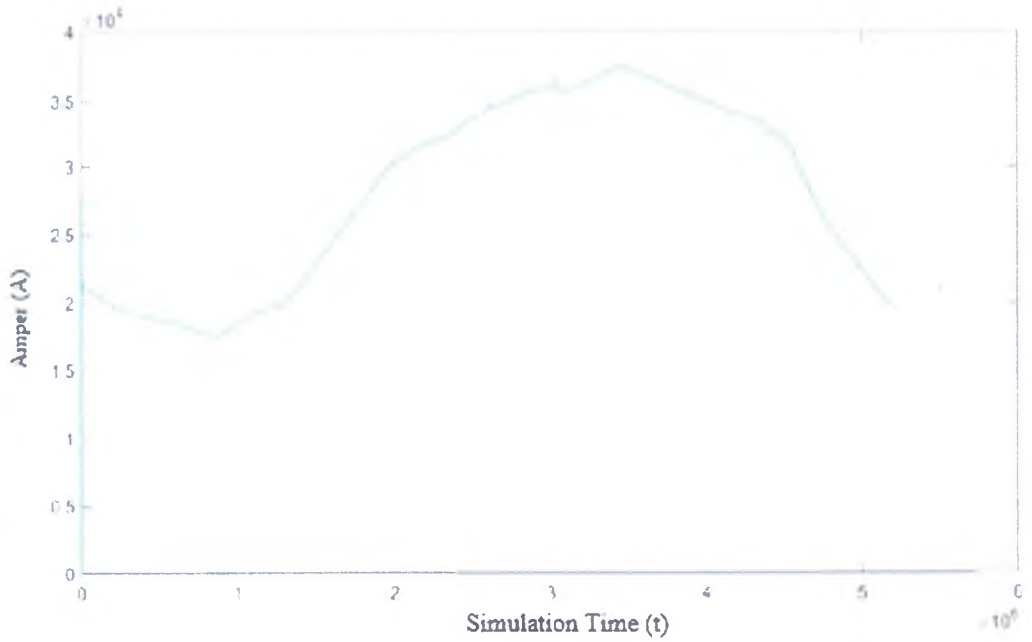

Figure 4.41. Current graph of bus 4 (I_{bus4})

Figure 4.42 shows us apparent power on bus5 which measures voltage and current of 10MW residential load and ASM, apparent power change with usage of system in first simulation there is no control so this curve shape with consumption data.

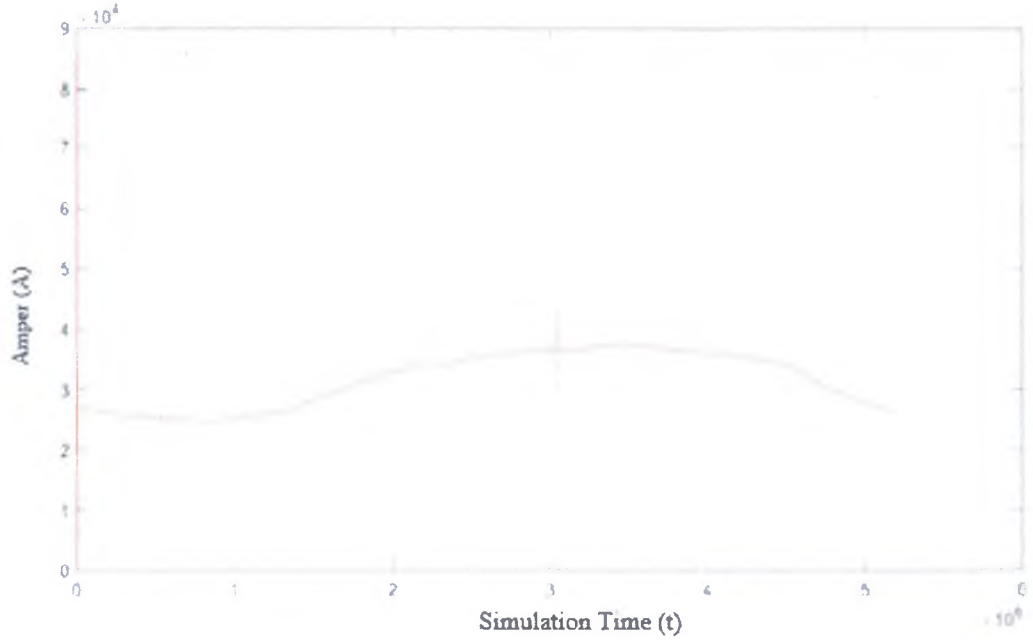

Figure 4.42. Current graph of bus 5 (I_{bus5})

Figure 4.43 shows us current flowing on load bus which is also inside of bus5 represent residential loads, current flowing change with usage of system in first simulation there is no control so this curve shape with consumption data.

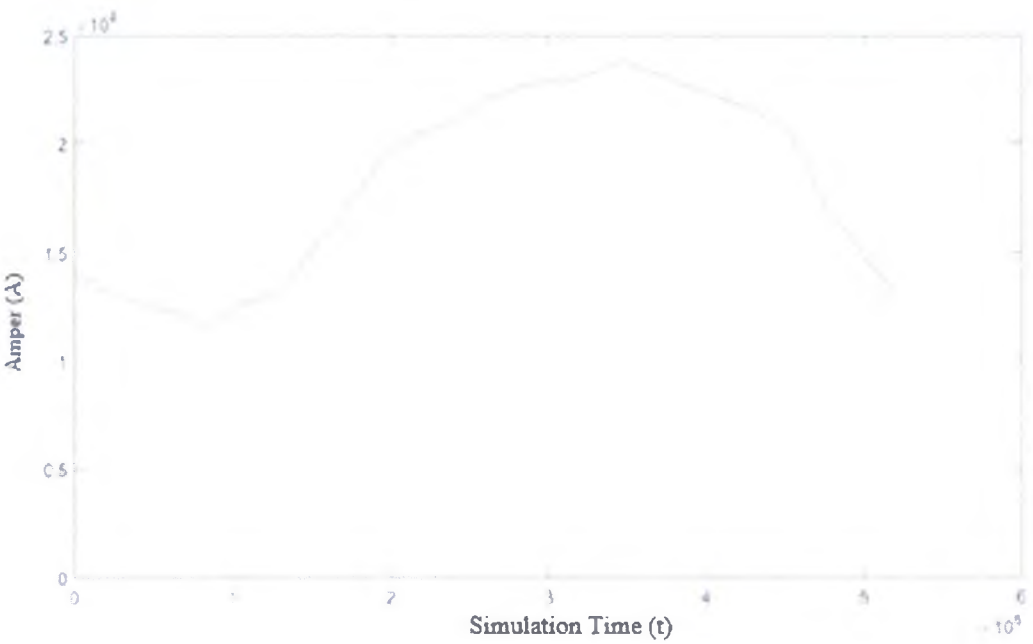

Figure 4.43. Current graph of load (I_{load})

Figure 4.44 shows us current flowing on PV bus. It changes parallel with irradiance data and PV system block produce maximum energy at 13:00-14:00.

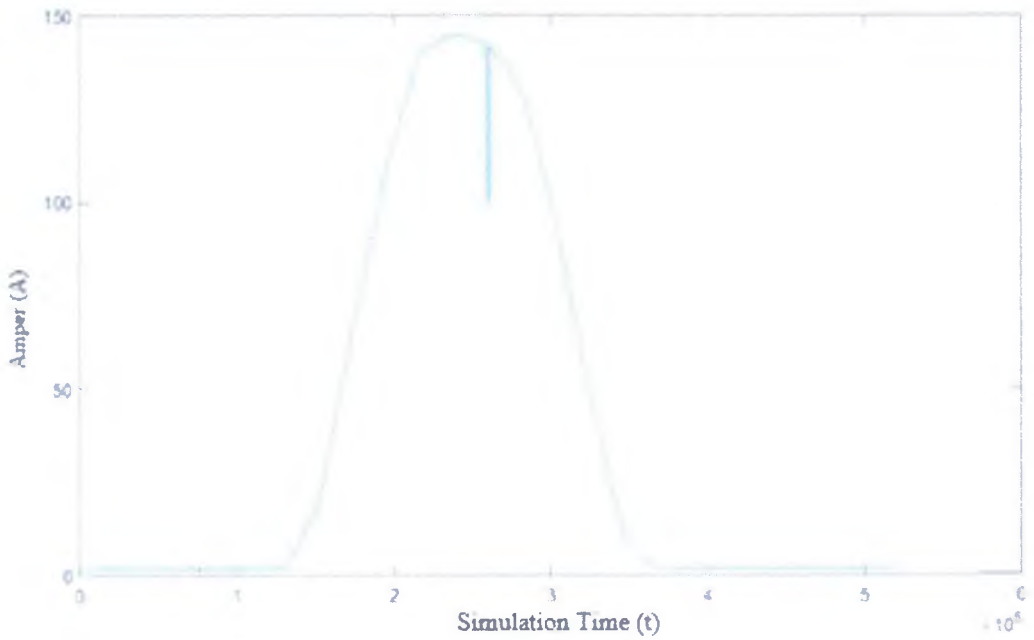

Figure 4.44. Current graph of PV (I_{PV})

Figure 4.45 shows us current flowing on ASM bus which is also inside of bus5, current flowing change with usage of system in first simulation there is no control so this curve shape with consumption data.

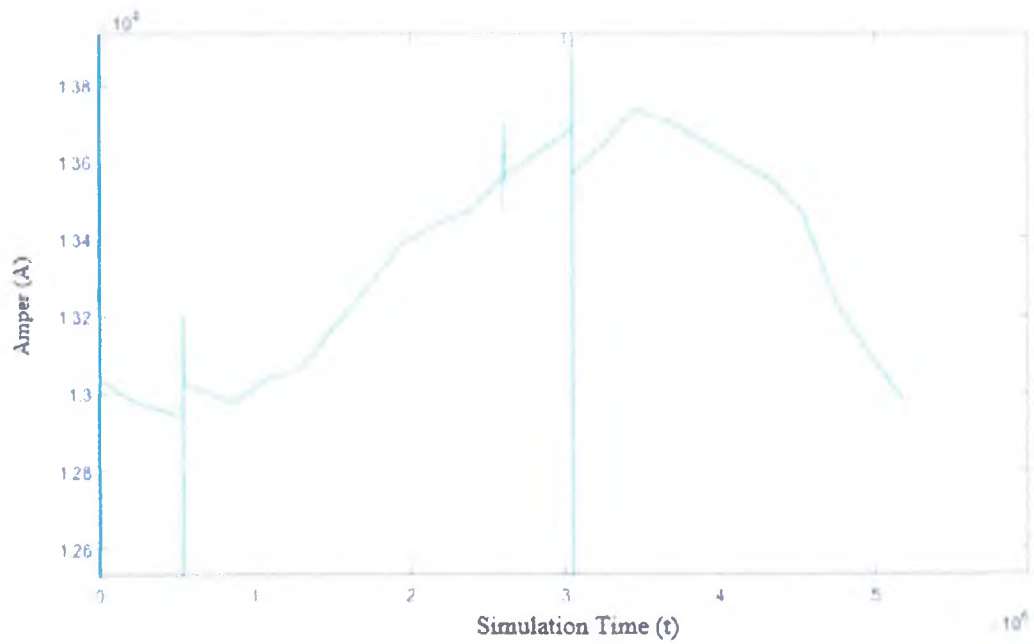

Figure 4.45. Current graph of ASM (I_{ASM})

This graph Figure 4.46 shows us current flowing on all buses.

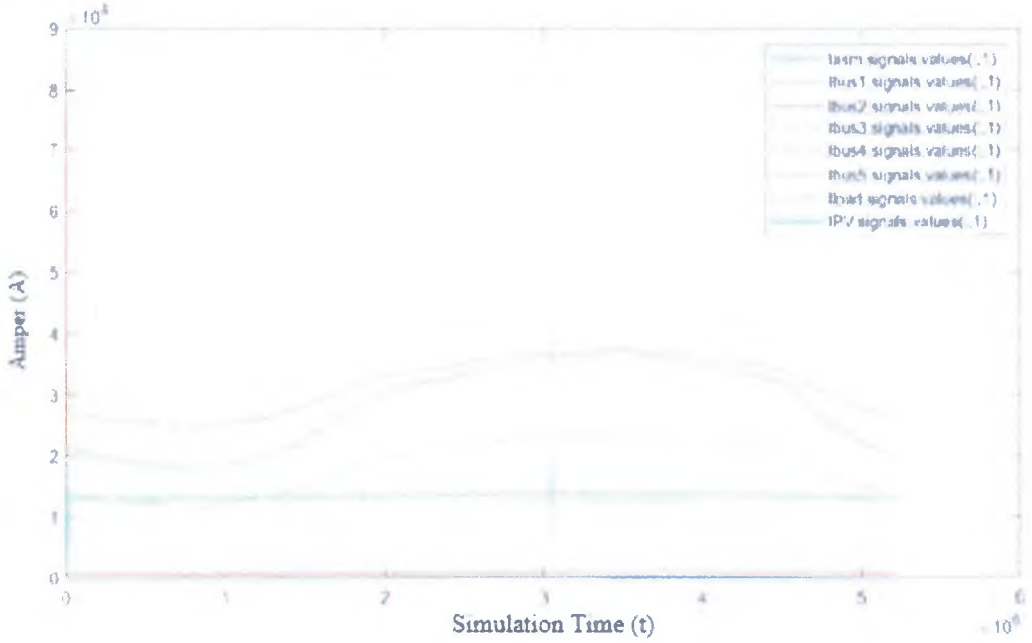

Figure 4.46. Current graphs of all (I_{all})

4.4. Case 2: All Graph with Controller

Figure 4.47 shows us voltage on bus1 which belongs to voltage source block before the OLTC voltage change with behavior of first system. In the second simulation there are three control strategies to regulate desire voltage and reactive power.

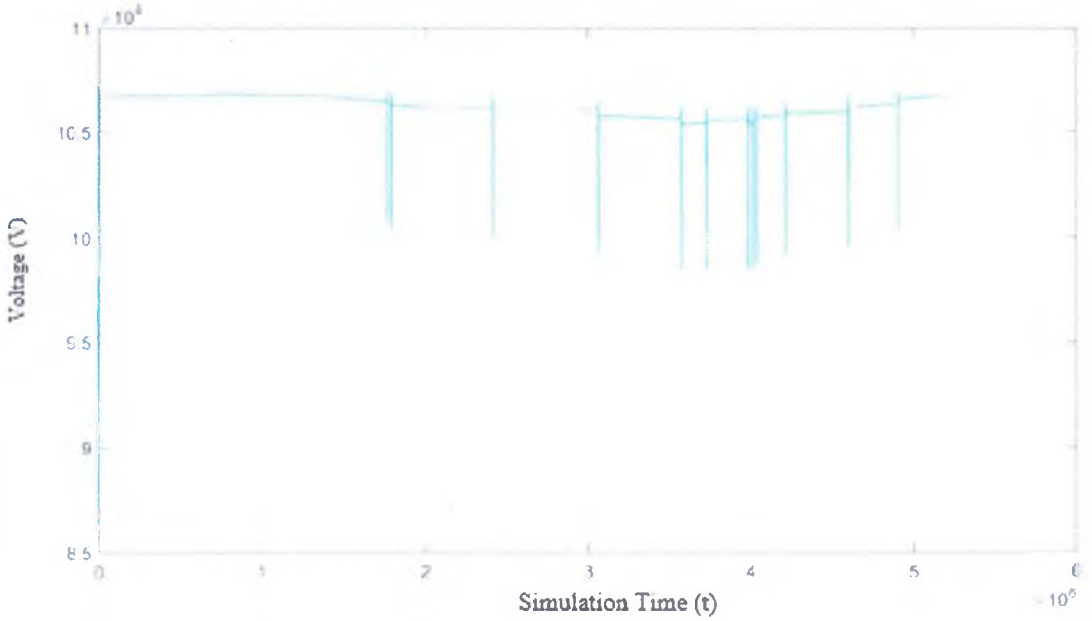

Figure 4.47. Voltage graph of bus 1 (V_{bus1})

Figure 4.48 shows us voltage on bus2 which belongs to voltage source block after the OLTC voltage change with behavior of first system. In the second simulation there are three control strategies to regulate desire voltage and reactive power.

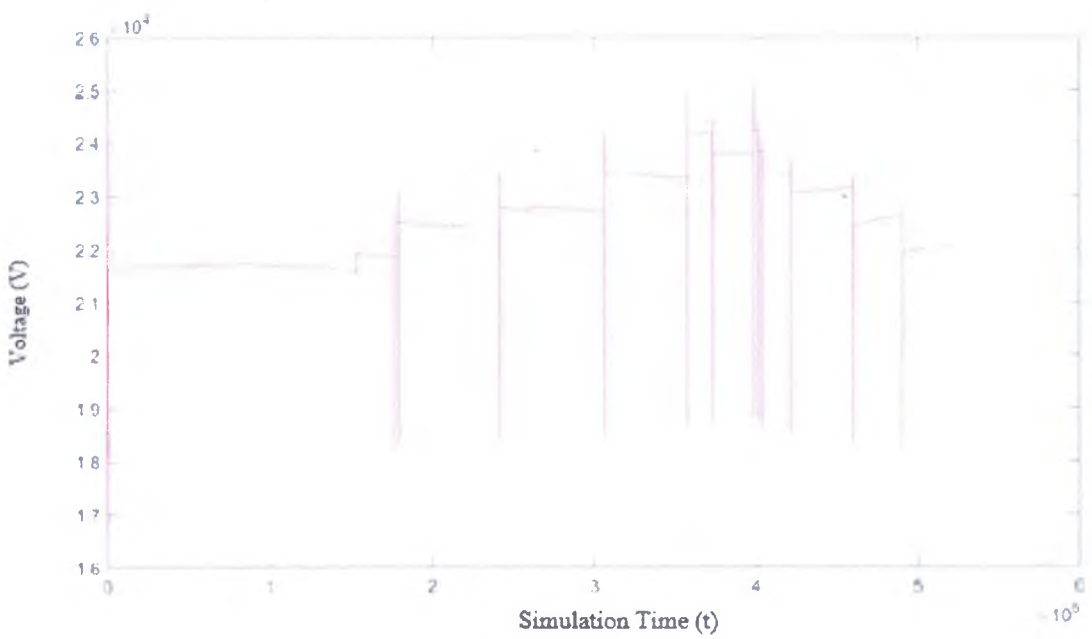

Figure 4.48. Voltage graph of bus 2 (V_{bus2})

This graph Figure 4.49 shows us voltage on bus3. This block measures voltage of diesel generator, voltage change with behavior of first system. In the second

simulation there are three control strategies to regulate desire voltage and reactive power.

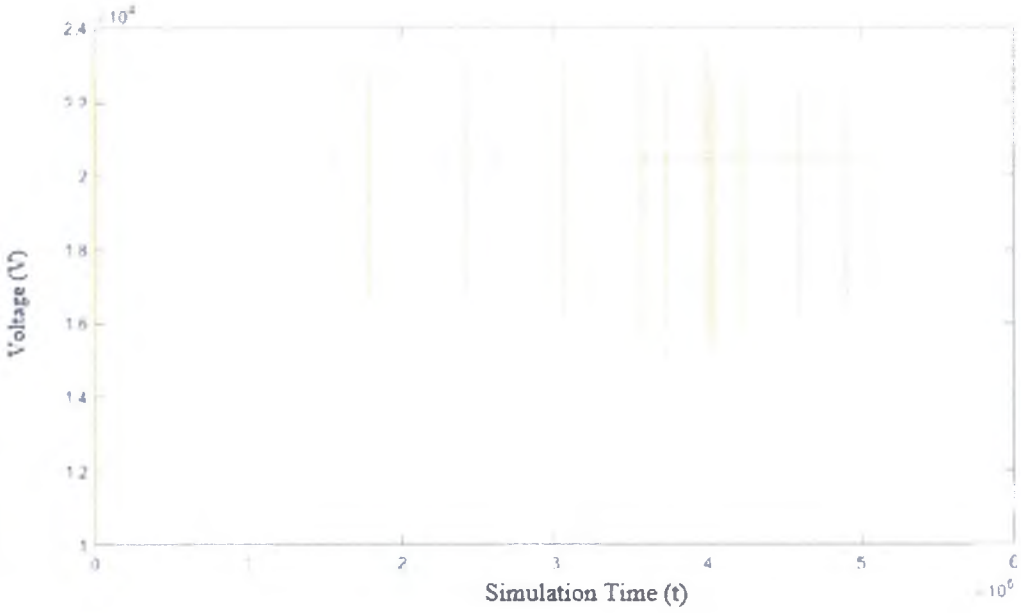

Figure 4.49. Voltage graph of bus 3 (V_{bus3})

Figure 4.50 shows us voltage on bus4 which measures the voltage of 15 MW residential load voltage change with behavior of first system. In the second simulation there are three control strategies to regulate desire voltage and reactive power.

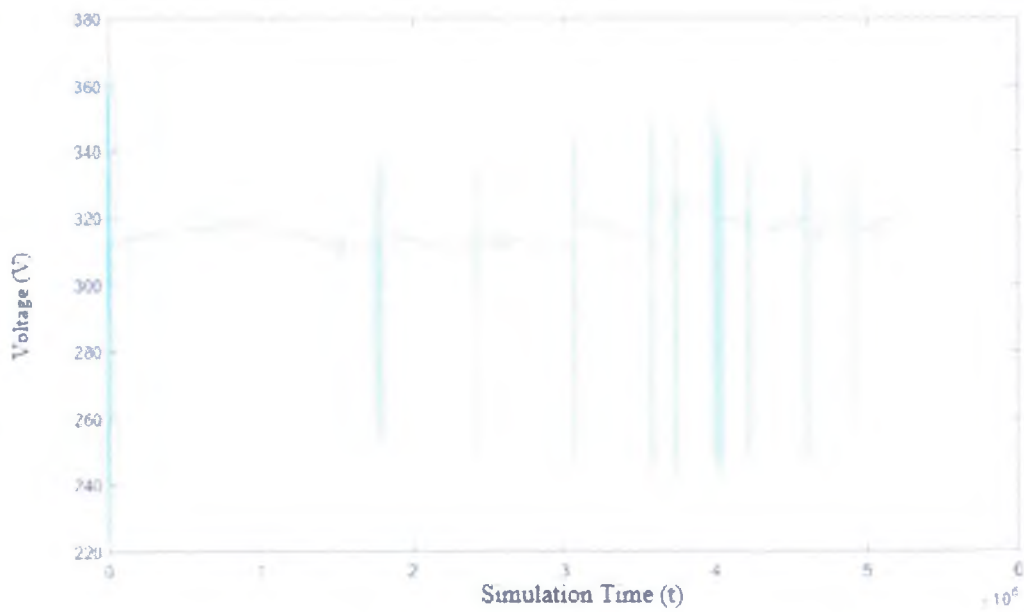

Figure 4.50. Voltage graph of bus 4 (V_{bus4})

Figure 4.51 shows us voltage on bus5 which measures voltage of 10MW residential load and ASM, voltage change with behavior of first system and In the second simulation there are three control strategies to regulate desire voltage and reactive power.

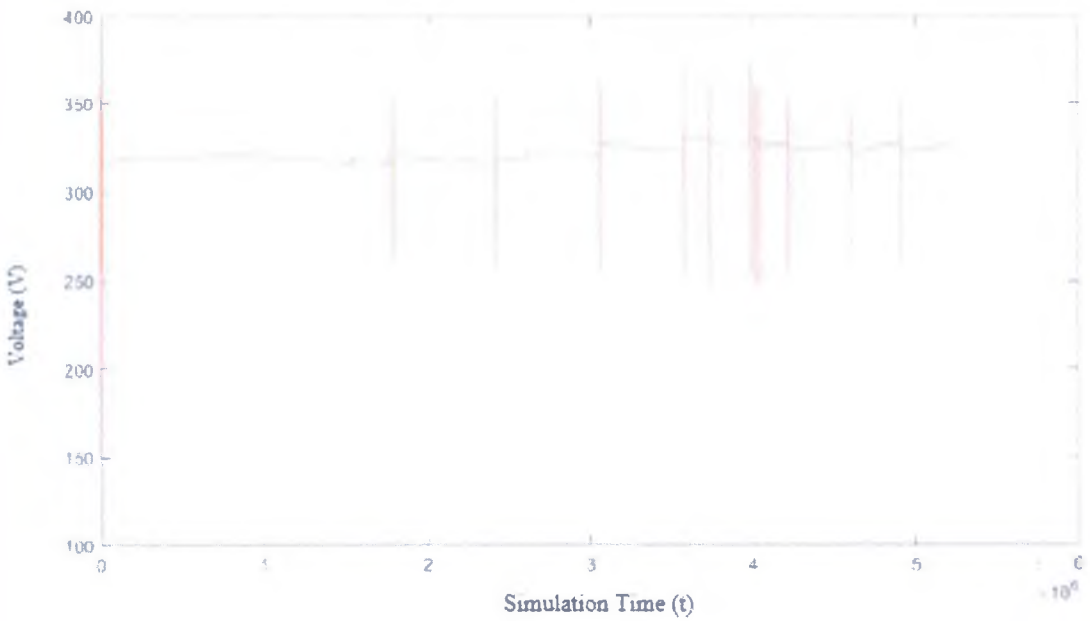

Figure 4.51. Voltage graph of bus 5 (V_{bus5})

Figure 4.52 shows us voltage on load bus which is also inside of bus5 representing residential loads, voltage change with behavior of first system. In the second simulation there are three control strategies to regulate desire voltage and reactive power.

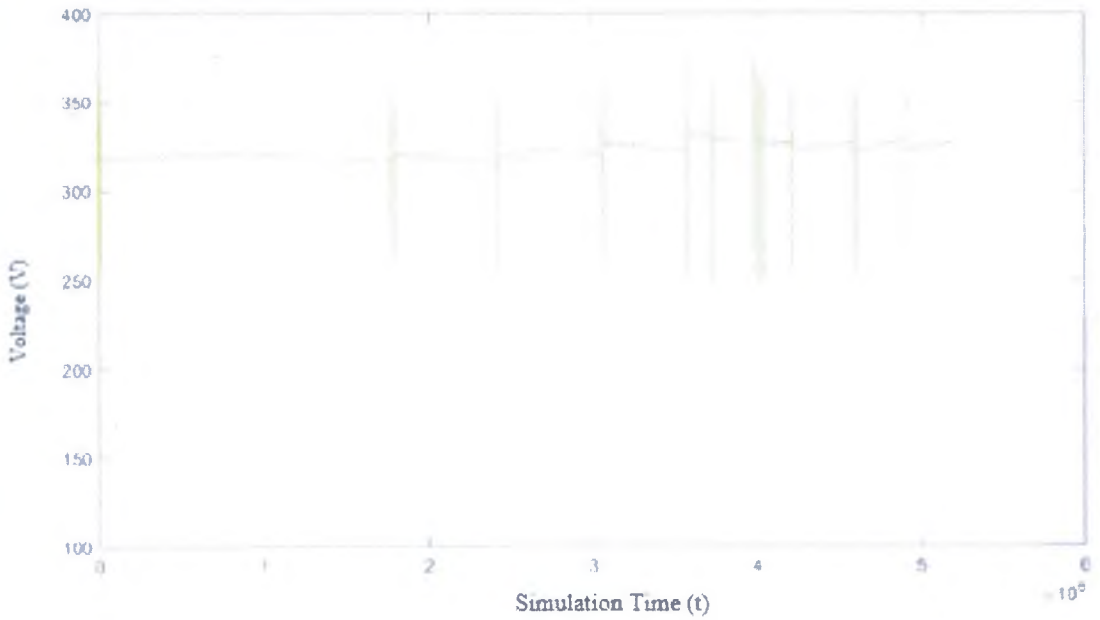

Figure 4.52. Voltage graph of load (V_{load})

Figure 4.53 shows us voltage on PV bus, actually voltage on this bus is the same as line voltage which 25kV, PV's are not producing any voltage in night time, also it can be seen on radiation data.

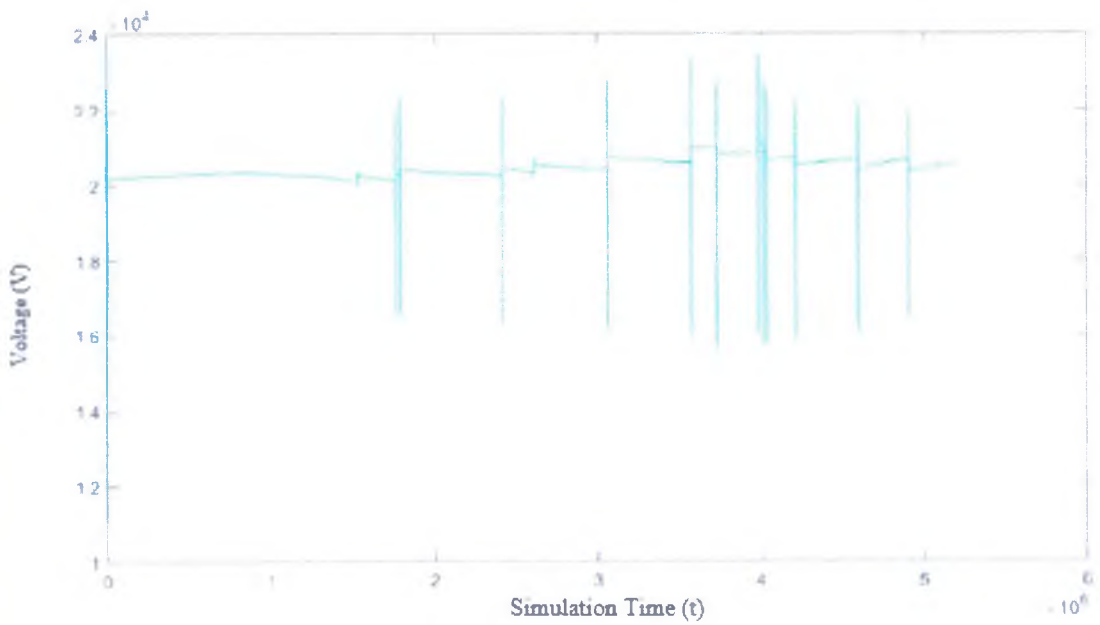

Figure 4.53. Voltage graph of PV (V_{PV})

Figure 4.54 shows us voltage on ASM bus which is also inside of bus5, voltage change with behavior of first system. In the second simulation there are three control strategies to regulate desire voltage and reactive power.

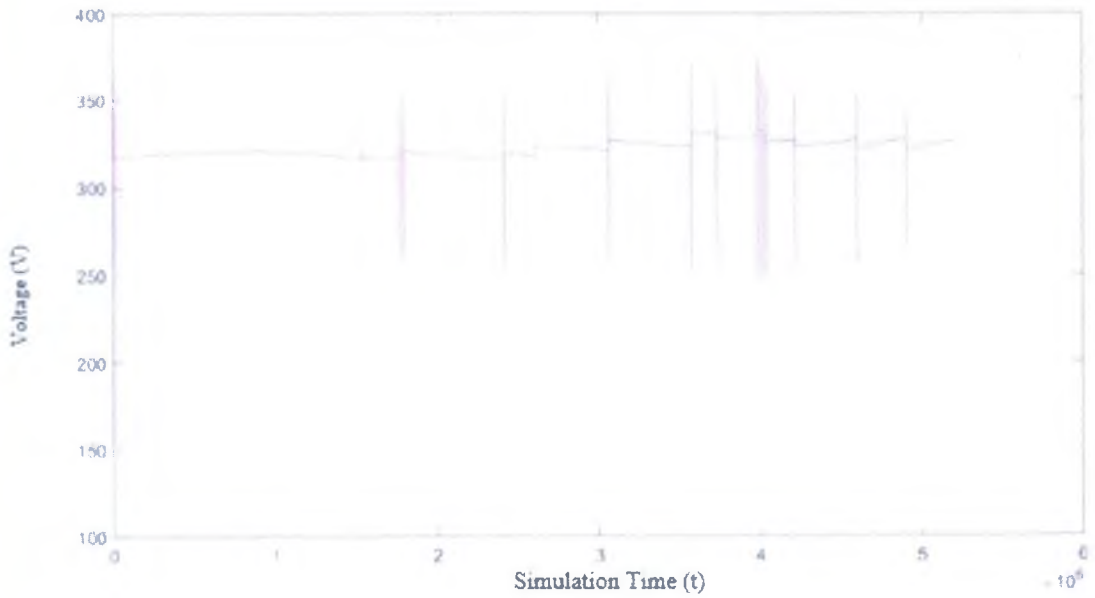

Figure 4.54. Voltage graph of ASM (V_{ASM})

Figure 4.55 shows us all voltages on all buses,

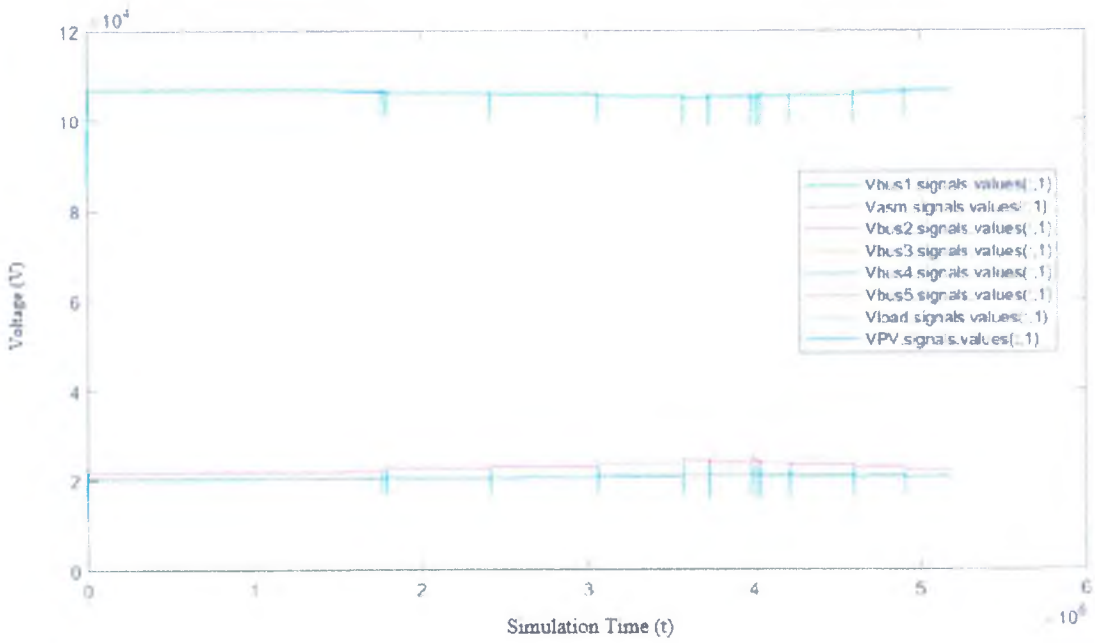

Figure 4.55. Voltage graphs of all (V_{all})

Figure 4.56 shows us active power on bus1 which belongs to voltage source block before the OLTC active power change with behavior of first system. In the second simulation there are three control strategies to regulate desire voltage and reactive power.

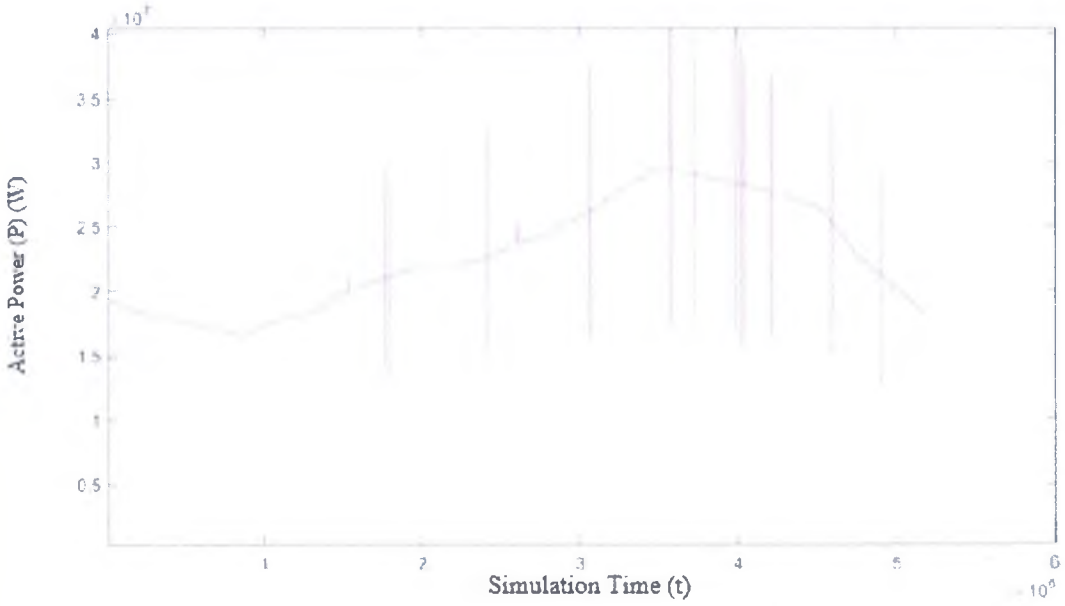

Figure 4.56. Active power graph of bus 1 (P_{bus1})

Figure 4.57 shows us active power on bus2. This bus belongs to voltage source block after the OLTC active power change with behavior of first system. In the second simulation there are three control strategies to regulate desire voltage and reactive power.

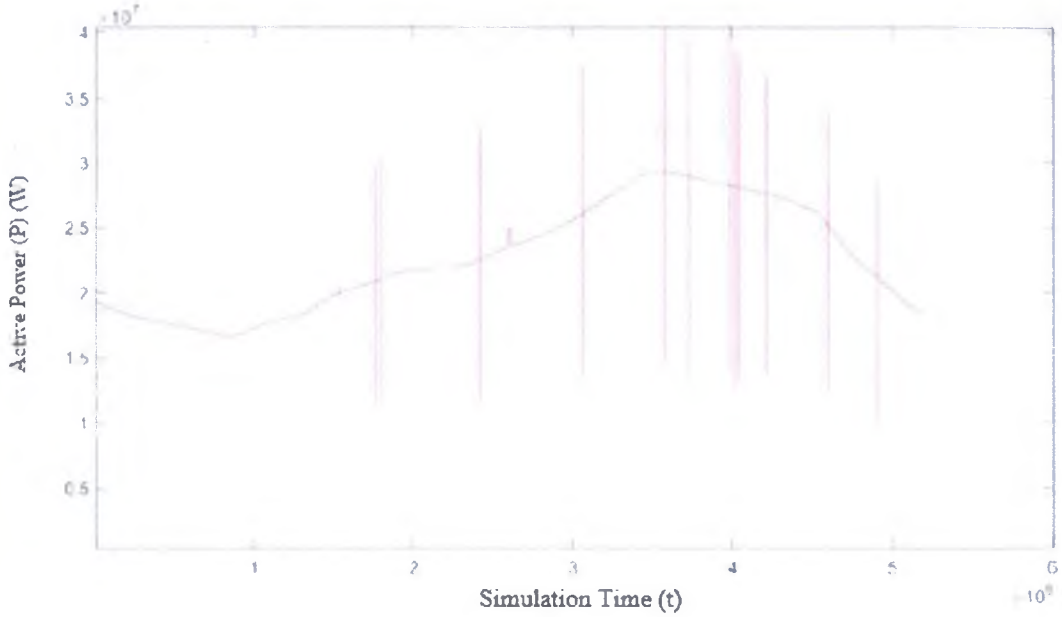

Figure 4.57. Active power graph of bus 2 (P_{bus2})

Figure 4.58 shows us active power on bus3, this block measures voltage of diesel generator, active power change with behavior of first system. In the second simulation there are three control strategies to regulate desire voltage and reactive power.

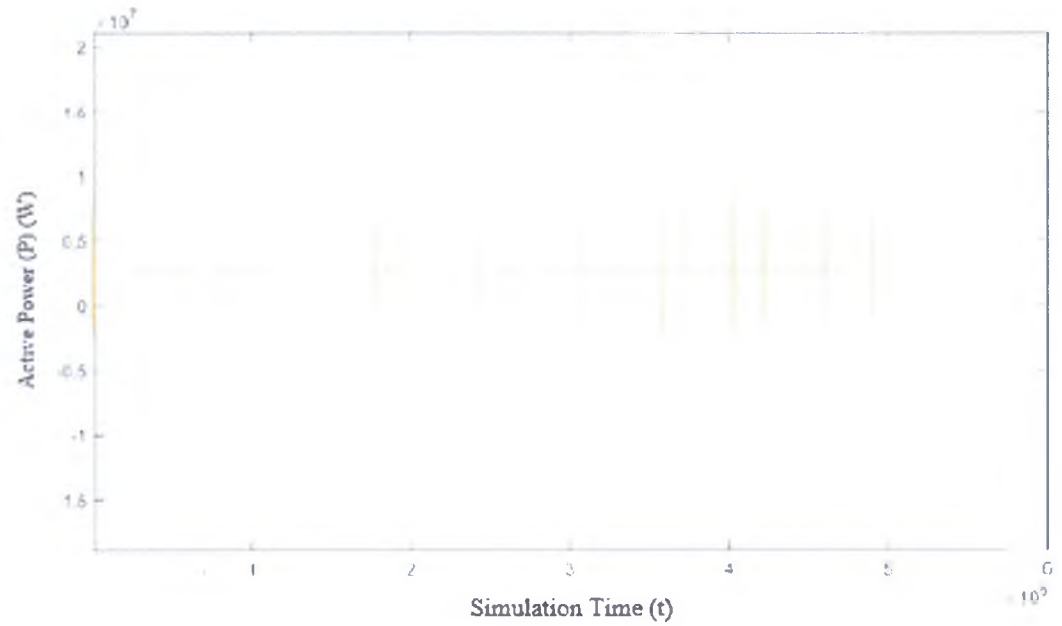

Figure 4.58. Active power graph of bus 3 (P_{bus3})

This graph Figure 4.59 shows us active power on bus4 which measures the voltage of 15 MW residential load active power change with behavior of first system. In the second simulation there are three control strategies to regulate desire voltage and reactive power.

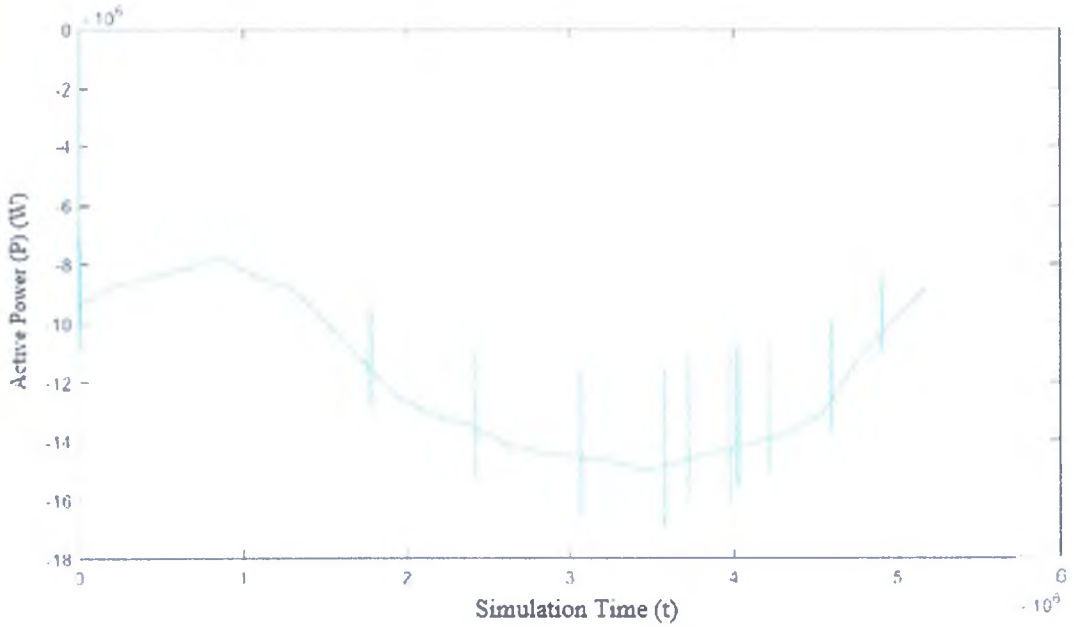

Figure 4.59. Active power graph of bus 4 (P_{bus4})

Figure 4.60 shows us active power on bus5 which measures voltage of 10MW residential load and ASM, active power change with behavior of first system. In the second simulation there are three control strategies to regulate desire voltage and reactive power.

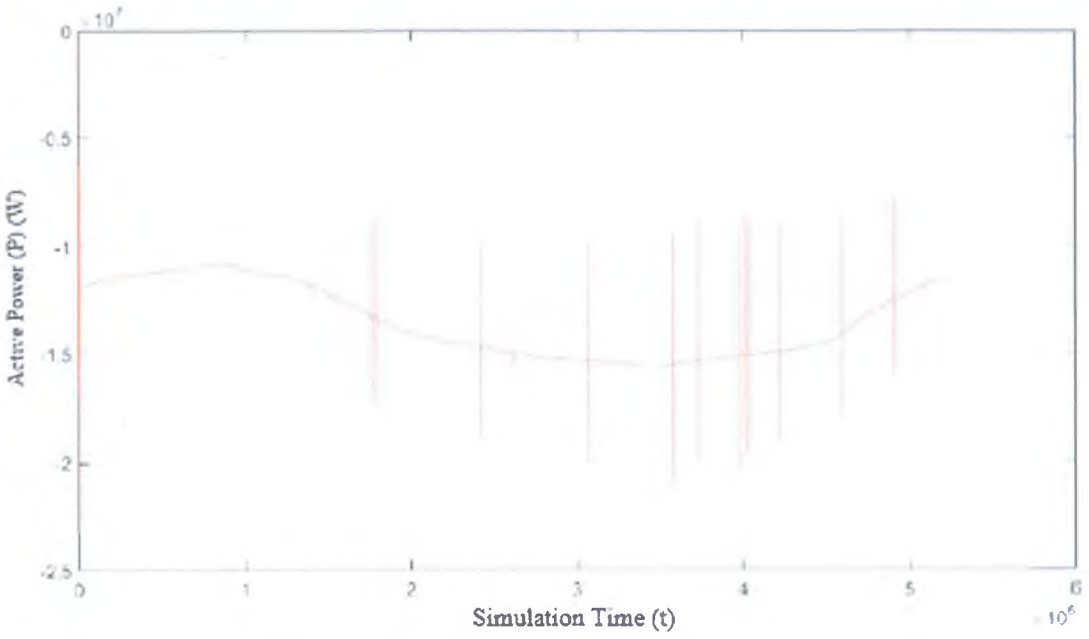

Figure 4.60. Active power graph of bus 5 (P_{bus5})

Figure 4.61 shows us active power on load bus which is also inside of bus5 represent residential loads, active power change with behavior of first system. In the second simulation there are three control strategies to regulate desire voltage and reactive power.

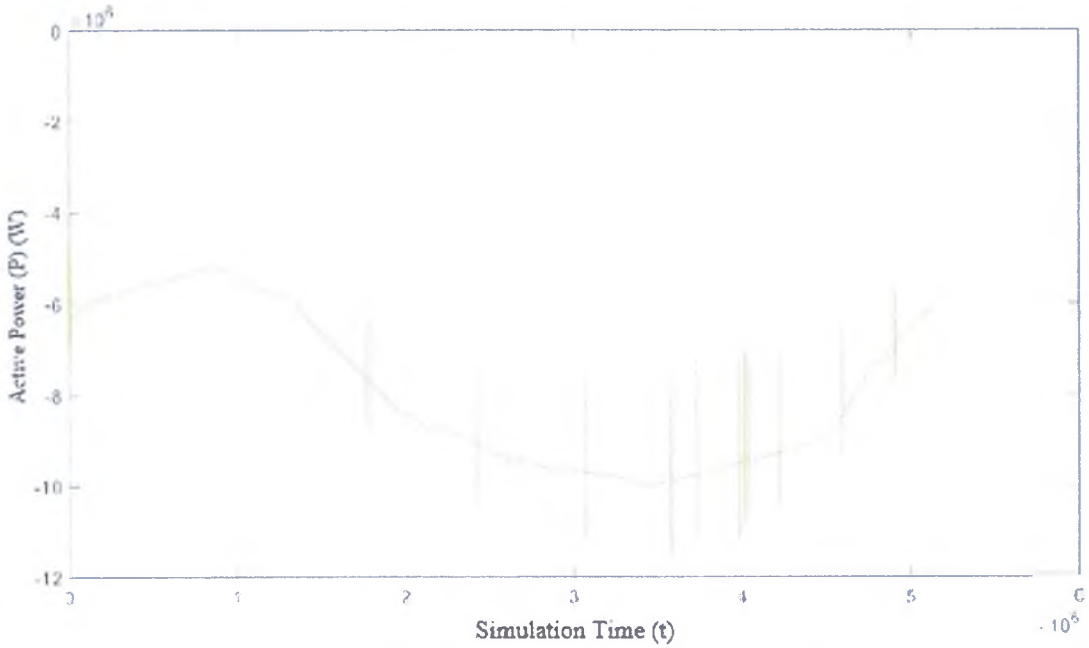

Figure 4.61. Active power graph of load (P_{load})

Figure 4.62 shows active power on PV bus which changes parallel with irradiance data and PV system block produce maximum energy at 13:00-14:00.

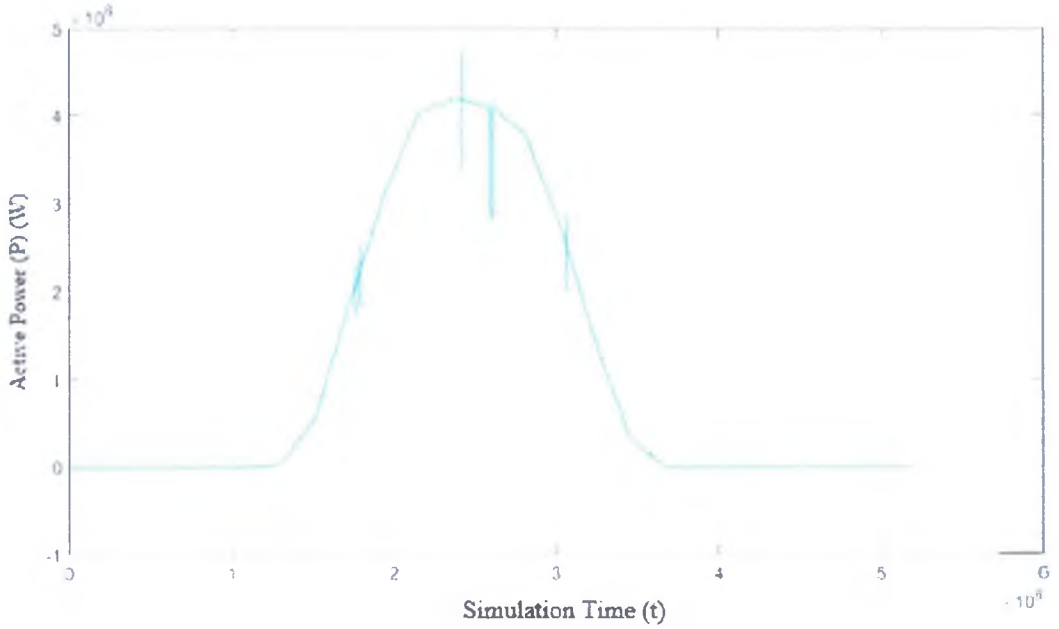

Figure 4.62. Active power graph of PV (P_{PV})

Figure 4.63 shows active power on ASM bus which is also inside of bus5, active power change with behavior of first system. In the second simulation there are three control strategies to regulate desire voltage and reactive power.

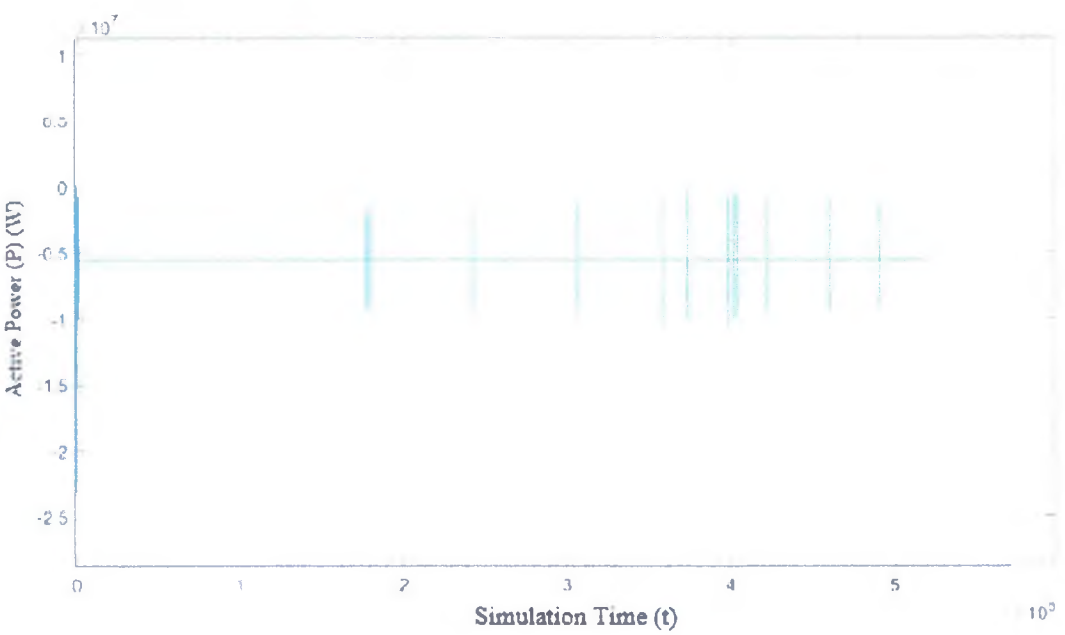

Figure 4.63. Active power graph of ASM (P_{ASM})

This graph Figure 4.64 shows us all active power on all buses,

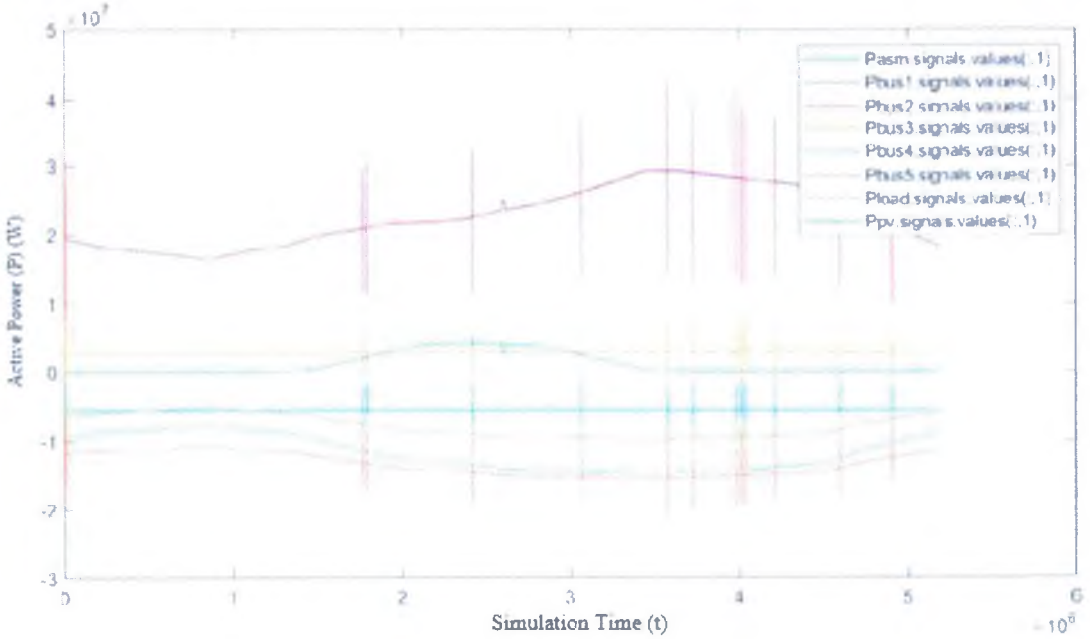

Figure 4.64. Active power graphs of all (P_{all})

This graph Figure 4.65 shows us reactive power on bus1, this bus belongs to voltage source block before the OLTC reactive power change with behavior of first system. In the second simulation there are three control strategies to regulate desire voltage and reactive power.

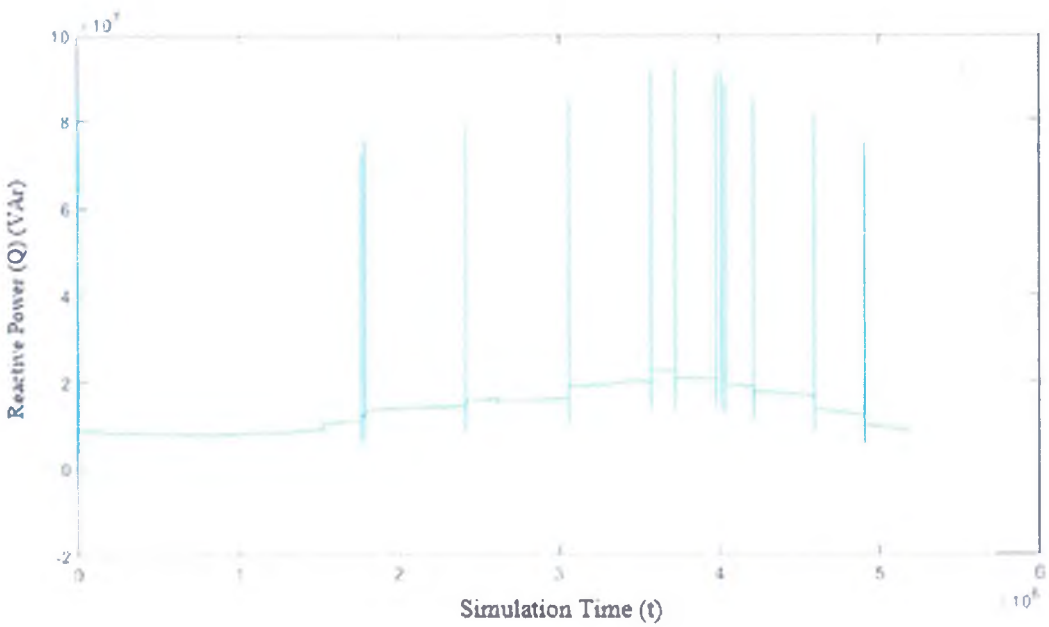

Figure 4.65. Reactive power graph of bus 1 (Q_{bus1})

This graph Figure 4.66 shows us reactive power on bus2 which belongs to voltage source block after the OLTC reactive power change with behavior of first system. In the second simulation there are three control strategies to regulate desire voltage and reactive power.

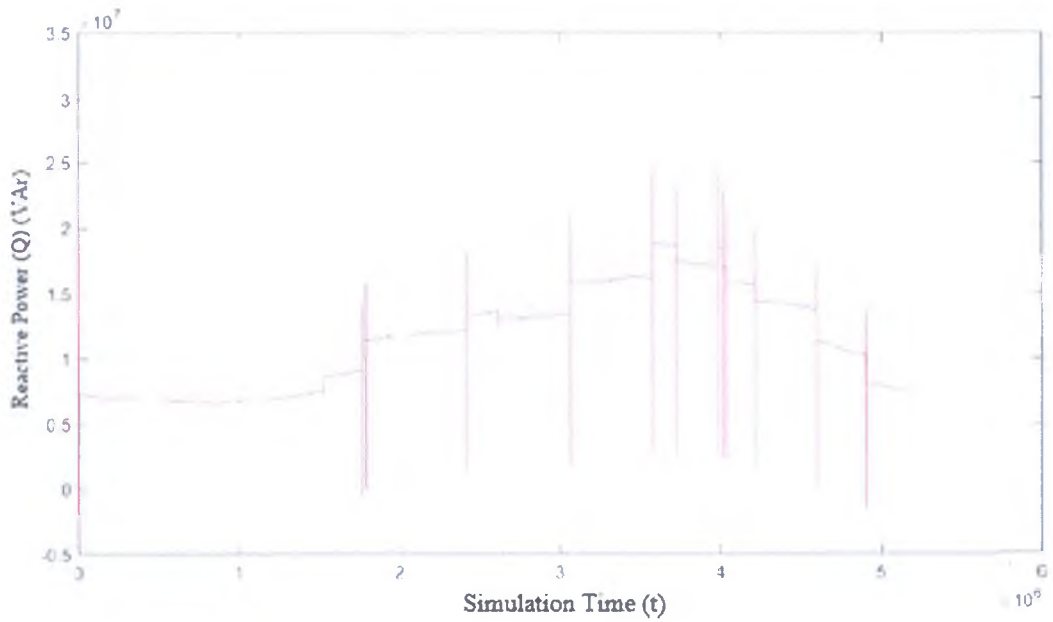

Figure 4.66. Reactive power graph of bus 2 (Q_{bus2})

This graph Figure 4.67 shows us reactive power on bus3 and this block measures voltage of diesel generator, reactive power change with behavior of first system. In the second simulation there are three control strategies to regulate desire voltage and reactive power.

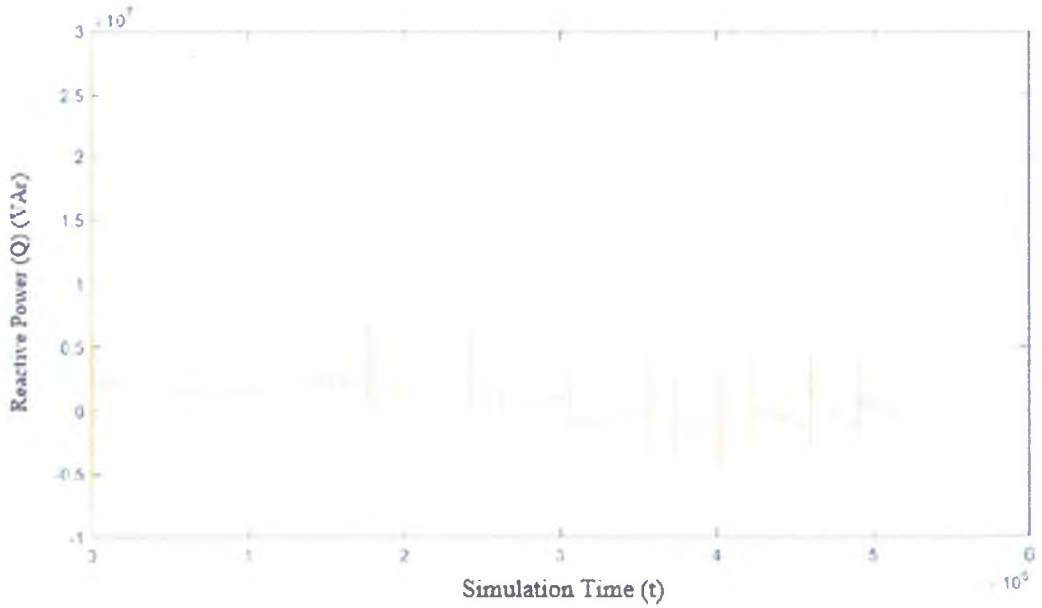

Figure 4.67. Reactive power graph of bus 3 (Q_{bus3})

This graph Figure 4.68 shows us reactive power on bus4 which measures the voltage of 15 MW residential load reactive power change with behavior of first system. In the second simulation there are three control strategies to regulate desire voltage and reactive power.

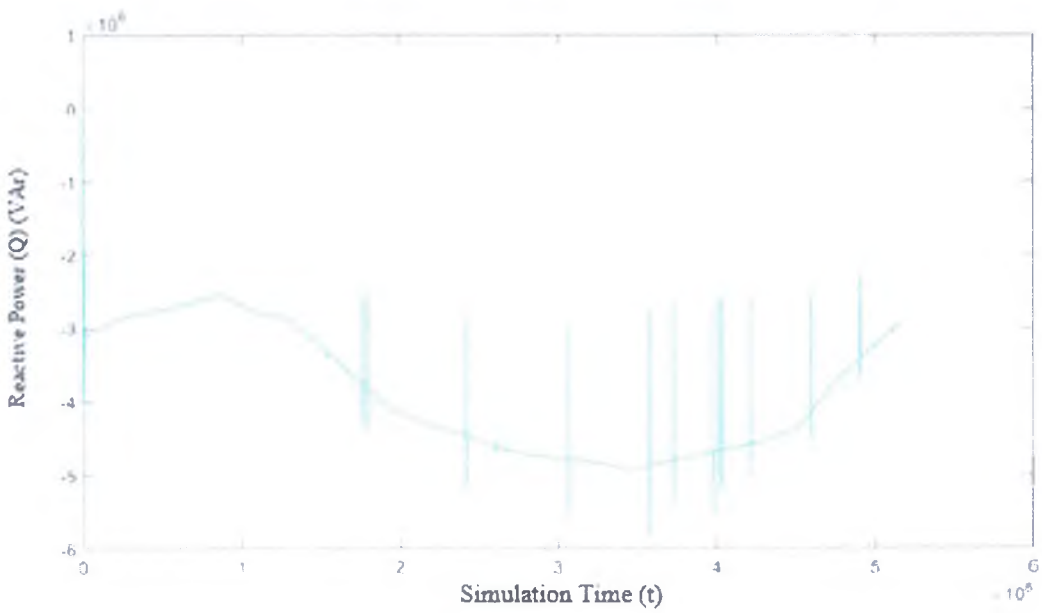

Figure 4.68. Reactive power graph of bus 4 (Q_{bus4})

Figure 4.69 shows us reactive power on bus5 which measures voltage of 10MW residential load and ASM, reactive power change with behavior of first system. In the second simulation there are three control strategies to regulate desire voltage and reactive power.

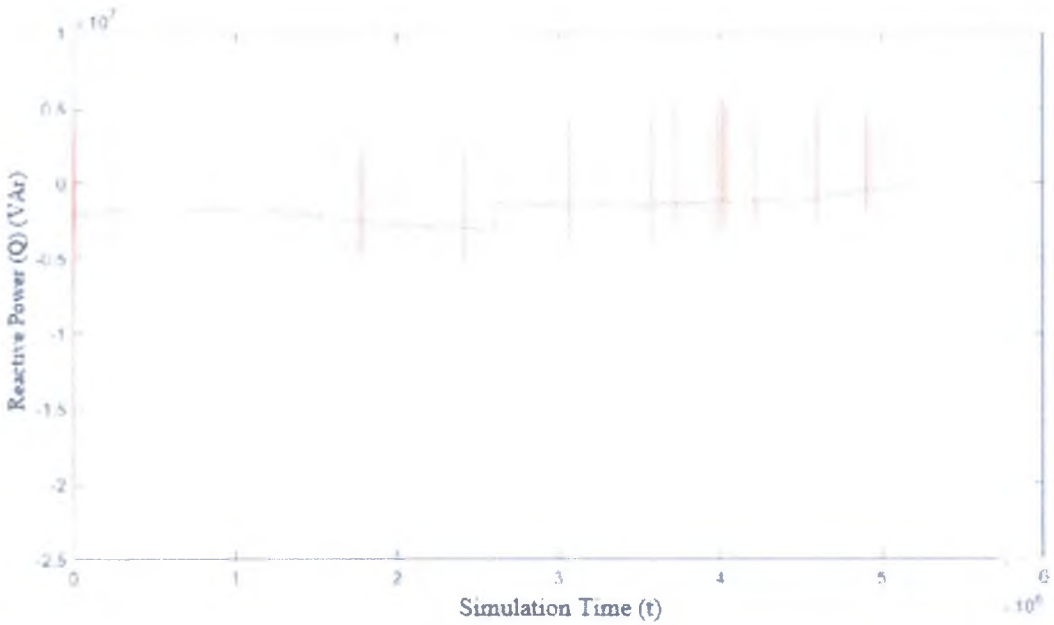

Figure 4.69. Reactive power graph of bus 5 (Q_{bus5})

Figure 4.70 shows us reactive power on load bus which is also inside of bus5 representing residential loads, reactive power change with behavior of first system. In the second simulation there are three control strategies to regulate desire voltage and reactive power.

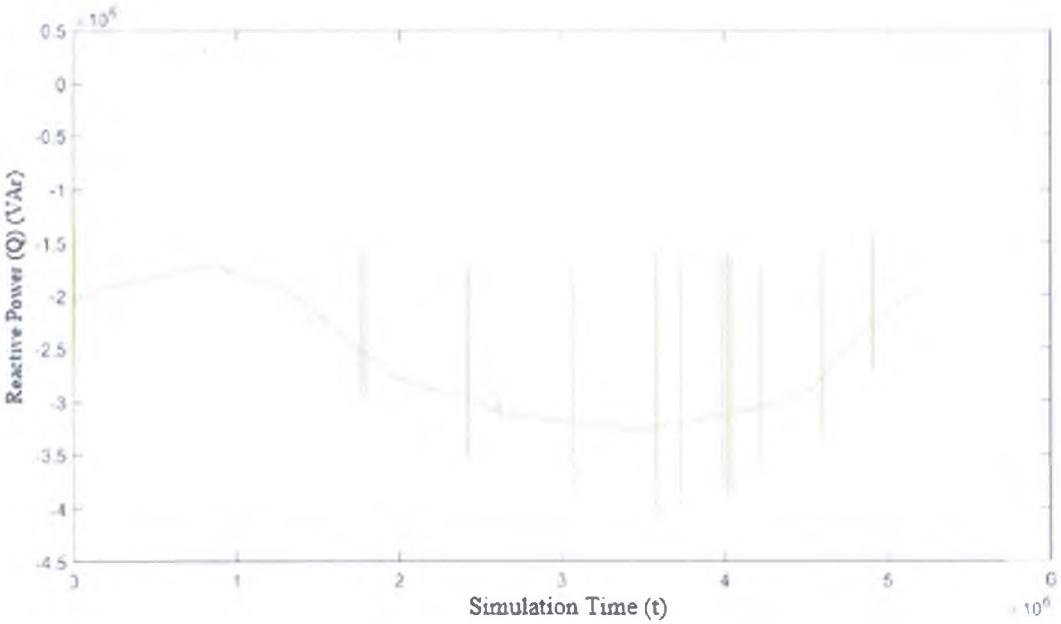

Figure 4.70. Reactive power graph of load (Q_{load})

Figure 4.71 shows us reactive power on PV bus, it changes parallel with irradiance data and PV system block produce maximum energy at 13:00-14:00.

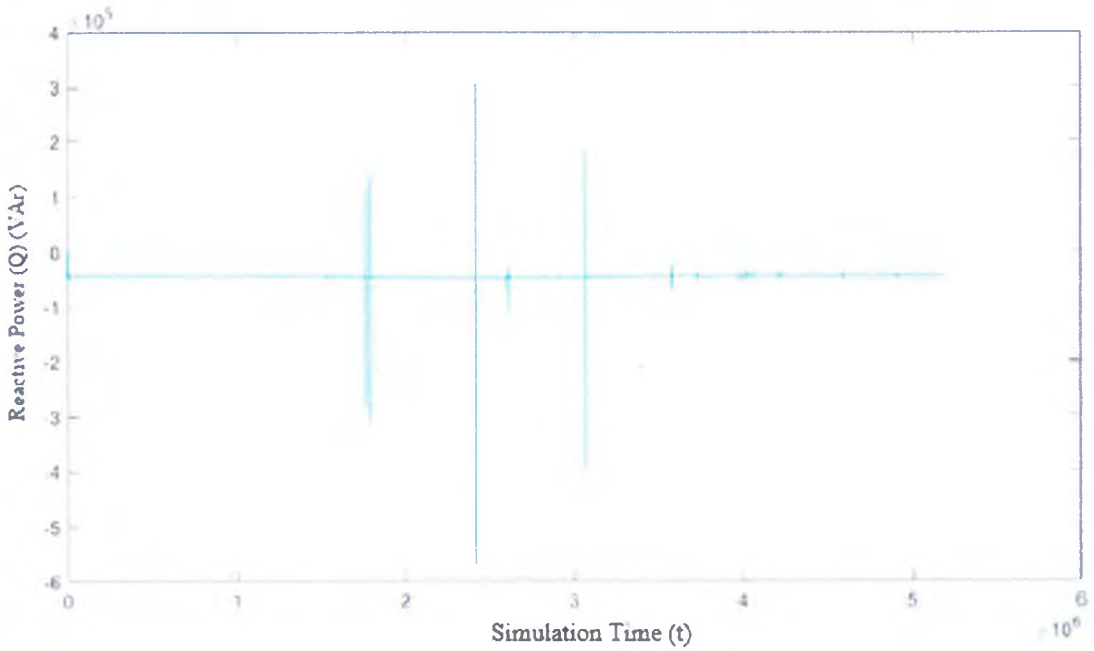

Figure 4.71. Reactive power graph of PV (Q_{PV})

Figure 4.72 shows us reactive power on ASM bus, which is also inside of bus5, reactive power change with behavior of first system. In the second simulation there are three control strategies to regulate desire voltage and reactive power.

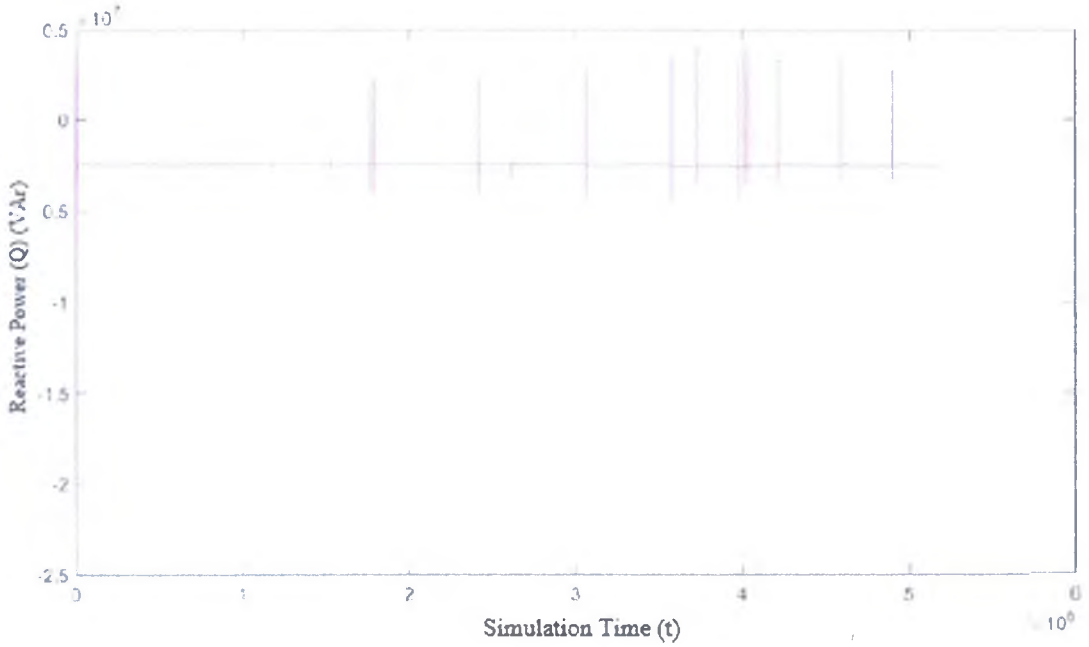

Figure 4.72. Reactive power graph of ASM (Q_{ASM})

Figure 4.73 shows us all reactive power on all buses,

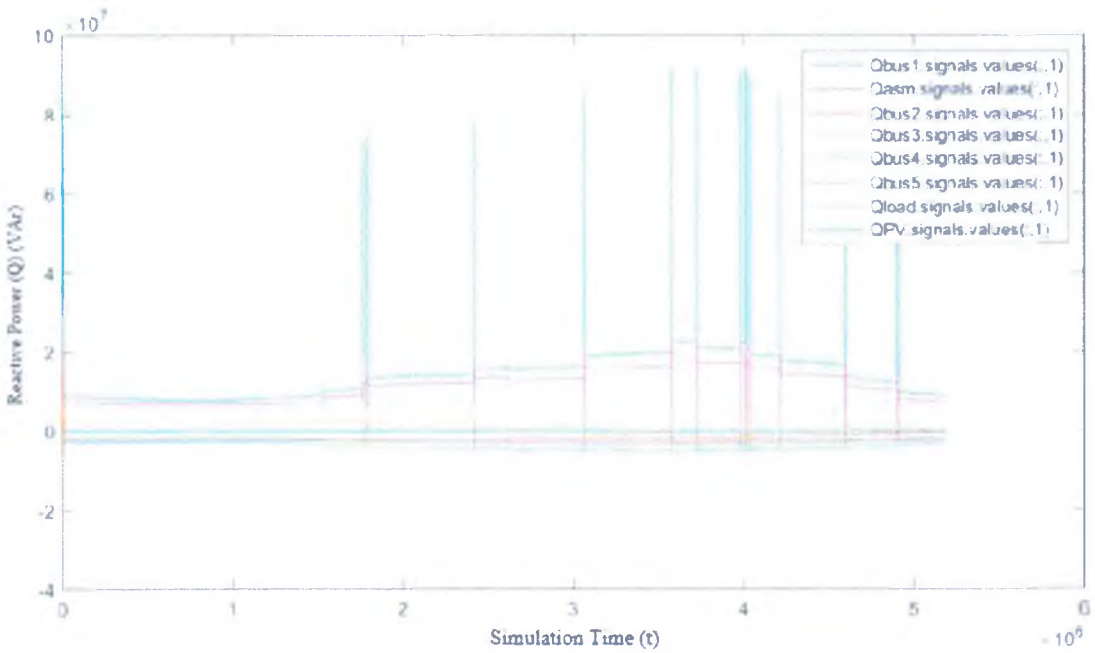

Figure 4.73. Reactive power graphs of all (Q_{all})

Figure 4.74 shows us apparent power on bus1 which belongs to voltage source block before the OLTC apparent power change with behavior of first system. In the second simulation there are three control strategies to regulate desire voltage and reactive power.

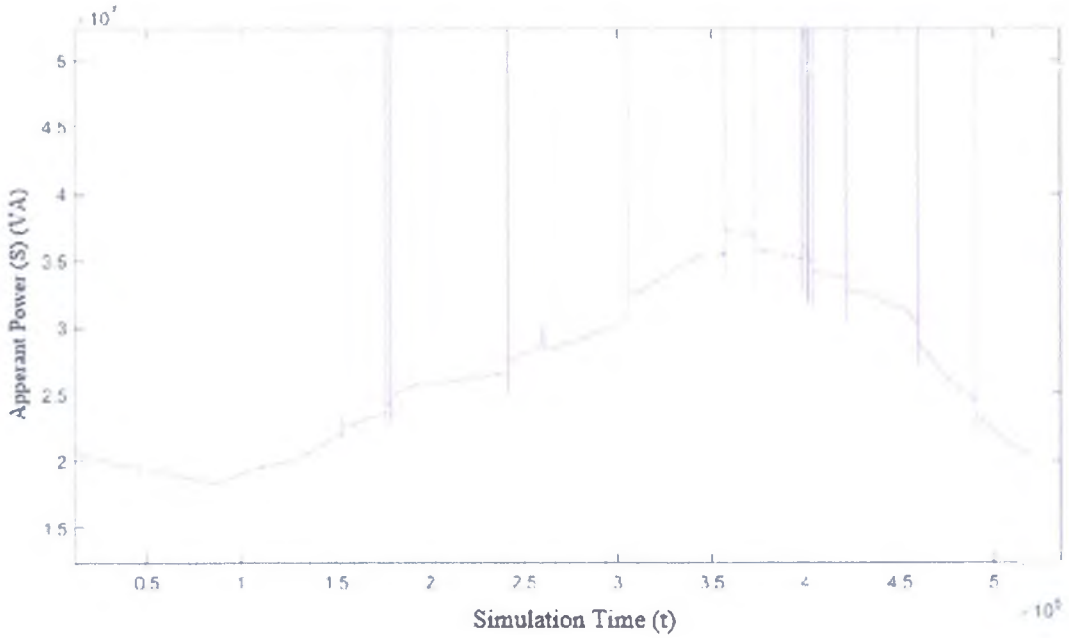

Figure 4.74. Apparent power graph of bus 1 (S_{bus1})

Figure 4.75 shows us apparent power on bus2 which belongs to voltage source block after the OLTC apparent power change with behavior of first system. In the second simulation there is three control strategies to regulate desire voltage and reactive power.

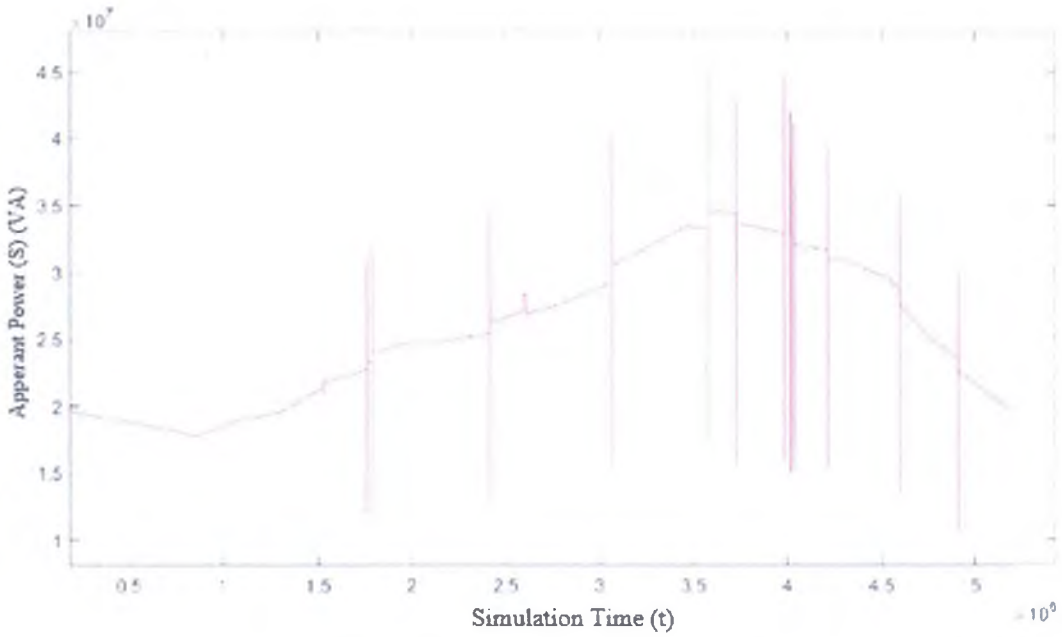

Figure 4.75. Apparent power graph of bus 2 (S_{bus2})

Figure 4.76 shows us apparent power on bus3. This block measures the voltage of diesel generator, apparent power change with behavior of first system. In the second simulation there are three control strategies to regulate desire voltage and reactive power.

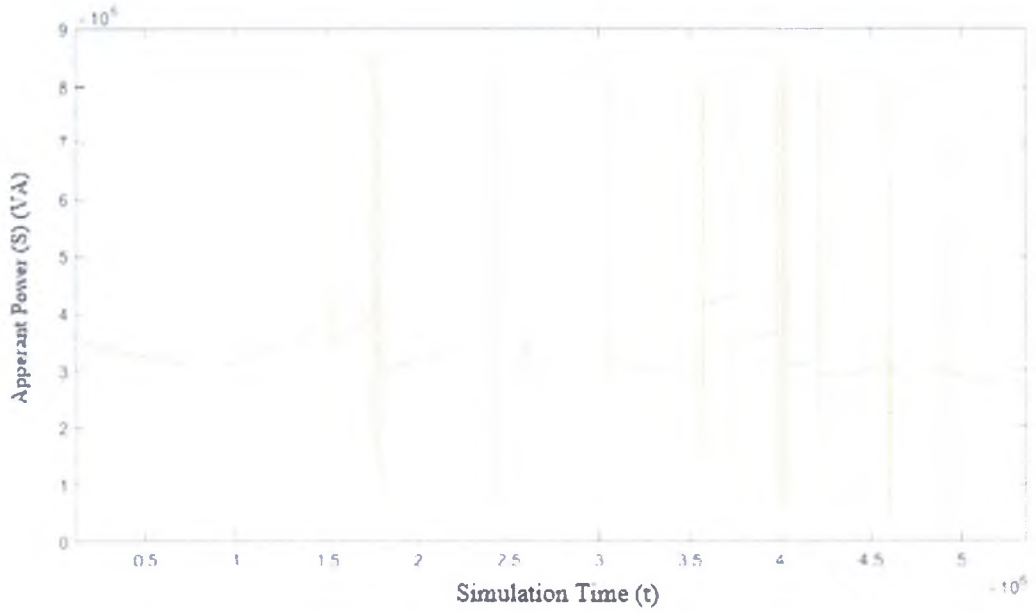

Figure 4.76. Apparent power graph of bus 3 (S_{bus3})

Figure 4.77 shows us apparent power on bus4 which measures the voltage of 15 MW residential load apparent power change with behavior of first system. In the second simulation there are three control strategies to regulate desire voltage and reactive power.

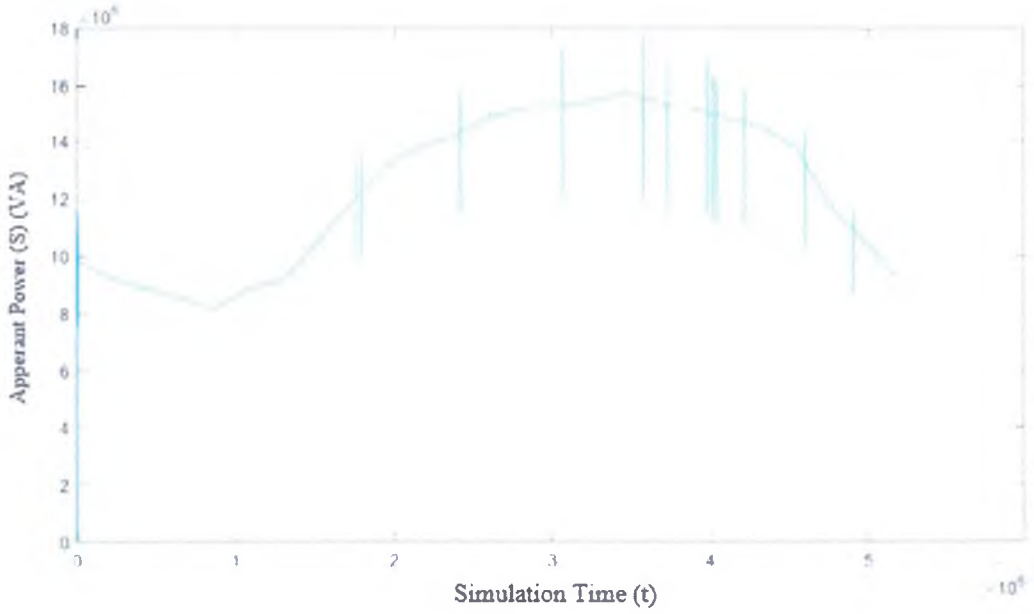

Figure 4.77. Apparent power graph of bus 4 (S_{bus4})

Figure 4.78 shows us apparent power on bus5 which measures voltage of 10MW residential load and ASM, apparent power change with behavior of first system. In the second simulation there is three control strategies to regulate desire voltage and reactive power.

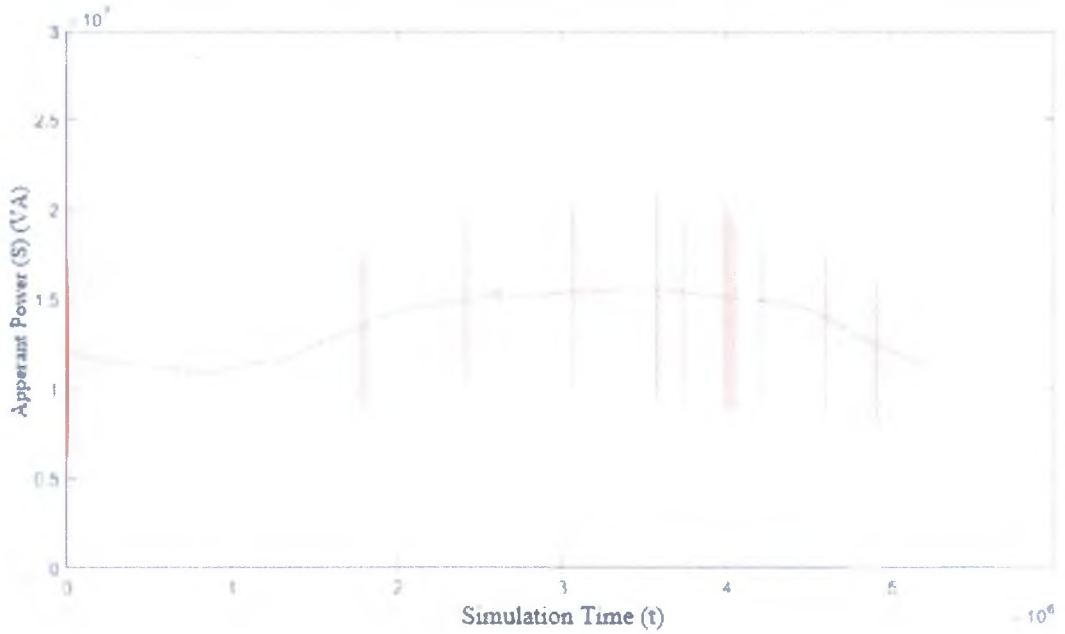

Figure 4.78. Apparent power graph of bus 5 (S_{bus5})

Figure 4.79 shows us apparent power on load bus which is also inside of bus5 representing residential loads, apparent power change with behavior of first system. In the second simulation there are three control strategies to regulate desire voltage and reactive power.

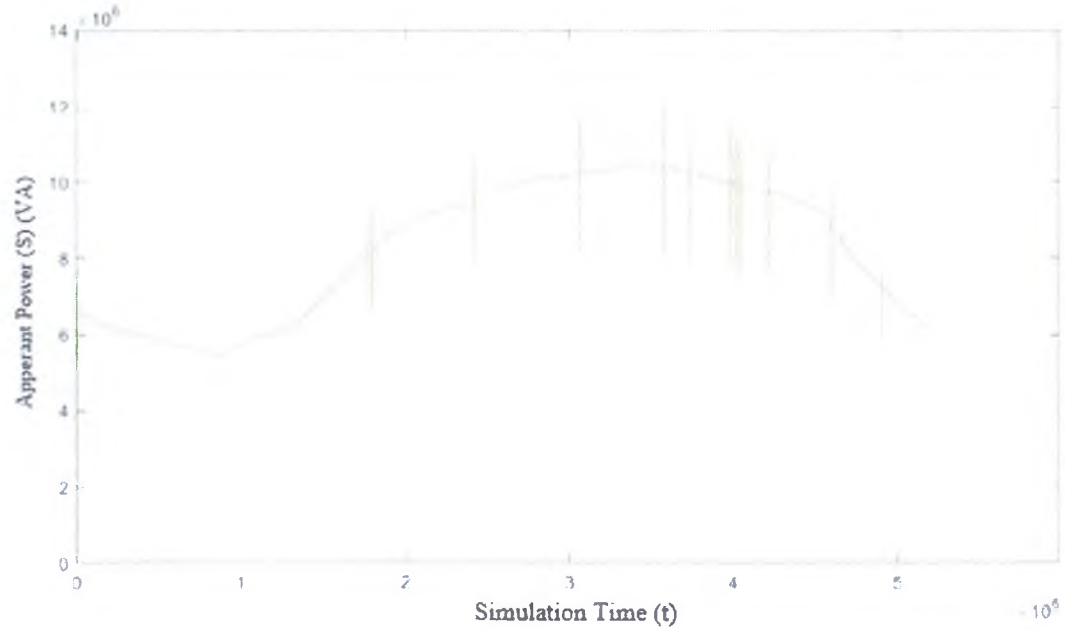

Figure 4.79. Apparent power graph of load (S_{load})

Figure 4.80 shows us apparent power on PV bus, it changes parallel with irradiance data and PV system block produce maximum energy at 13:00-14:00.

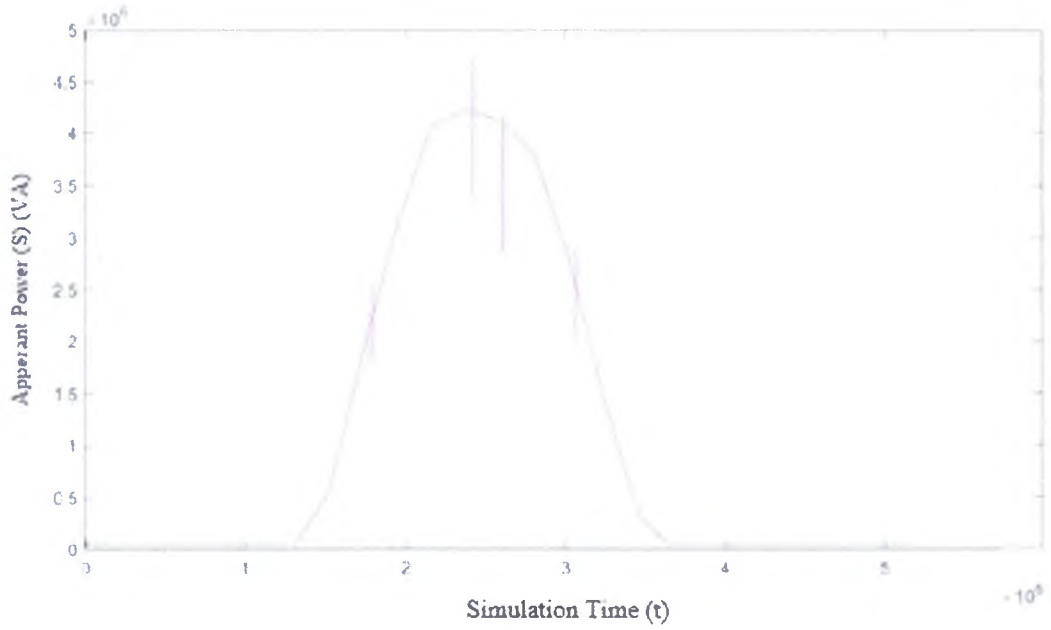

Figure 4.80. Apparent power graph of PV (S_{PV})

Figure 4.81 shows us apparent power on ASM bus which is also inside of bus5, apparent power change with behavior of first system. In the second simulation there are three control strategies to regulate desire voltage and reactive power.

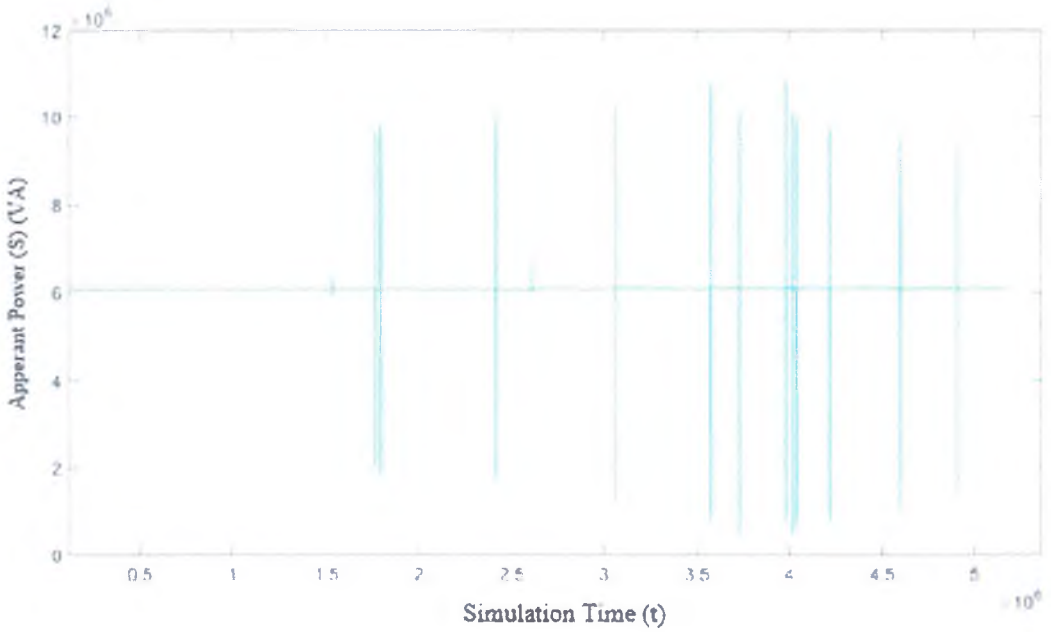

Figure 4.81. Apparent power graph of ASM (S_{ASM})

Figure 4.82 shows us all apparent power on all buses,

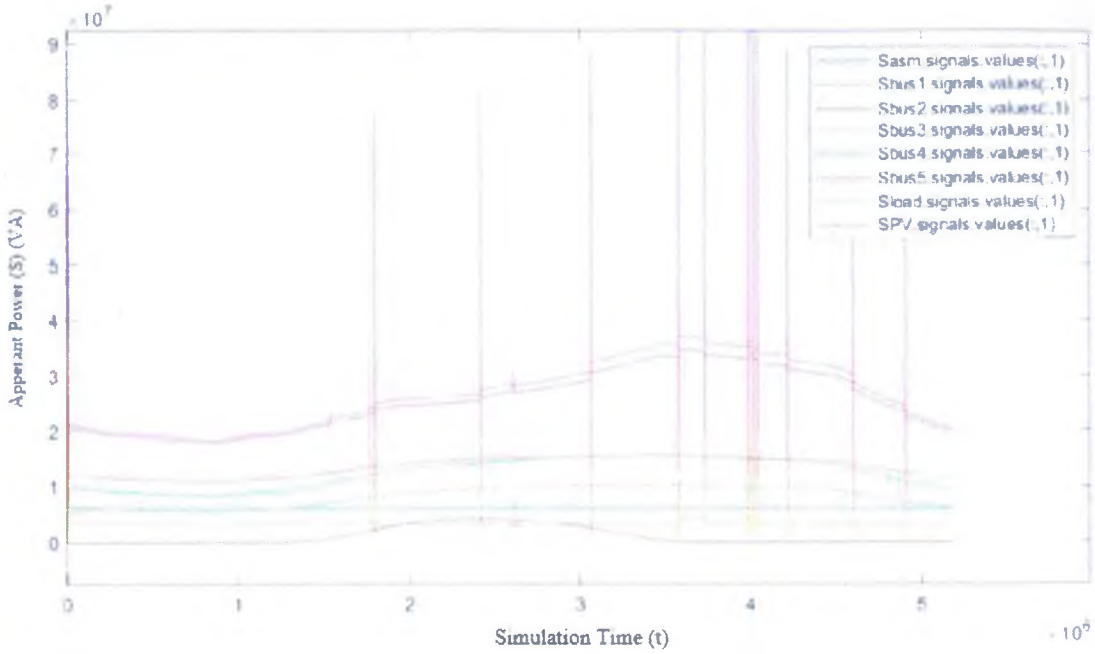

Figure 4.82. Apparent power graphs of all (S_{all})

Figure 4.83 shows us current flow on bus1 which belongs to voltage source block before the OLTC current flow change with behavior of first system. In the second simulation there is three control strategies to regulate desire voltage and reactive power.

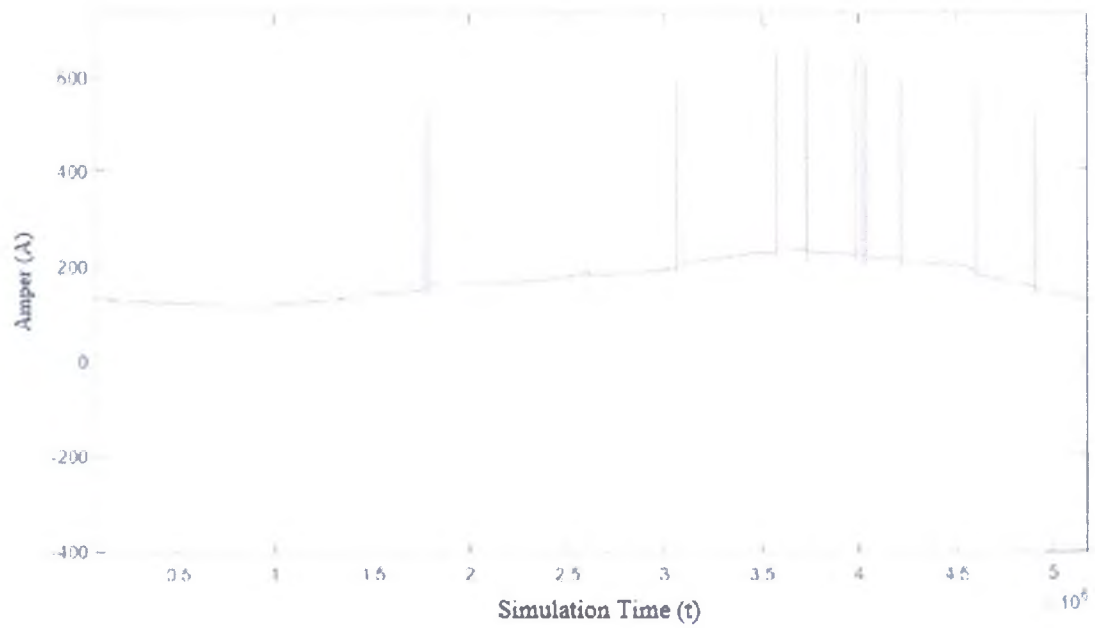

Figure 4.83. Current graph of bus 1 (I_{bus1})

Figure 4.84 shows us current flow on bus2 which belongs to voltage source block after the OLTC current flow change with behavior of first system. In the second simulation there is three control strategies to regulate desire voltage and reactive power.

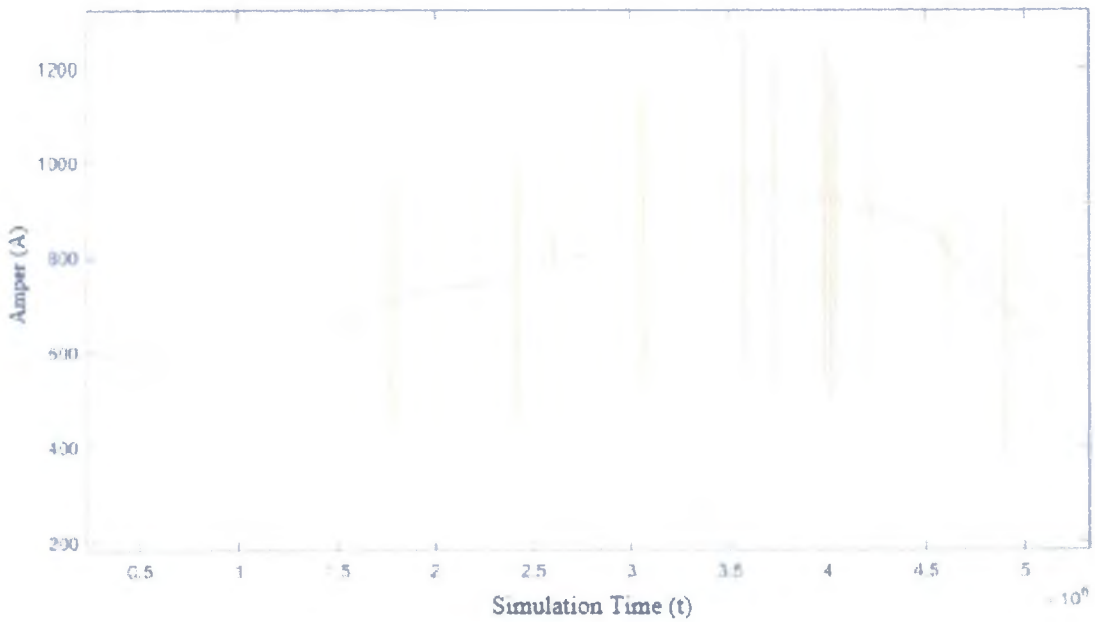

Figure 4.84. Current graph of bus 2 (I_{bus2})

Figure 4.85 shows us current flow on bus3. This block measures the voltage of diesel generator, current flow change with behavior of first system. In the second simulation there are three control strategies to regulate desire voltage and reactive power.

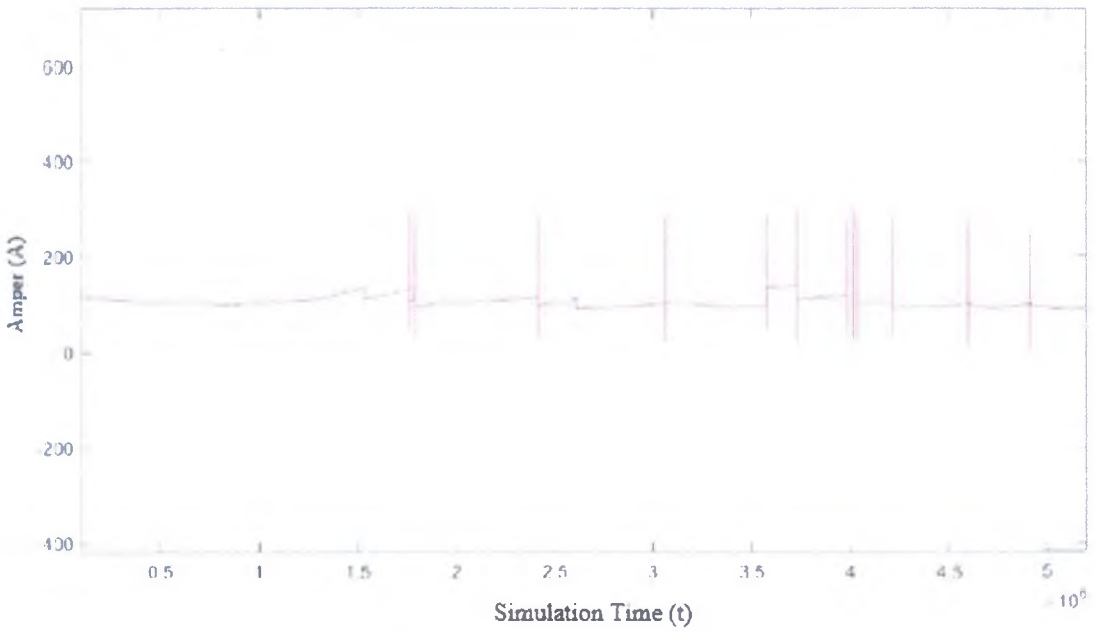

Figure 4.85. Current graph of bus 3 (I_{bus3})

Figure 4.86 shows us current flow on bus4 which measures the voltage of 15 MW residential load, current flow change with behavior of first system. In the second simulation there are three control strategies to regulate desire voltage and reactive power.

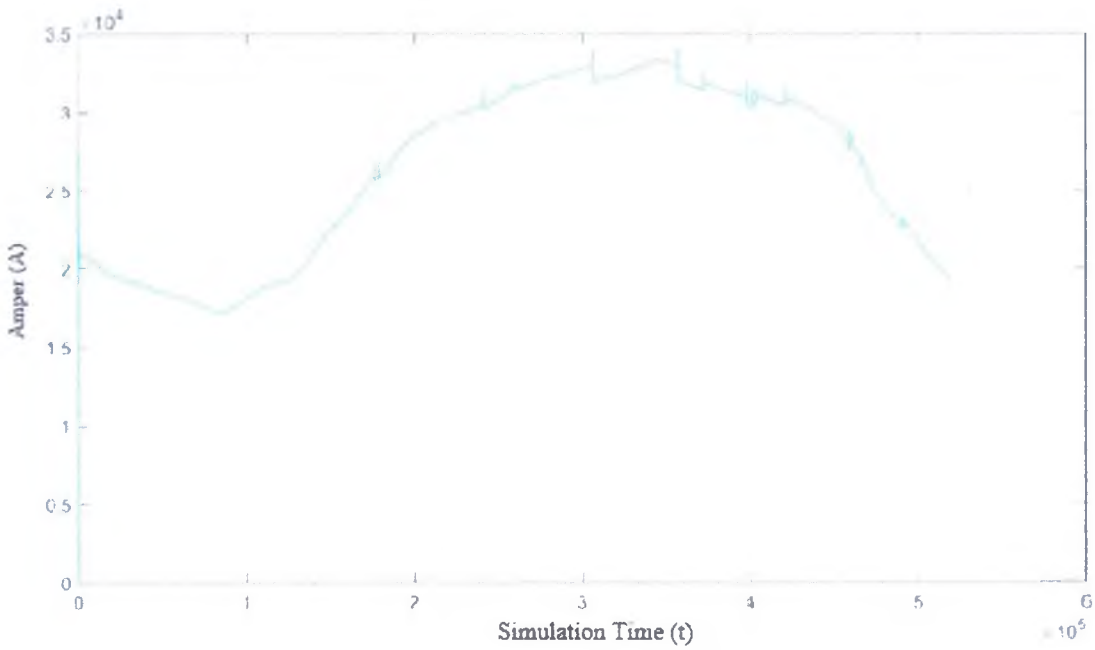

Figure 4.86. Current graph of bus 4 (I_{bus4})

Figure 4.87 shows us current flow on bus5 which measures the voltage of 10MW residential load and ASM, current flow change with behavior of first system. In the second simulation there is three control strategies to regulate desire voltage and reactive power.

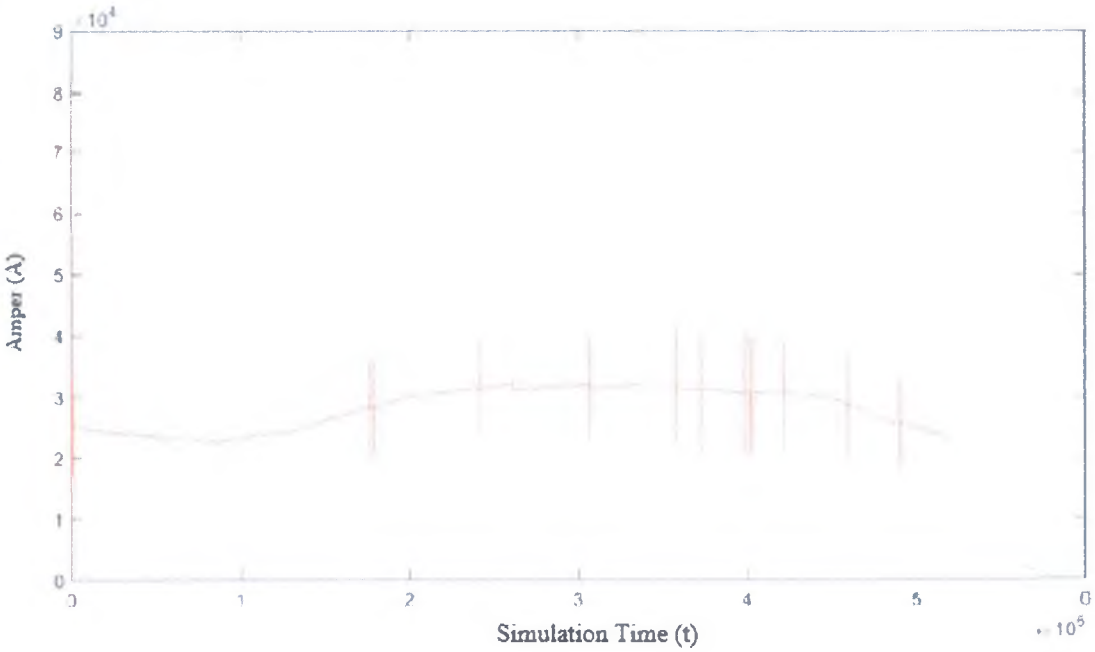

Figure 4.87. Current graph of bus 5 (I_{bus5})

Figure 4.88 shows current flow on load bus which is also inside of bus5 represent residential loads, current flow change with behavior of first system. In the second simulation there are three control strategies to regulate desire voltage and reactive power.

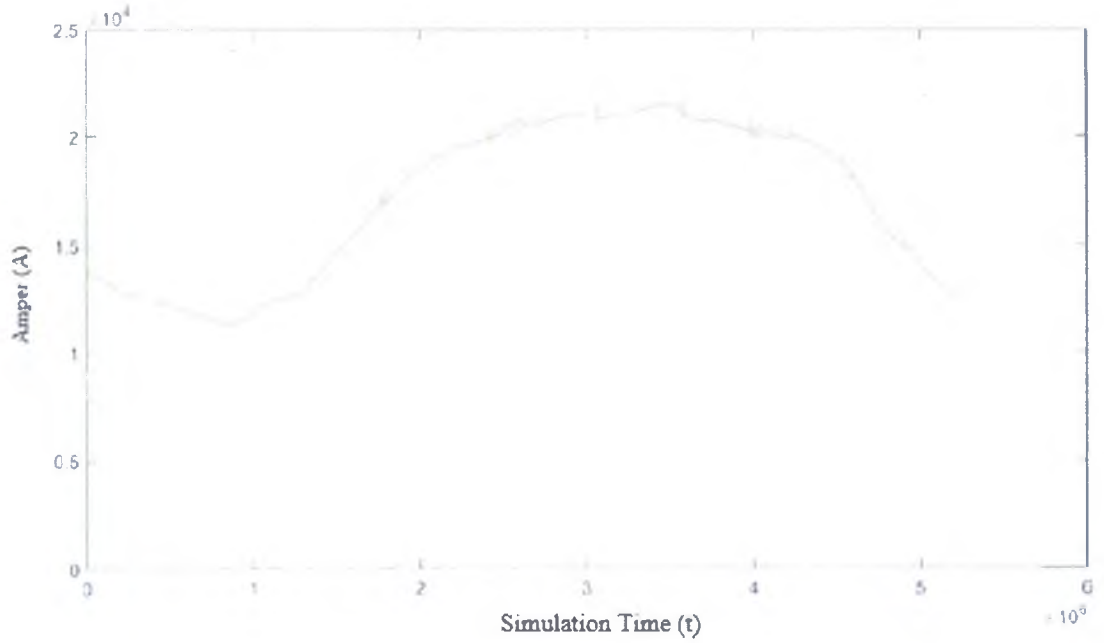

Figure 4.88. Current graph of Load (I_{load})

Figure 4.89 shows us current flow on PV bus, it changes parallel with irradiance data and PV system block produce maximum energy at 13:00-14:00.

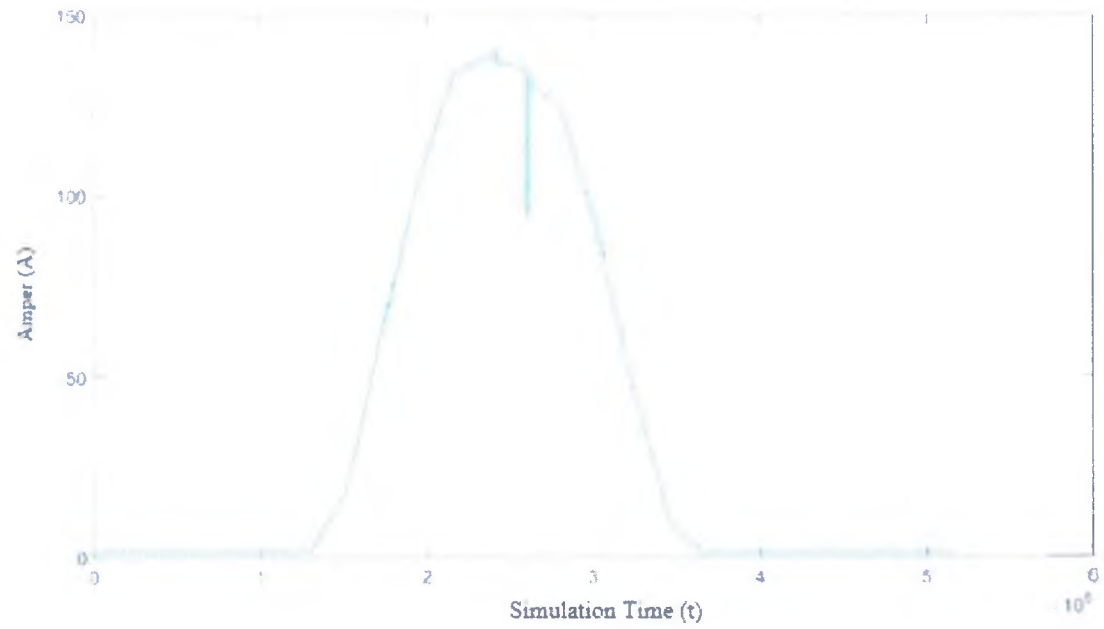

Figure 4.89. Current graph of PV (I_{PV})

Figure 4.90 shows us current flow on ASM bus which is also inside of bus5, current flow change with behavior of first system. In the second simulation there are three control strategies to regulate desire voltage and reactive power.

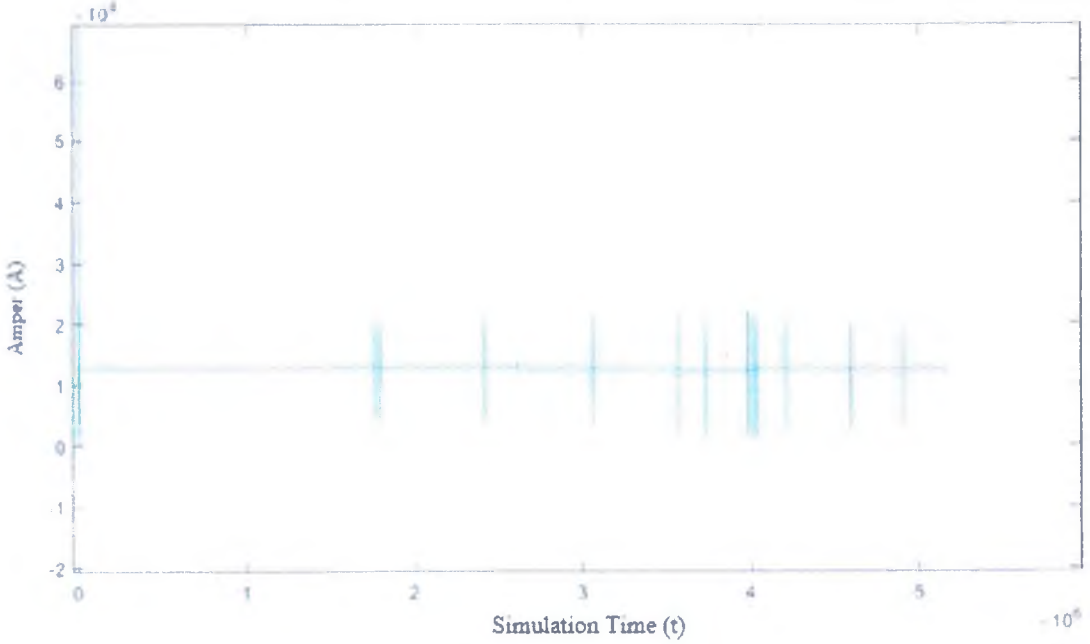

Figure 4.90. Current graph of ASM (I_{ASM})

Figure 4.91 shows us current flow on all buses,

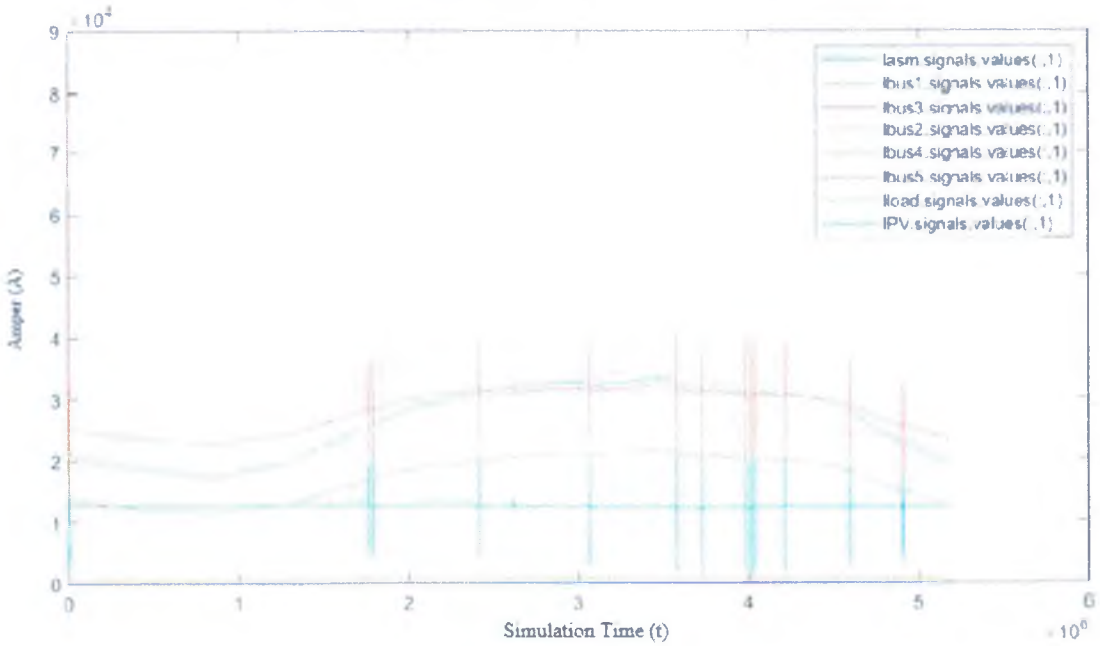

Figure 4.91. Current graphs of all (I_{all})

4.5. Case 1: Implementing Nine Zone Diagram

The uncontrolled nine zone diagram is given in Table 4.34.

Table 4.34. Implementing nine zone diagram without controller

TIME	CURRENT SITUATION FOR BUS1(SOURCE)					ZONE	what we will do /NINE ZONE DIAGRAM	
	V	Q	P	S	I		OLTC (V)	SVC (Q)
10	↓	↑	↑	↑	↑	8	increase V	decrease Qc
21	↑	↓	↓	↓	↓	4	decrease V	increase Qc
TIME	CURRENT SITUATION FOR BUS2					ZONE	what we will do /NINE ZONE DIAGRAM	
	V	Q	P	S	I		OLTC (V)	SVC (Q)
10	↓	↑	↑	↑	↑	8	increase V	decrease Qc
21	↑	↓	↓	↓	↓	4	decrease V	increase Qc
TIME	CURRENT SITUATION FOR BUS3 DIESEL SOURCE					ZONE	what we will do /NINE ZONE DIAGRAM	
	V	Q	P	S	I		OLTC (V)	SVC (Q)
10	↔	↑	↔	↑	↑	7	No changeV	decrease Qc
21	↔	↓	↔	↓	↓	3	No changeV	increase Qc
TIME	CURRENT SITUATION FOR BUS4 (LOAD)					ZONE	what we will do /NINE ZONE DIAGRAM	
	V	Q	P	S	I		OLTC (V)	SVC (Q)
10	↓	↑	↑	↑	↑	8	increase V	decrease Qc
21	↑	↓	↓	↓	↓	4	decrease V	increase Qc
TIME	CURRENT SITUATION FOR BUS5					ZONE	what we will do /NINE ZONE DIAGRAM	
	V	Q	P	S	I		OLTC (V)	SVC (Q)
10	↓	↑	↑	↑	↑	8	increase V	decrease Qc
21	↑	↓	↓	↓	↓	4	decrease V	increase Qc
TIME	CURRENT SITUATION FOR LOAD					ZONE	what we will do /NINE ZONE DIAGRAM	
	V	Q	P	S	I		OLTC (V)	SVC (Q)
10	↓	↑	↑	↑	↑	8	increase V	decrease Qc
21	↑	↓	↓	↓	↓	4	decrease V	increase Qc
TIME	CURRENT SITUATION FOR PV FARM					ZONE	what we will do /NINE ZONE DIAGRAM	
	V	Q	P	S	I		OLTC (V)	SVC (Q)
10	↓	↔	↑	↑	↑	1	increase V	No changeQc
21	↑	↔	↔	↔	↔	5	decrease V	No changeQc
TIME	CURRENT SITUATION FOR ASM					ZONE	what we will do /NINE ZONE DIAGRAM	
	V	Q	P	S	I		OLTC (V)	SVC (Q)
10	↓	↔	↔	↔	↔	1	increase V	No changeQc
21	↑	↔	↔	↔	↔	5	decrease V	No changeQc

For example, the status update for bus1 (source), where the nine zone diagram is in the area of, OLTC and SVC support to the system are currently being added. Here;

Time 10: It is seen that the voltage value decreases in the current status column for bus1 and the other parameters increase. The Nine zone diagram is in the 4th zone. In this case, voltage increase in OLTC, reactive power reduction occurs in SVC.

Time 21: It is seen that the voltage value increases in the current status column for bus1 and the other parameters decrease. The Nine zone diagram is in the 4th zone. In this case, voltage decrease in OLTC, reactive power increment occurs in SVC.

Similar comments can be made for other cases.

4.6. Case 2: Implementing Nine Zone Diagram

The controlled nine zone diagram is given in Table 4.35 briefly. For example, the status update for bus1 (source), where the nine zone diagram is in the area of, OLTC and SVC support to the system are currently being added.

Time 10: It is observed that in the current status column for bus1, there is no change in the voltage value and in the other parameters an increase. The Nine zone diagram is in the 7th zone. In this case, there is no reactive power reduction in the SVC while there is no change in OLTC.

Time 21: In the current status column for Bus1, there is no change in the voltage value while the other parameters show a decrease. Nine zone diagram is in zone 3. In this case there is no change in OLTC and reactive power increase in SVC.

Similar comments can be made for other situations

Table 4.35. Implementing nine zone diagram with controller

TIME	CURRENT SITUATION FOR BUS1(SOURCE)					ZONE	what we will do /NINE ZONE DIAGRAM	
	V	Q	P	S	I		OLTC (V)	SVC (Q)
10	↔	↑	↑	↑	↑	7	No change V	decrease Qc
21	↔	↓	↓	↓	↓	3	No change V	increase Qc
TIME	CURRENT SITUATION FOR BUS2					ZONE	what we will do /NINE ZONE DIAGRAM	
	V	Q	P	S	I		OLTC (V)	SVC (Q)
10	↑	↑	↑	↑	↑	6	decrease V	decrease Qc
21	↓	↓	↓	↓	↓	2	increase V	increase Qc
TIME	CURRENT SITUATION FOR BUS3 DIESEL SOURCE					ZONE	what we will do /NINE ZONE DIAGRAM	
	V	Q	P	S	I		OLTC (V)	SVC (Q)
10	↔	↑	↔	↑	↔	7	No changeV	decrease Qc
21	↔	↓	↔	↓	↔	3	No changeV	increase Qc
TIME	CURRENT SITUATION FOR BUS4 (LOAD)					ZONE	what we will do /NINE ZONE DIAGRAM	
	V	Q	P	S	I		OLTC (V)	SVC (Q)
10	↔	↑	↑	↑	↑	7	No change V	decrease Qc
21	↔	↓	↓	↓	↓	3	No change V	increase Qc
TIME	CURRENT SITUATION FOR BUS5					ZONE	what we will do /NINE ZONE DIAGRAM	
	V	Q	P	S	I		OLTC (V)	SVC (Q)
10	↑	↑	↑	↑	↑	6	decrease V	decrease Qc
21	↔	↓	↓	↓	↓	3	No change V	increase Qc
TIME	CURRENT SITUATION FOR LOAD					ZONE	what we will do /NINE ZONE DIAGRAM	
	V	Q	P	S	I		OLTC (V)	SVC (Q)
10	↓	↑	↑	↑	↑	8	increase V	decrease Qc
21	↔	↓	↓	↓	↓	3	No change V	increase Qc
TIME	CURRENT SITUATION FOR PV FARM					ZONE	what we will do /NINE ZONE DIAGRAM	
	V	Q	P	S	I		OLTC (V)	SVC (Q)
10	↑	↓	↔	↑	↑	4	decrease V	increase Qc
21	↓	↔	↔	↔	↔	1	increase V	No changeQc
TIME	CURRENT SITUATION FOR ASM					ZONE	what we will do /NINE ZONE DIAGRAM	
	V	Q	P	S	I		OLTC (V)	SVC (Q)
10	↓	↓	↔	↔	↔	2	increase V	increase Qc
21	↔	↔	↔	↔	↔	0	No change V	No changeQc

CHAPTER V

CONCLUSIONS AND FUTURE WORKS

5.1. Conclusions

In this master thesis we investigated the voltage and reactive power regulation of Distribution grid with controlled nine zone diagram algorithm. For implementation and analysis of nine zone algorithm, a real transmission line and microgrids (MG) was simulated. The main reason for connecting microgrid to the distribution system; which has PV plant and Diesel Generator, is to see the effects of supplement sources on the main grid. Phasor type simulation was used because it allows us to simulate a long period of time like one day, one month, etc. The developed system is composed of Voltage Source which is the main generator of system and OLTC (On load tap changer), SVC (Static VAr compensator), PV array, residential loads, diesel generator, and asynchronous motor used as representing factorial loads. Matlab/Simulink was used as simulation software.

After deciding all components of simulation, our main motivation is making the simulation as real as possible so we collect consumer usage data from energy suppliers at our city for using as energy consumption data in simulation for one day. We used these data reference to residential loads and with this loads act as a variable load and consumption will change every hour of the day so we can collect better result instead of using fixed loads. Also, we checked irradiance data and compared with the data belong to our city for getting an idea about our region needing.

For best comparison, simulation run two times, first one not have any external control algorithm and second one is controlled by nine zone diagram algorithm.

1. All simulation results were collected and nine zone diagram implemented to these results. For example, when voltage and reactive power rises or decreases

dramatically on a specific bus we decided to implement which zone of diagram to system for reaching zero point of diagram.

2. According to the first results of simulation specific control algorithim is implemented to the OLTC for controlling rising and decease of voltage, SVC for compensating reactive power on specific bus also PV array controller used for controlling reactive power of system. Controller of system working with previous data of system and it get feedback signals from system for controlling undesired situation. With controlled system we can barely see that voltage and reactive power values reach the desired condition in table 4.10 uncontrolled voltage and reactive power result for bus5 given and if compare this result with table 4.26 which controlled version of simulation result for same bus we see that voltage and reactive power chage with control mechanism effects table 4.26 and in table 4.10 it follows the consumption data where is consumtion high voltage is low but in second result this effect eliminated.

5.2. Future Works

In this study, voltage regulation in transmission lines was performed by using reactive power. Nine zone diagram method was used for the application of reactive power to the system.

In this study, three separate controllers were used for OLTC, SVC, and PV Array. In this respect, the work can be used as a general controller for future work.

Besides, the method can also be simulated using the wind turbine and the results are comparable. Similarly, the operation of the system can be simulated using the PV array and the wind turbine together.

The optimization methods considering the uncertainties in the system such as the variations in loads and active power generation of the DGs should also implemented.

REFERENCES

A. Bedeloğlu, A. Demir, and Y. Bozkurt, (2010) "Fotovoltaik teknolojisi: Türkiye ve dünyadaki durumu, genel uygulama alanları ve fotovoltaik tekstiller". Tekstil Teknolojileri Elektronik Dergisi, 2010. 4(2): p. 43-58.

A. Goldthau, (2008). "Rhetoric versus reality: Russian threats to European energy supply". Energy Policy, 36(2): p. 686-692.

A. Kusko, and M.T. Thompson, (2007) Power quality in electrical systems. Vol. 23. McGraw-Hill.

A. Pan, Tian, Y., Zhao, H., Yang, X., & Jin, J. (2012). Power quality analysis of PV system of summer and winter.

A. Safari, and S. Mekhilef, (2011) "Simulation and hardware implementation of incremental conductance MPPT with direct control method using cuk converter". IEEE transactions on industrial electronics, 58(4): p. 1154-1161.

A. Salam, A. Mohamed, and M. Hannan, (2008) "Technical challenges on microgrids". ARPN Journal of engineering and applied sciences, 3(6): p. 64-69.

A. Testa, et al. (2012) "A buck-boost based dc/ac converter for residential PV applications". in Power Electronics, Electrical Drives, Automation and Motion (SPEEDAM), 2012 International Symposium on. IEEE.

A., Baggini, (2008) Handbook of power quality. John Wiley & Sons.

B. Vermulst, C. Wijnands, and J. Duarte. (2012) "Isolated high-efficiency DC/DC converter for photovoltaic applications". in IECON 2012-38th Annual Conference on IEEE Industrial Electronics Society. 2012. IEEE.

B.J. Rani, G.S. Ilango, and C. Nagamani, (2013) "Enhanced power generation from PV array under partial shading conditions by shade dispersion using Su Do Ku configuration". IEEE Transactions on sustainable energy, 4(3): p. 594-601.

C.K. Sao, and P.W. Lehn, (2008) "Control and power management of converter fed microgrids". IEEE Transactions on Power Systems, 23(3): p. 1088-1098.

D. Middleton, I.o. Electrical, and E. Engineers, (1996) An introduction to statistical communication theory. IEEE press Piscataway, NJ..

D. Parlak, (2014) 12 Darbeli Tiristör Kontrollü Reaktör Tabanlı Reaktif Güç Kompanzasyonu Sistemlerinin Gerilim Regülasyonu İçin Tasarım, Uygulama Ve Mühendislik Yönleri, in Elektrik Elektronik Mühendisliği Bölümü.Orta Doğu Teknik Üniversitesi: Ankara.

D. Riawan, and C. Nayar. (2007) "Analysis and design of a solar charge controller using cuk converter". in Power Engineering Conference, AUPEC 2007. Australasian Universities. IEEE.

D. Song, et al. (2012) "Progress in n-type Si solar cell and module technology for high efficiency and low cost. in Photovoltaic Specialists Conference (PVSC)", 38th IEEE.

D.P. Shankar, U. Govindarajan, and K. Karunakaran, (2013) "Period-bubbling and mode-locking instabilities in a full-bridge DC-AC buck inverter". IET Power Electronics, 6(9): p. 1956-1970.

E. Barklund, et al., (2008) Energy management in autonomous microgrid using stability-constrained droop control of inverters.

E. Filoğlu, (2011) Türkiye'de Mikro Kojenerasyon, 2. Elektrik Tesisat Ulusal Kongresi Bildirileri, 2011.

E. Fuchs, and M.A. Masoum, (2011) Power quality in power systems and electrical machines. Academic press.

E.İ.G. Müdürlüğü, and U.E.T. (1997) Merkezi, Sanayide Enerji Yönetimi Esasları, Cilt IV, Ocak.

F. Blaabjerg, and D.M. Ionel, (2017) Renewable Energy Devices and Systems with Simulations in MATLAB® and ANSYS®. CRC Press.

F. Katiraei, and M.R. Iravani, (2006) "Power management strategies for a microgrid with multiple distributed generation units". IEEE transactions on power systems, 21(4): p. 1821-1831.

F.A. Viawan, and D. Karlsson. (2008) "Coordinated voltage and reactive power control in the presence of distributed generation". in Power and Energy Society General Meeting-Conversion and Delivery of Electrical Energy in the 21st Century, IEEE.

F.S. Gazijahani, et al. (2017) "Optimal day ahead power scheduling of microgrids considering demand and generation uncertainties". in Electrical Engineering (ICEE), 2017 Iranian Conference on. IEEE.

F.Z. Peng, Y.W. Li, and L.M. Tolbert. (2009) "Control and protection of power electronics interfaced distributed generation systems in a customer-driven

microgrid". in Power & Energy Society General Meeting, 2009. PES'09. IEEE.

G. Chicco, J. Schlabbach, and F. Spertino, (2009) "Experimental assessment of the waveform distortion in grid-connected photovoltaic installations". Solar Energy, 83(7): p. 1026-1039.

G. Diaz,et al., (2010) "Scheduling of droop coefficients for frequency and voltage regulation in isolated microgrids". IEEE Transactions on Power Systems, 25(1): p. 489-496.

H. Hanaoka, M. Nagai, and M. Yanagisawa. (2003) "Development of a novel parallel redundant UPS". in Telecommunications Energy Conference, INTELEC'03. The 25th International. IEEE.

H., Erdoğan, et al., (2009) "Yoğunlaştırıcılı Güneş Enerji Santralleri Ve Ilısu Hes'e Alternatif Olarak Güneydoğu Anadolu Bölgesine Uygulanabilirliği" V. Yenilenebilir Enerji Kaynakları Sempozyumu, Diyarbakır.

H., Kanchev, et al., (2011) "Energy management and operational planning of a microgrid with a PV-based active generator for smart grid applications". IEEE transactions on industrial electronics, 58(10): p. 4583-4592.

H., Saadat, (1999) Power System Analysis McGraw-Hill Series in Electrical Computer Engineering.

H.B. Çetinkaya, and F. Dumlu, (2013) "Dağıtık Üretim Tesislerinin Şebeke Entegrasyonunda Yaşanabilecek Olası Problemler ve Entegrasyon Analizleri". Akıllı Şebekeler ve Türkiye Elektrik Şebekesinin Geleceği Sempozyumu.

H.-C. Chin, (1995) "Optimal shunt capacitor allocation by fuzzy dynamic programming". Electric Power Systems Research, 35(2): p. 133-139.

I.O.f. Standardization, and I.E. Commission, (2001) Software Engineering--Product Quality: Quality model. Vol. 1. ISO/IEC.

J. Rocabert, et al., (2012) "Control of power converters in AC microgrids". IEEE transactions on power electronics, 27(11): p. 4734-4749.

J. Von Appen,et al., (2013) "Time in the sun: the challenge of high PV penetration in the German electric grid". IEEE Power and Energy magazine, 2013. 11(2): p. 55-64.

J., Hernández, et al., (2011) "Guidelines for the technical assessment of harmonic, flicker and unbalance emission limits for PV-distributed generation". Electric Power Systems Research, 81(7): p. 1247-1257.

J.J. Burke, (1994) Power distribution engineering: fundamentals and applications. CRC Press.

K. Basaran, N.S. Cetin, and S. Borekci, (2016) "Energy management for on-grid and off-grid wind/PV and battery hybrid systems". IET Renewable Power Generation, 11(5): p. 642-649.

K. Fekete, Z. Klaic, and L. Majdandzic, (2012) "Expansion of the residential photovoltaic systems and its harmonic impact on the distribution grid". Renewable Energy, 43: p. 140-148.

K.H. Chua, et al., (2011) "Mitigation of voltage unbalance in low voltage distribution network with high level of photovoltaic system". Energy Procedia, 12: p. 495-501.

L. Freris, and D. Infield, Renewable energy in power systems. (2008). John Wiley & Sons.

L. Jun-Wei, et al., (2015) Analysis of Nine zone diagram for voltage control of substation Considering the Load characteristics.

L. Jun-Wei, et al., (2015) Analysis of Nine zone diagram for voltage control of substation Considering the Load characteristics.

M. Abdollahi, and S. Bathaee. (2008) "Sliding mode controller for stability enhancement of MicroGrids". in Transmission and Distribution Conference and Exposition, T&D. IEEE/PES-2008.

M. Meiqin, L. Chang, and D. Ming. (2008) "Integration and intelligent control of micro-grids with multi-energy generations: A review". in Sustainable Energy Technologies, ICSET 2008. IEEE International Conference on. 2008. IEEE.

M. Ortega, J. Hernández, and O. García, (2013) "Measurement and assessment of power quality characteristics for photovoltaic systems: Harmonics, flicker, unbalance, and slow voltage variations". Electric Power Systems Research, 96: p. 23-35.

M., Bayat, et al., (2016) "Coordination of distributed energy resources and demand response for voltage and frequency support of MV microgrids". IEEE Trans. Power Syst, 31(2): p. 1506-1516.

M., Shamshiri, C.K. Gan, and C.W. Tan. (2012) "A review of recent development in smart grid and micro-grid laboratories". in Power Engineering and Optimization Conference (PEDCO) Melaka, Malaysia, 2012 IEEE International.

M.A. Eltawil, and Z. Zhao, (2010) "Grid-connected photovoltaic power systems: Technical and potential problems—A review". Renewable and Sustainable Energy Reviews, 14(1): p. 112-129.

M.K. Daugherty, and V.R. Carter, (2010) "Renewable energy technology". Technology and Engineering Teacher, 69(5): p. 24.

M.R. Miveh, S. Mirsaeidi, and M. Gandomkar, (2012) Fundamental Key Issues and Analysis of Symmetrical Current Components in Micro-Grids.

N.M., Tabatabaei, et al., (2017) Reactive Power Control in AC Power Systems.

P. Chopade, et al. (2011) "Reactive power management and voltage control of large Transmission System using SVC (Static VAR Compensator)". in Southeastcon, 2011 Proceedings of IEEE.

R. Gazete, (2010) Elektrik Piyasasında Lisanssız Elektrik Üretimine İlişkin Yönetmelik.

R. González, et al., (2007) "Transformerless inverter for single-phase photovoltaic systems". IEEE Transactions on Power Electronics, 22(2): p. 693-697.

R. Idris, and N. Zaid. (2016) "Optimal shunt capacitor placement in radial distribution system". in Power and Energy (PECon), 2016 IEEE International Conference on.

R.H. Lasseter, (2011) Smart distribution: Coupled microgrids. Proceedings of the IEEE, 99(6): p. 1074-1082.

S. Chattopadhyay, M. Mitra, and S. Sengupta, (2011) Electric power quality, in Electric Power Quality. Springer. p. 5-12.

S. Chiang, H.-J. Shieh, and M.-C. Chen, (2009) "Modeling and control of PV charger system with SEPIC converter". IEEE Transactions on Industrial Electronics, 56(11): p. 4344-4353.

S. Chowdhury, and P. Crossley, (2009) Microgrids and active distribution networks. The Institution of Engineering and Technology.

S. Ozdemir, N. Altin, and I. Sefa, (2014) "Single stage three level grid interactive MPPT inverter for PV systems". Energy Conversion and Management, 80: p. 561-572.

S. Saridakis, E. Koutroulis, and F. Blaabjerg, (2013) "Optimal design of modern transformerless PV inverter topologies". IEEE transactions on energy conversion, 28(2): p. 394-404.

S., Borlase, (2016) Smart grids: infrastructure, technology, and solutions.CRC press.

S., Conti, et al., (2012) "Optimal dispatching of distributed generators and storage systems for MV islanded microgrids". IEEE Transactions on Power Delivery, 27(3): p. 1243-1251.

S.K. Gawre, N. Patidar, and R. Nema, (2012) "Application of wavelet transform in

power quality: a review". Power, 39(18).

S.K. Mazumder, M. Tahir, and K. Acharya, (2008) "Master-slave current-sharing control of a parallel dc-dc converter system over an RF communication interface". IEEE transactions on industrial electronics (1982), 55(1): p. 59.

S.-l. Lei, et al., (2013) "Research of Voltage and Reactive Power Control Strategy Based on Fuzzy Logic Control in Three Winding Step-Down Substation". Journal of Chongqing University of Technology (Natural Science), 27: p. 90-95.

S.M. Sharkh, et al., (2014) Power electronic converters for microgrids. John Wiley & Sons.

T.C. Green, and M. Prodanović, (2007) "Control of inverter-based micro-grids". Electric power systems research, 77(9): p. 1204-1213.

V. Quaschning, (2016) Understanding renewable energy systems. Routledge.

W. Kersting, (2009) "The modeling and application of step voltage regulators". in Power Systems Conference and Exposition, PSCE'09. IEEE/PES. 2009. IEEE.

W.N. Macêdo, and R. Zilles, (2009) "Influence of the power contribution of a grid-connected photovoltaic system and its operational particularities". Energy for Sustainable Development, 13(3): p. 202-211.

W.-Q. Han, et al., (2012) Study of area substation voltage and reactive power control based on load forecasting. Power System Protection and Control, 40(8): p. 68-72.

X. Huijie, et al. (2010) "Design and implementation of a PV DC/DC converter with high efficiency at low output power". in Power System Technology (POWERCON), 2010 International Conference on. IEEE.

X. Wang, F. Blaabjerg, and W. Wu, (2014) "Modeling and analysis of harmonic stability in an AC power-electronics-based power system". IEEE Transactions on Power Electronics, 29(12): p. 6421-6432.

X., Wang, et al., (2012) "A review of power electronics based microgrids". Journal of Power Electronics, 12(1): p. 181-192..

Y. Du, et al., (2013) "Modeling and analysis of current harmonic distortion from grid connected PV inverters under different operating conditions". Solar Energy, 94: p. 182-194.

Y.S. Lim, and J.H. Tang, (2014) "Experimental study on flicker emissions by photovoltaic systems on highly cloudy region: A case study in Malaysia". Renewable Energy, 64: p. 61-70.

Y.-z., Zhang, W.-z. XU, and H.-y. FU, (2009) "Voltage and reactive power control

on global optimization control based on sensitivity" [J]. Power System Protection and Control.

Z. Peng-hui, S. Shi-Ping, and H. Yan, (2014) "Reactive power control method for substation based on the modified nine zone diagram". Modern Electronics Technique, 37: p. 152-159.

Z., Zhang, et al., (2010) "A load-sharing control scheme for a microgrid with a fixed frequency inverter". Electric Power Systems Research, 80(3): p. 311-317.

Z.E. Aygen, (2002) Elektrik enerji sistemlerinde genetik algoritma kullanarak optimizasyona yeni bir yaklaşım. Fen Bilimleri Enstitüsü.